Simulated Hydrologic Responses to Climate-Change Projections for the Lake Tahoe Basin

Michael Dettinger
Seshadri Rajagopal

March 2023

Publication No. 41292

Prepared by
Division of Hydrologic Sciences, Desert Research Institute

Prepared for
California Tahoe Conservancy

THIS PAGE INTENTIONALLY LEFT BLANK

EXECUTIVE SUMMARY

Background

Climate change is already impacting the Lake Tahoe Basin and even more change will come in coming decades. In response, agencies and communities throughout the Basin are beginning to develop plans and actions to enhance their capacity to adapt to climate change. An early step towards adaptation was an integrated vulnerability assessment in 2018 that provided state-of-the-science information on how climate is likely to change and how these changes will impact the Tahoe environment. However, the spatial resolution of climate and hydrologic projections available at that time was relatively coarse, and the present study provides a new set of more highly resolved projections of snowpack and streamflow responses to climate changes.

The new projections provided here are detailed enough to represent contrasts and commonalities across the diverse hydrologic settings of the Basin more completely than previous studies, and thus are an opportunity to anticipate future trends and transformations in the Basin, as well as climate-change hotspots and refuges in ways not possible with previous projections.

Methods

For more than a decade, the Desert Research Institute (in collaboration with the U.S. Geological Survey) has been developing hydrologic models of the watersheds, streams, and groundwater systems that encircle Lake Tahoe. One of the resulting models—the Precipitation-Runoff Modeling System (PRMS) model used here–has the advantage over simulations used by earlier assessments that it simulates hydrology at highly resolved, 1/29-square-mile grid cells compared to the 14-square-mile grid cells used in the most recent previous assessment. Results from the PRMS model are typically output for each of 60 subbasins that together comprise the Tahoe Basin and represent all the various streams that flow into the Lake. Following an analysis to determine how well the PRMS simulates various aspects of current Basin hydrology (more on this below), downscaled 1950-2099 climate-change projections from eight global climate models (GCMs) responding to two different assumptions about future global greenhouse-gas emissions (labeled RCP4.5 and RCP8.5) were input to the PRMS model to simulate an “ensemble” (or collection) of plausible hydrologic responses. A probabilistic ensemble approach is used here because we have little or no way to determine which of the GCMs to “believe” most, or even what emissions will look like in the future, so that a focus on ranges and averages of possible impacts is the safest approach. The simulated hydrologic responses to these 16 climate-change projections, and summaries of their statistics, are the principle products of the present study.

Results

The full report describes projected changes in:

- average temperatures
- heat waves
- total precipitation
- total snowmelt
- snowmelt timing
- streamflow totals

- timing of precipitation
- precipitation extremes
- April 1 snow-water amounts
- snow-season lengths
- streamflow timing
- streamflow extremes
- rain-on-snow events.

The complete and detailed projections are being made available online so that interested parties will be able to do their own analyses and develop their own conclusions and uses for the new projections. Some key results follow:

Climate Change

Projected warming and changes in precipitation totals (expressed as changes from historical norms at subbasin scales) are spatially fairly uniform across the Lake Tahoe Basin. Climate responses to increasing greenhouse-gas concentrations in the global atmosphere are, after all, global phenomena acting over distances and times far larger than the Tahoe Basin and most individual weather events. Consequently, most of the subbasin-to-subbasin variations in hydrologic responses reported here are reflections of the ways that the different terrains, forest covers, and soils in the various subbasins repond to fairly similar climate changes.

Overall, by end of century, temperatures are projected to increase by about +4ºF to +9ºF with large warming in response to greater greenhouse-gas emissions (RCP8.5; Figure E.1a), as also in the California Fourth Climate Change Assessment Sierra Nevada Region Report (2018). Annual precipitation totals are on average projected to increase (in the ensemble of climate models evaluated here) by about 0 to 15%, depending on emissions (Figure E.4). However, these

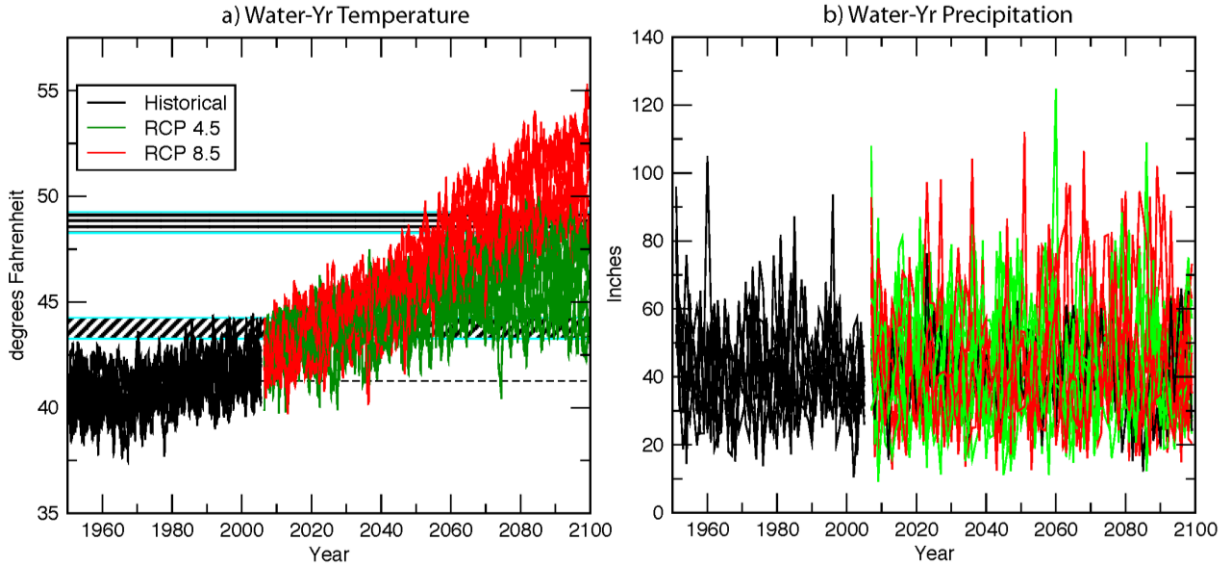

Figure E.1. Ensemble of projected changes in (a) air temperatures and (b) precipitation totals, over the Upper Truckee River subbasin, as an example of the changes projected by eight climate models downscaled and run through the basin PRMS model. RCP 4.5 greenhouse-gas emissions are less than RCP 8.5 emissions, especially after mid 21st Century. Hachured horizontal bars in (a) indicate warming of 2-3ºF and 7-8F warmer than the 1971-2000 historical norm (dashed line).

ensemble-average precipitation changes differ considerably from climate model to climate model, and are small compared to the range of historical year-to-year precipitation variations, indicating that the long-term annual-precipitation changes will very likely be well within the large range of historical variations that we already are used to. Thus the projection that precipitation will increase overall ends up being the least confident projection by this study.

On the other hand, precipitation extremes, like annual maximum 1- and 3-day precipitation totals, are projected to increase by about 10–25% depending on the future emissions assumed. These increases in precipitation extremes are smaller than the scatter between GCMs, indicating significant agreement among models, making this a reasonably confident projection.

Snowpack Changes

In response to the projected warming, large snowpack declines are to be expected. April 1 snow-water equivalents (SWEs) and annual snowmelt totals (as a simple measure of how much snowpack forms overall) decline substantially in the projections, with the greatest declines in subbasins along the north and east sides of the Lake (Figure E.2). April 1 SWEs all but disappear in the northern and eastern subbasins and decline by about 80% in the rest of the Basin when future emissions are large (RCP8.5). This decline reflects projections of less snowfall and snowpack overall as well as of earlier snowmelt. Snow-season lengths are projected to be a month to more than three months shorter by end of century, depending on location and emissions, and the "center" of snowmelt timing arrives about 20 to 50 days earlier in the year. Precipitation timing is not projected to change much but, mostly because of the warming-induced snowfall and snowmelt changes, the center of streamflow timing is also projected to arrive about 20 to 50 days earlier on average (Figure E.3), in agreement with more coarsely resolved "North Sierra" projections in the California Fourth Assessment Sierra Nevada Region Report (2018) and in most previous studies.

Streamflow Changes

Annual streamflow totals do not decline on long-term average, despite increasing overall evaporative demands (i.e., atmospheric "thirst"). Indeed, flows increase overall (Figure E.4), reflecting a combination of the modest ensemble-average precipitation increases (Figure E.4) and the fact that much more future runoff occurs before the summer upturn in the atmospheric thirst for evaporation and plant transpiration. The largest streamflow increases are projected for the east side of the Lake. Year-to-year streamflow fluctuations also grow (not shown here), resulting in increased episodes of hydrologic whiplash between drought conditions and flood.

Annual streamflow maxima (peak flows) are projected to increase considerably with maximum 3-day flow totals in a few subbasins almost tripling by end of century under the greater RCP8.5 emissions. More typically, peak flows increase by about 30-150% more than their historical averages (right maps in Figure E.5). These large increases in flood flows reflect the more extreme storms (left maps in Figure E.5) but are amplified versions of those precipitation extremes because more high-altitude catchment areas receive rainfall rather than

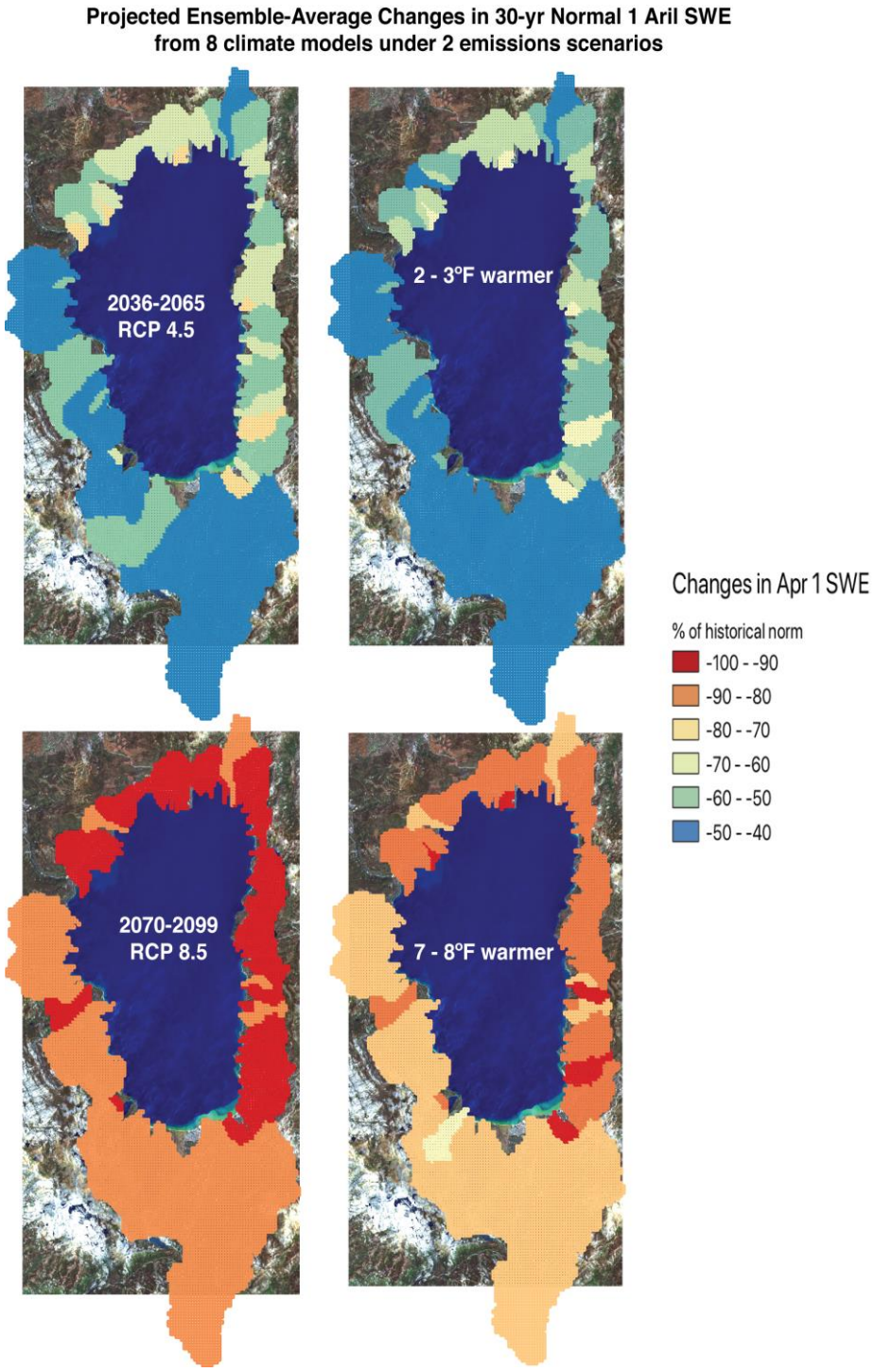

Figure E.2. Ensemble-average declines in 30-yr normal April 1 snow-water equivalents (SWE) over the Tahoe basin, as projected by eight climate models downscaled and run through the basin PRMS model (left) and for nonoverlapping 30-yr segments from the overall ensemble with average warming in the hachured ranges in Figure E-1a (right). Percentage of normal is reported such that "+90%" means the future value is 1.9 times the historical norm.

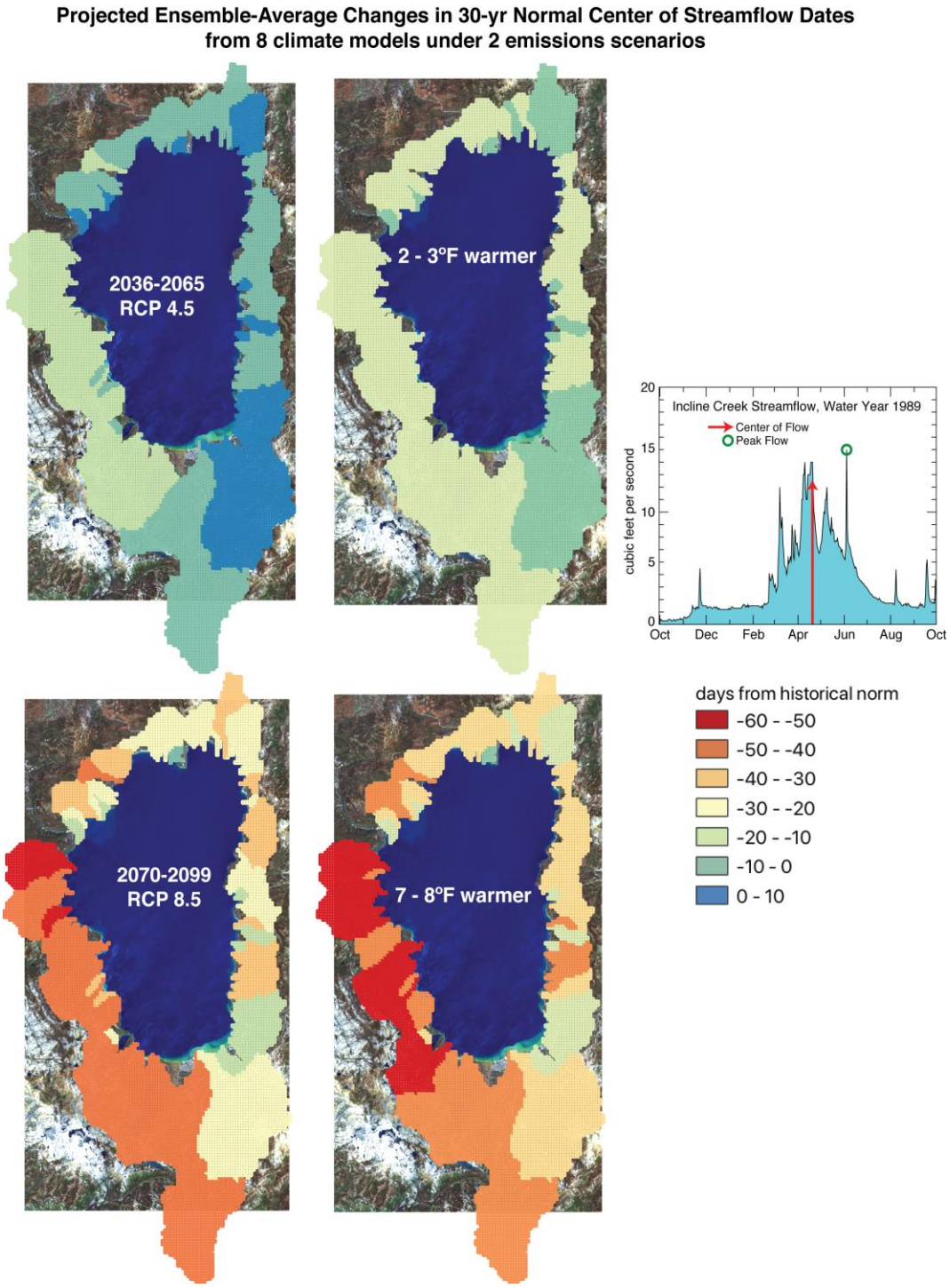

Figure E.3. As in Figure E.2 except for "center of streamflow" timing changes (see inset for example comparison of center of streamflow vs. annual maximum-daily flow timing for observed flows in Incline Creek).

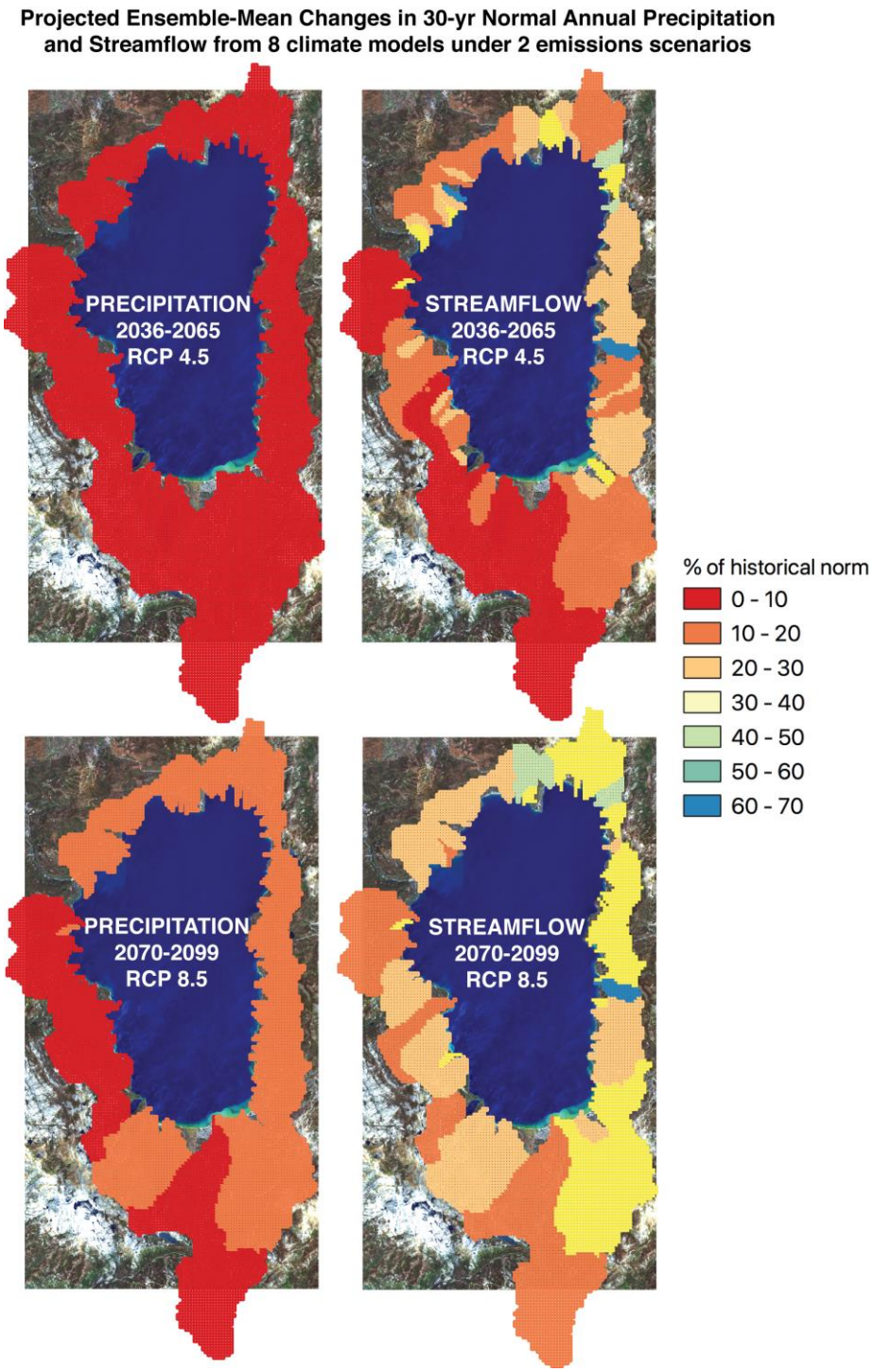

Figure E.4. As in left side of Figure E.2 except for changes in annual precipitation (left) and annual streamflow (right).

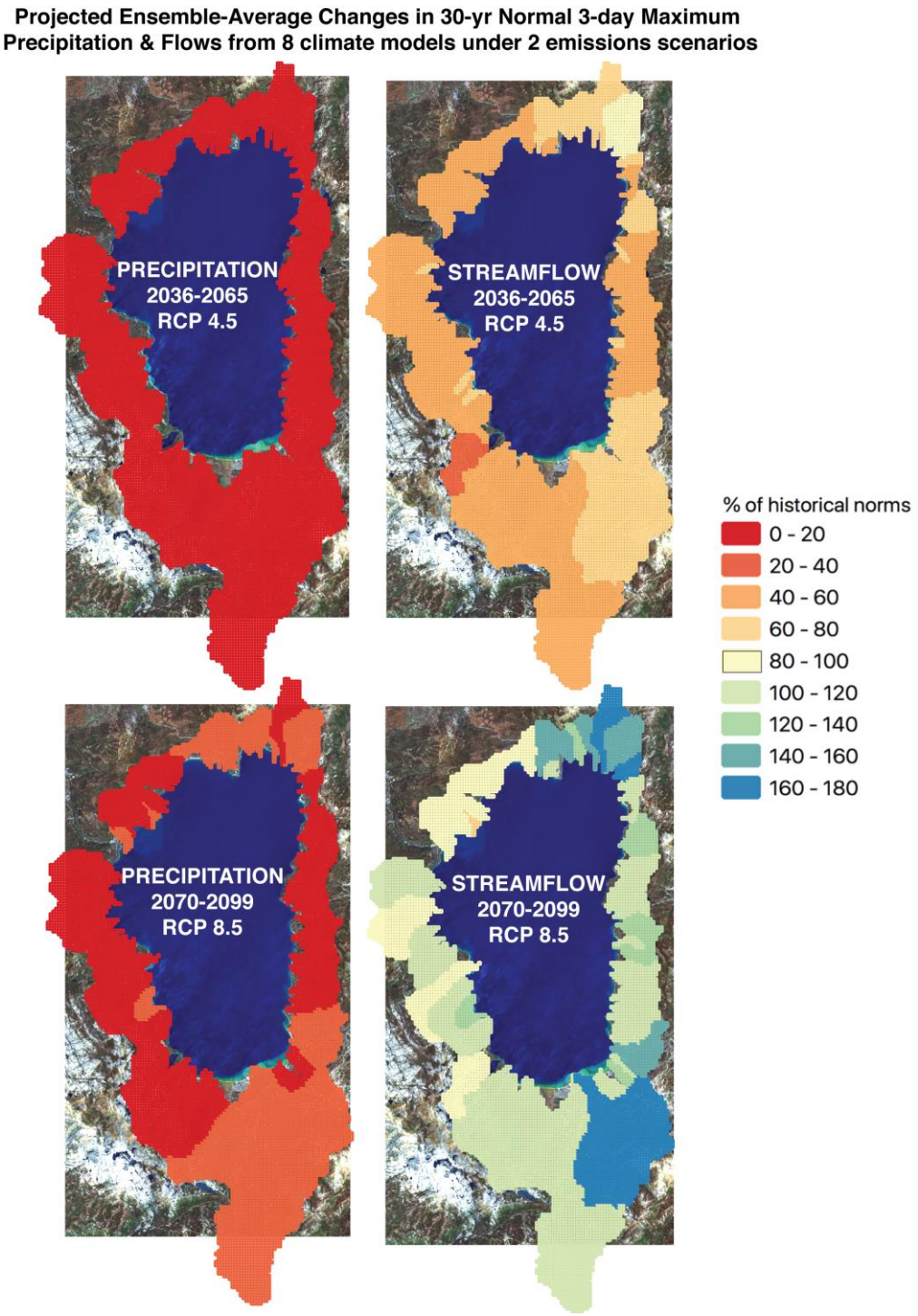

Figure E.5. As in Figure E.4 except for changes in 3-day maximum precipitation (left) and streamflow (right).

snowfall in the warmer future storms. These projected increases mean that more flow will enter the Lake at higher rates in shorter periods of time; that is, inflows to the Lake will be concentrated into shorter, more intense bursts overall, potentially challenging some sediment- and nutrient-inflow management efforts, all other things being equal.

Hot Spots and Refuges

Each of the subbasins responds to climate changes in its own way, reflecting distinctive elevations, aspects, distances from the main ridgeline of the Sierra Nevada and thus precipitation regimes, forest patterns, and so on. Subbasin responses differ in terms of their changes in snowpacks, streamflow totals, and flood regimes. For planning purposes, it will be useful to be able to distinguish which subbasins are more vulnerable overall to climate change and which are less so. Such distinctions could provide a basis for deciding where to invest to hold the line against future changes ("hot spots"), versus areas where relatively muted future changes might provide some refuge against the worst climate-change impacts.

An example of such a "hot spot versus refuge" mapping is shown in Figure E.6, where projected percentage and day-of-year changes (e.g., from Figures E.4 and E.2) at each of the 60 subbasins were ranked separately for each of 10 measures of climate-change reponse. Then at each subbasin the 10 ranks were averaged to distinguish the overall most-responsive subbasins from less-responsive subbasins.

Overall, subbasins on the north and east sides of the Basin respond more than the west and south sides. At a finer scale, for this 30-yr period and the higher emissions scenario, Trout Creek in the southeast corner of the Basin, and Mill Creek in the Incline Village area, are subbasins that are most impacted on average and might be examples of hot spots for climate change. Eagle and Cascade Creeks near Emerald Bay are projected to be least impacted overall. Results of hot-spot determinations will depend on the particular decades and emissions analyzed, as well as on the particular subset of impacts ranked but, in consultation with agencies of the Basin, hotspot-versus-refuge analyses can add geographic detail to planning and adaptation efforts.

Limitations and Ways Forward

As noted earlier, PRMS model errors were evaluated by comparing historical streamflow simulations to historical observations at nine stream gages around the Basin. The comparisons indicate that the PRMS model used here is capable of simulating streamflows around the Basin under a wide range of historical climatic conditions and during medium to high flows. The comparisons indicated that the model is probably not as capable of providing reliable low-flow projections, and so the present study could not confidently project changes in the low warm-season flows or soil- and fuels-moisture. A more inclusive, well-calibrated, groundwater-surface water model (e.g., the GS-FLOW model) will be needed for reliable projections of future dry seasons.

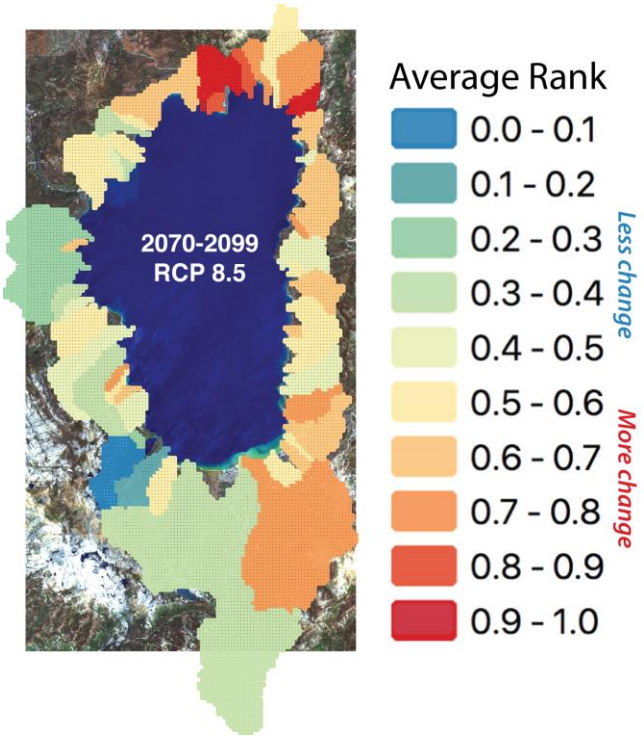

Figure E.6. Overall average of subbasin ranks of projected climate-change impacts in the Tahoe basin by end of 21st Century under RCP8.5 emissions. Measures included in this calculation are the projected changes of (1) annual precipitation, (2) maximum 3-day precipitation totals, (3) April 1 SWE, (4) snow-season length, (5) snowmelt timing, (6) annual snowmelt, (7) annual streamflow, (8) streamflow timing, (9) maximum 3-day streamflow totals, and (10) amount of rainfall on snow. Measure-by-measure, the subbasin responses are ranked from smallest to largest, and then all the ranks for each subbasin are averaged to arrive at a single average ranking for the subbasin. Then those average ranks are rescaled from 0 (subbasin with lowest average rank) to 1 (subbasin with highest average rank).

The simulations summarized here do not include hydrologic effects of forest changes under historical or climate-changed conditions (e.g., from past or future wildfires), but could—in principle--be modified to preliminarily explore such effects, if changes in forest cover were made available for use as externally-provided time-varying conditions that could be imposed in the PRMS model.

A new generation of climate projections will become available in the next year or so for the upcoming California Fifth Climate Change Assessment. If the different generations of climate-change projections that have emerged for use in assessments since about 2000 is our guide, ensemble-average precipitation patterns may be expected to change somewhat and projected warming may increase modestly (as local temperature impacts of snow-cover loss are currently being integrated into the new projections). These changes in projections may modify hydrologic responses but, for the most part, the vulnerabilities emphasized in the present study are likely to remain broadly representative.

THIS PAGE INTENTIONALLY LEFT BLANK

CONTENTS

LIST OF FIGURES

LIST OF ACRONYMS

CCC4A	California's Fourth Climate Change Assessment
CMIP	Coupled Model Intercomparison Project
DRI	Desert Research Institute
DWR	Department of Water Resources
GCM	Global Climate Model
HRU	Hydrologic Response Unit
IPCC	Intergovernmental Panel on Climate Change
LOCA	Localized Constructed Analogs
MACA	Multivariate Adaptive Constructed Analogs
NCA	National Climate Assessments
PRISM	Relationships on Independent Slopes Model
PRMS	Precipitation-Runoff Modeling System
ROS	Rain-On-Snow
SWE	Snow-Water Equivalents
TCAAP	Tahoe Climate Adaptation Action Plan
USGS	U.S. Geological Survey

1. INTRODUCTION

Climate change is already impacting the Lake Tahoe Basin, and the Sierra Nevada more broadly, with much more change to come (e.g., Coats *et al.*, 2013). In response, agencies and communities throughout the Basin are developing plans and actions to enhance their capacity to adapt to climate change. The Tahoe Climate Adaptation Action Plan (TCAAP; https://tahoe.ca.gov/programs/climate-change/) is a primary example, convening and developing information resources and strategic community-based planning to accelerate resource management, infrastructure, and economy adaptations to climate change. An early step in the TCAAP was development of an integrated vulnerability assessment (https://tahoe.ca.gov/wp-content/uploads/sites/257/2020/04/Integrated-Vulnerability-Assessment-of-Climate-Change-in-the-Lake-Tahoe-Basin_2020.pdf) to provide residents, visitors, businesses, and public agencies with state-of-the-science information on how temperature and precipitation will change, and how these patterns will affect aspects of the Tahoe environment that people care about. However, the spatial resolution of climate projections available at that time was relatively coarse. For the landscape and community-scale planning being undertaken as part of TCAAP, more highly resolved spatial projections of climate change and, especially, its impacts would be desirable.

The TCAAP vulnerability assessment was based on scientific projections of how climate will change in the Basin and where and how those changes will be impactful. A key resource for that assessment was projections of temperature and precipitation changes in coming decades, and simulations of hydrologic responses to those climate changes, made available as part of California's Fourth Climate Change Assessment (CCC4A; https://Cal-Adapt.org). The CCC4A projections were formulated and provided on a 1/16º latitude-longitude (roughly 4 mile) spatial grid over California (and Nevada), which was a resolution suitable for the state- and regional-scale assessment activities undertaken by that assessment. These grid cells amount to about 14 square miles—9000 acres--each. At this resolution, the entire Tahoe Basin is represented by parts of about 36 grid cells, which provided the Vulnerability Assessment with information to digest and interpret at the basin scale. However, to put this resolution into a more local context, Blackwood Creek above Lake Tahoe drains 11 square miles; Incline Creek, 7 square miles; and the large Upper Truckee drainage above South Lake Tahoe is 55 square miles. The City of South Lake Tahoe (CA) encompasses 17 square miles, and Incline Village (NV) about 22 square miles. Thus Blackwood and Incline Creeks, and South Lake and Incline Village, are each represented by one or two grid cells (if the grid was perfectly placed and oriented for each basin and city, which it is not). The Upper Truckee drainage might be described by 4 grid cells in total. Figure 1.1 illustrates how this grid looks over the Tahoe Basin. All the climate variations and differences, and all of the hydrologic processes and responses, are simulated in terms of these few grid cells. The projections provided information at the scale of the Basin as a whole and a few patterns across this domain. A limitation of this data set is that the grid cells routinely encompass both sides of the surrounding mountain ridges, extending both inside and outside of the Basin, so that important properties like aspect (which time of day a slope receives most of its sunshine and for how long) and elevation ranges are not restricted to just the catchments that drain into the Tahoe Basin.

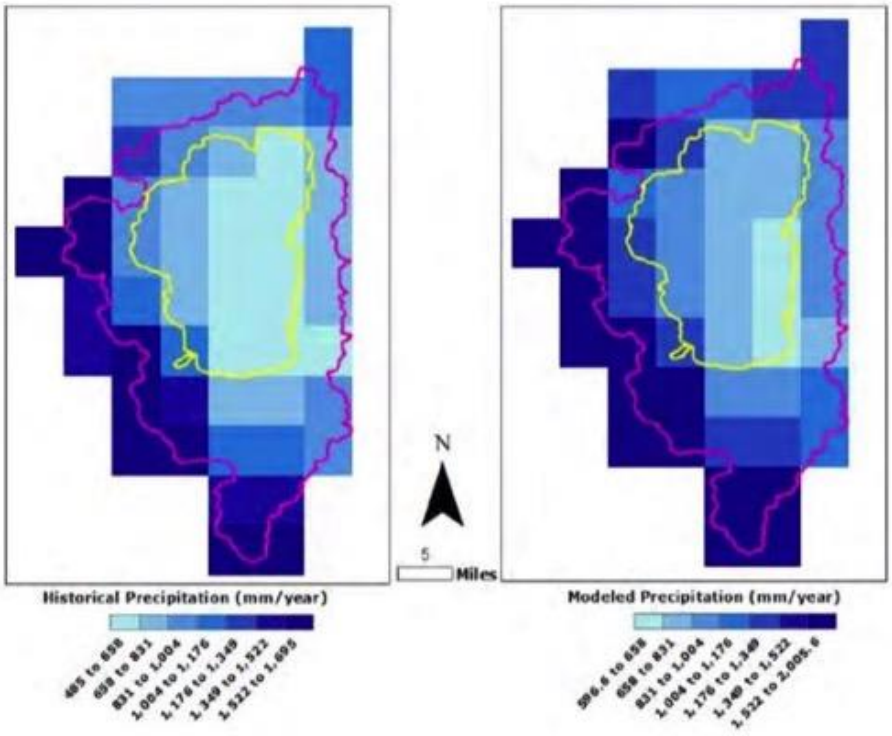

Figure 1.1. Example of simulated precipitation patterns from climate-change scenarios on the 1/16º-resolution grid provided by the CCC4A and used for the TCAAP Vulnerability Assessment (2020), where this figure is described as "comparison of mean historical precipitation (1950-2005) and modeled future precipitation under RCP8.5 (2070-2099)"—the RCP8.5 terminology will be explained later in this report.

For more than a decade, studies at the Desert Research Institute (often in collaboration with the U.S. Geological Survey) have been developing and calibrating a collection of hydrologic models of the catchments, river basins, and groundwater systems that encircle Lake Tahoe. The available models are either based on the USGS's Precipitation-Runoff (surface-water) Modeling System (PRMS) or their GS-FLOW groundwater-surface water flow-modeling system (which combines the USGS's MODFLOW groundwater-flow model with the PRMS model). The entirety of the Basin is now well represented by the PRMS model, which has been used to simulate hydrologic responses to most of the same climate-change projections as used in the CCC4A; in particular, this PRMS model was used in the DRI-led Water for the Seasons project in 2018-2020 (Erkman *et al.*, 2020). The quality of performance of the GS-FLOW model of the Tahoe Basin is less certain, for a variety of reasons, most particularly because much less observational data is available to characterize (calibrate) groundwater patterns and fluctuations in the complex terrain of the Basin.

The PRMS model of the Basin has the advantage over the CCC4A simulations in that it simulates hydrologic processes and climate-change responses on the basis of variations in land-surface features (e.g., soils, vegetation, topography) at a highly resolved 300 meter scale

(yielding 1/29 square mile grid cells). The CCC4A hydrologic-response simulations used in the TCAAP vulnerability assessment were derived from the Variable Infiltration Capacity macroscale hydrologic model (Liang *et al.,* 1994) on the same 14-square-mile grid as the climate projections themselves.

Simulation results from the PRMS model are typically output for the Basin as a whole, or for each of 60 subbasins individually that together comprise the Tahoe Basin and represent all the various streams that flow into the Lake. However, when warranted, the PRMS outputs can be provided for each of the original 300-m grid cells. (For comparison to the CCC4A resolution described earlier, at this PRMS resolution the Blackwood Creek drainage is represented by over 300 grid cells, and South Lake Tahoe encompasses 500 cells.) Figure 1.2—in comparison to Figure 1.1—provides a sense of the additional resolution that the PRMS and GS-FLOW models provide (although the two figures are mapping different quantities). With this resolution, spatial differences in hydrologic conditions and responses can be identified and visualized from between individual subbasins, along subbasin and stream channel axes, and across elevation zones. Similarly, simulated responses could be evaluated within all manner of jurisdictional boundaries in the Tahoe Basin (not shown).

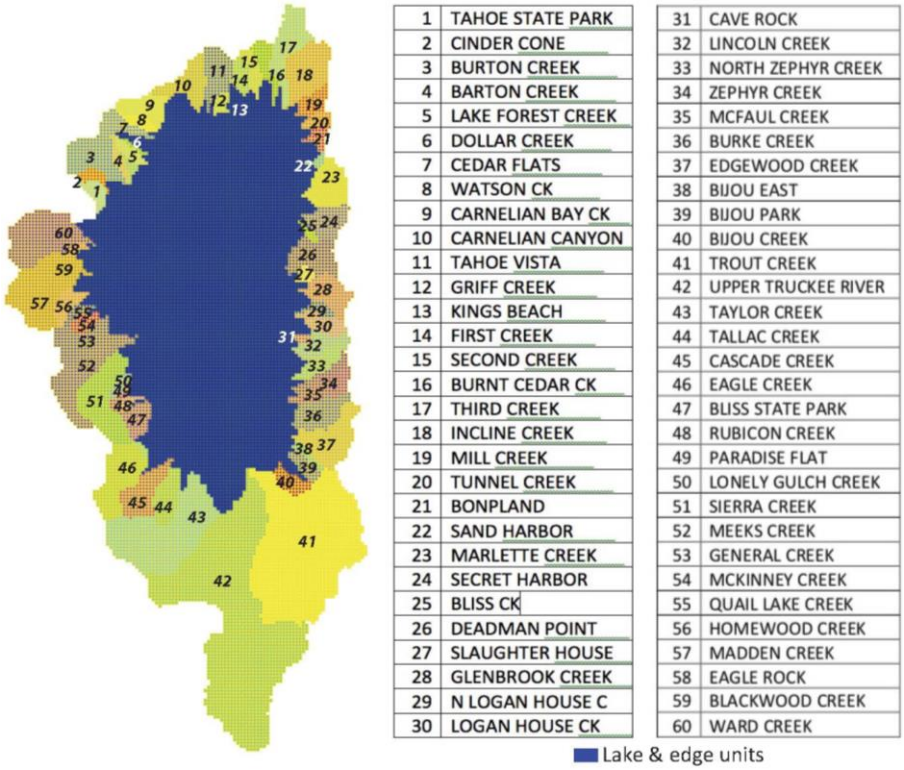

Figure 1.2. PRMS model subbasins, with indications of grid cells comprising the subbasins, for the Lake Tahoe Basin. Subbasins are randomly colored; note pattern and scale of 300-m grid cells that are most visible around subbasins 52, 53, and 28.

This study applies a collection (ensemble) of eight models used for climate-change projections during the CCC4A era to the PRMS model of the Tahoe Basin, and revisits some of the responses discussed in the TCAAP Vulnerability Assessment in greater spatial detail. This higher resolution allows the present study to evaluate the PRMS model's accuracy in historical simulations on a subbasin-by-subbasin basis as well as in terms of specific aspects of subbasin snow and flow characteristics. This allowed propoer focus to be placed on the modeled climate-change impacts that are most likely to be accurately projected. The CCC4A projections were too coarsely resolved to allow such model validations. The higher resolution of the PRMS model also allows the hydrologic responses of individual subbasins to be compared, which provides a basis for delineation of areas within the basin that are likely to be most impacted by climate change, versus subbasins that are likely to be less impacted, in terms of specific kinds of climate-change impacts (e.g., flow amounts, flow timing, and so on) as well as in aggregate for many different kinds of impacts, which permits potential climate-change "hot spots" and "refuges" within the Basin to be identified.

The following sections of this report describe the various models and methods used to simulate and analyze the hydrologic responses to projected climate changes in the Tahoe Basin (section 2), followed by a detailed appraisal of how well the models combine to reproduce historical hydrologic variations in the Basin (section 3), which provides a basis for deciding which simulated responses merit attention here. Section 4 then describes the climate changes projected for the Basin, and section 5 presents the simulated hydrologic responses to climate changes projected by midcentury and end of century. Chapter 6 presents an alternative way of evaluating the projections, based on summaries of the hydrologic responses to 30-yr periods by which Basin temperatures have risen by 2-3º, 4.5-5.5º, and 7-8ºF in a given climate model-emissions scenario combination, rather than depending on pre-set future time periods across all projections. Chapter 7 discusses results, limitations, and identifies the subbasins that are simulated to be most vulnerable to climate changes versus those that are least vulnerable.

2. MODELS AND METHODS

2.1. MODELS

A combination of three sets of models are connected in tandem to generate the hydrologic projections presented here: (1) Outputs from an ensemble of eight different global climate models, which are (2) downscaled by a statistical method called Local Constructed Analogs with Multivariate Adaptive Constructed Analogs, and used as inputs to (3) a surface-water hydrologic model called the Precipitation Runoff Modeling System (PRMS). This section is organized such that the PRMS model, the climate models, and the downscaling methods are discussed in turn.

Precipitation-Runoff Modeling System

Hydrologic responses in the Lake Tahoe Basin to projected climate changes are simulated here by application of a large, multi-subbasin model of land-surface and shallow subsurface hydroclimate and hydrologic processes using the Precipitation-Runoff Modeling System (PRMS) as applied over a 300-m resolution plan-view grid aggregated to 60 subbasins that together represent the runoff-generating parts of the Basin. PRMS is a physically based, deterministic, distributed-parameter model designed to simulate precipitation and snowmelt runoff as well as alpine snowpack accumulation and snowmelt processes. It was designed to evaluate streamflow and general watershed responses to various combinations of climate and land use by the U.S. Geologic Survey (Leavesley *et al.*, 1983; Markstrom *et al.*, 2008). The PRMS model as applied to the Tahoe Basin was developed by the Desert Research Institute (DRI) and U.S. Geological Survey over the past couple of decades. An early set of PRMS models for the Basin was developed by the USGS (Jeton, 1999) and a modern version was begun with work near Incline Village by Huntington and Niswonger (2012) using the USGS surface- and groundwater flow modeling system (GS-FLOW, Markstrom *et al.*, 2008), which includes PRMS. The version applied here (PRMS 5.0.6007, 2013-09-27) was developed and used subsequently as part of the USBR Truckee Basin Study (2015). This model uses daily temperature and precipitation data as inputs to simulate Basin hydrologic variations and responses, for various historical, projected, and hypothetical conditions.

In PRMS the spatial variations of land characteristics that affect snowpack, evapotranspiration, soil-moisture recharge-storage-discharge, and ultimately the runoff within and from watersheds are accounted for in terms of disaggregation of modeled areas into parcels known as hydrologic response units (HRU's). HRU's are characterized by the physiographic properties that determine their hydrologic responses, including altitudes, slopes, aspects, vegetation, soil properties, and climate. These properties are represented as being uniform within each HRU but differ from HRU to HRU. In the Tahoe Basin PRMS model, each 300-m grid cell (Figure 1.2) is defined to be a separate HRU. The weighted-sum of daily hydrologic stores and fluxes from all HRU’s within a given basin or subbasin is the simulated basin or subbasin’s overall hydrologic responses. Processes represented in the PRMS simulations include all those indicated in Figure 2.1 above the capillary fringe, with streamflow (one of the more important outputs) being the sum of surface runoff (overland flow), and deep and shallow subsurface runoffs (interflows and shallow components of base flow). The snowpack (not shown in Figure 2.1) is represented by two layers, an upper boundary a few inches thick and the rest of the pack. Snow accumulation depends on the form of precipitation (snowfall vs rainfall) which in turn depends on air temperatures during the day in question. Snowmelt also depends on air temperatures, as well as on day of year (to represent length of daylight considerations) and a simple representation of the internal temperature of the snowpack.

Changes in moisture in each HRU are represented as flows to, through, and from a series of conceptual reservoirs, as illustrated schematically by Figure 2.2. The soil column is depicted

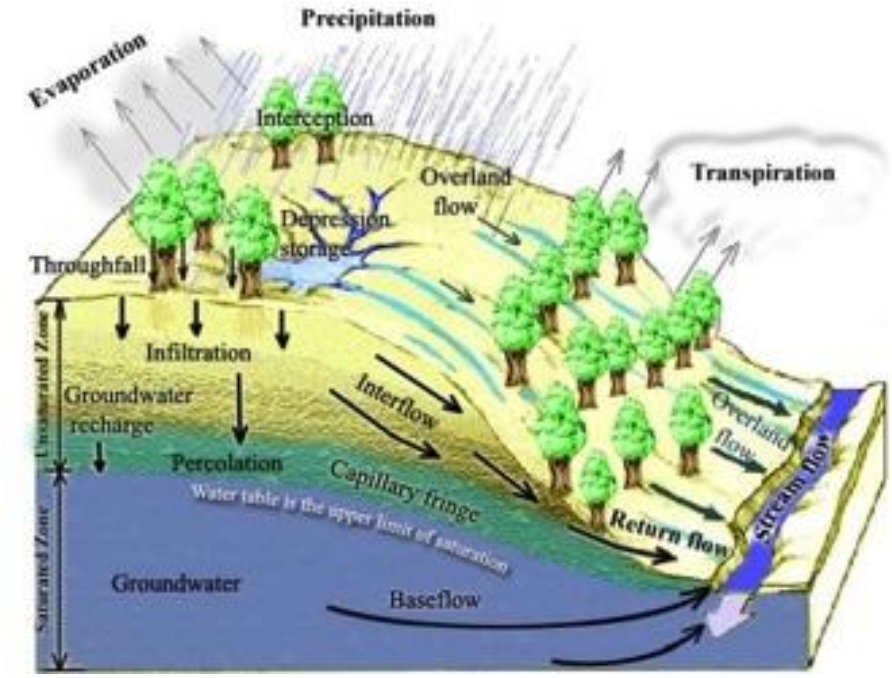

Figure 2.1. Conceptual depiction of hydrologic processes simulated by the Precipitation-Runoff Modeling System (PRMS). In the PRMS as applied in this study, return flows, capillary fringe, groundwater storage and flows are not included. Source: Tarboton (2003).

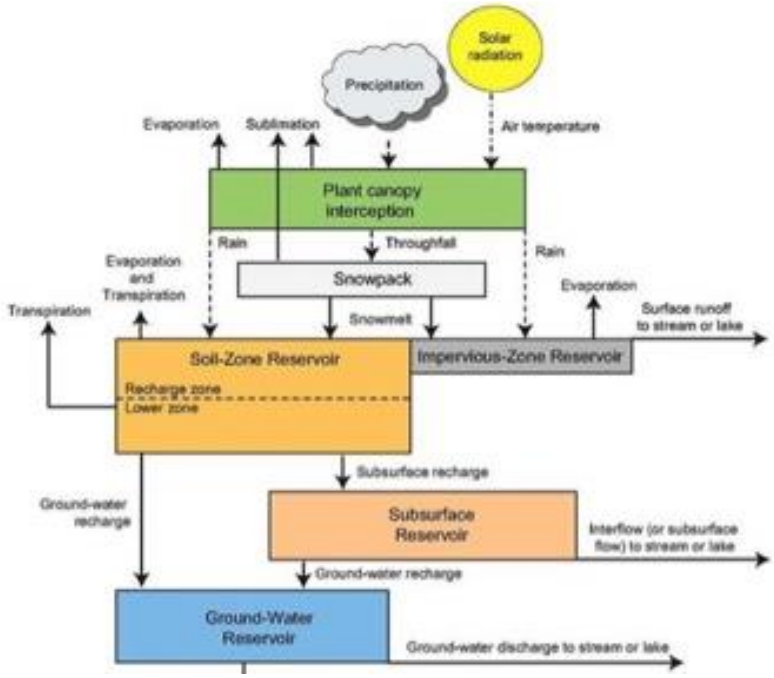

Figure 2.2. Schematic of the Precipitation-Runoff Modeling System (PRMS). In the PRMS as applied in this study, solar radiation is not included as a direct input. Modified from: Leavesley *et al.* (1983) and Markstrom *et al.* (2008).

by three different depth-zone reservoirs, of increasing depth and slowness of response. In the present study, characteristics of air temperatures, precipitation, snowpack, and streamflow (the aggregated daily total runoff rates) will be evaluated under climate change conditions projected by eight different global climate models under two different greenhouse-gas emissions scenarios.

The PRMS models of the Basin were calibrated using historical periods of daily meteorological and streamflow measurements. Section 3 of this report will show and discuss how well historical hydrology is simulated when the PRMS model is forced by a 30-year historical record of Basin meteorology and by historical-period climate simulations from eight climate models. Other details of the structure and development of the Tahoe Basin PRMS model (as part of a larger set of 2015 USBR Truckee Basin models) are described Erkman *et al.* (2020).

Climate Models

For the purposes of the present study, daily-level projections of historical and future climates are needed as inputs for the PRMS hydrologic model. A general-circulation, global-climate model (GCM; Figure 2.3) can be used to generate simulated climate variables and variations that can then be input to hydrology models to simulate climate-change responses of snowpacks and streamflow for use in hydrologic-change assessments. These GCMs (in their modern formulations) are numerical representations of the governing equations and climate processes that dictate coupled atmospheric, oceanic, cryospheric, and terrestrial aspects of climate variation and change on time scales from hours to centuries, and over the entire globe. They simulate heat, energy, water, and momentum balances and fluxes in the atmosphere and oceans. They simulate precipitation, radiation fluxes, winds and currents, as well as snow and ice, vegetation and land cover processes, and more, to achieve realistic representations and "realizations" of weather, oceanography, and climate on land and seas.

Because the global climate is a complex, chaotic dynamic system (Ghil and Childress 1987), and given that GCMs are moderately comprehensive representations thereof, climate simulations are as subject to the "butterfly effect" or "sensitive dependence on initial conditions" as is the real-world climate system (Lorenz 1963). As a consequence, any two simulations, even by the exact same GCM starting from extremely (but not exactly) similar initial conditions will yield different climate variations after just a few weeks. This is not a limitation of the models but a feature of the real world that any acceptable model will share. Despite these day-to-day and even year-to-year differences between climate predictions longer than about monthly time frames—which are due to sensitive responses to the precise initial conditions from which simulations are started—the longer term responses (often in the form of climate-change trends) to long-term changes in greenhouse-gas concentrations are generally more or less the same in multiple projections by the same model responding to the same concentrations. But different GCMs do tend to differ in their sensitivity to the greenhouse gases in (generally) subtle ways that can yield different amounts of warming and heat trapped as the decades pass in the 21st Century. And we have little or no way to decide exactly which of the GCMs is going to prove most correct in the future. Together these differences, chaotic fluctuations, and different sensitivities

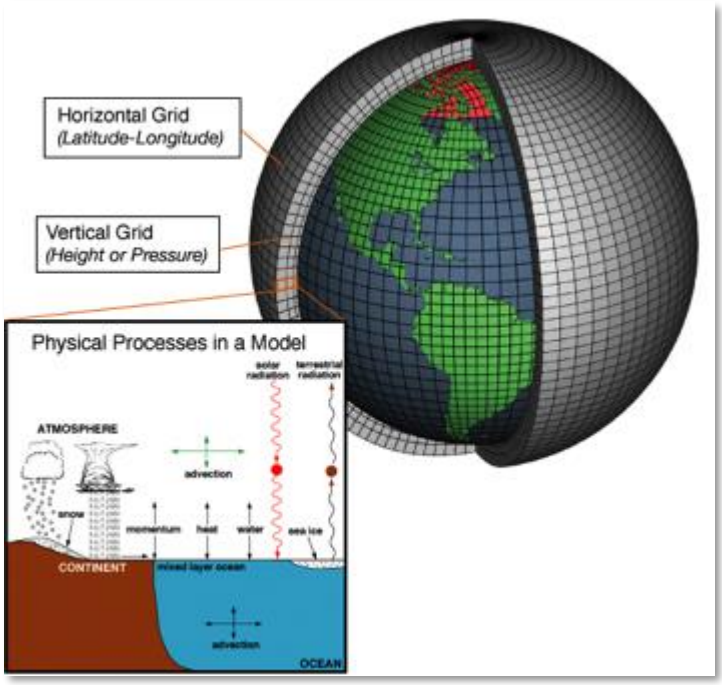

Figure 2.3. Conceptual diagram depicting the coverage and resolution of atmospheric parts of general-circulation models, with an inset listing just a few of the physical processes that are simulated at these scales.

mean that the best way to interpret climate-change projections is to consider a number of different projections from a number of different models responding to a range of possible future greenhouse conditions (e.g., Christensen and Lettenmaier 2007). Comparing these results allows us to identify what changes are shared by the various projections to what extent, and how much those projections diverge (or not) from the range of natural climate variations in the historical period (mostly from before climate change was much of a concern). This study will pursue that strategy, as do almost all modern climate-change assessments.

Several generations of GCMs, with new or evolving GCMs appearing in each generation, have been used by the United Nations Intergovernmental Panel on Climate Change (IPCC) for its regular IPCC Assessments since the early 2000s, with outputs that have been archived by the Coupled Model Intercomparison Project (CMIP; https://pcmdi.llnl.gov/index.html; Touze-Peiffer 2020) at Lawrence Livermore Laboratory. A representative subset of projections from 8 GCMs from the 5th IPCC Assessment and archived by the 5th CMIP (CMIP5, ca. 2013) were used in the Water for the Seasons project (which laid the groundwork for the present study), due to constraints on time and availability. Projections by these models responding to two greenhouse-gas emissions scenarios (to be discussed in section 5.1) form a 16-member ensemble (8 GCMs x 2 emissions scenarios) that will be used here to explore the range, unanimity, and character of climate changes, and hydrologic responses, that might be expected to affect the Tahoe Basin during the 150 years between 1950 and 2099.

Six of the eight GCMs used by the Water for the Seasons study were members of a group of 10 GCMs that the California Department of Water Resources (DWR) determined, through a technical-advisory group study, to provide the best CMIP5-era simulations of the historical-era climate based on a selection of global, regional, and California-centered climate statistics (Figure 2.4). The study (California DWR CCTAG, 2015) started with 31 CMIP5 GCMs and scored them according to their abilities to reproduce these metrics in agreement with historical observations. The objective was to cull the worst performers, rather than to identify the "best" model. There are sufficient differences between GCMs and their projections, and no one knows which one is going to prove to be most accurate as the century progresses, so that no single GCM can be trusted, nor expected, to yield the "best" projections. Thus (a) the target of this analysis was to identify a manageable number of "good" GCMs that could be used in CCC4A studies, and (b) a sufficient number of models were needed so that a reasonably full range of possible futures would be available to provide some sense of uncertainties and ranges of possibilities. Evaluation of a global round of metrics led to rejection of 12 GCMs as being less globally skillful. The regional round of model culling removed four additional GCMs. The remaining 15 GCMs were evaluated with statistics considered locally relevant to the California climate and water resources to arrive at a final 10 GCMs. (However, the senior author here was part of this analysis and can report that the final number of models "retained" (10) was more a result of negotiation with DWR—based on their perception of how many scenarios they could handle with their available computational resources— rather than reflecting any notable "break" between the skills of the models above and below the 10-model threshold that was settled on).

In choosing GCMs for the Water for the Seasons study, only some of the GCMs included all the data that was necessary to meet their study demands for the best possible estimates of evaporation from Lake Tahoe. This objective required projections of humidity, winds, and solar radiation, in addition to the temperatures and precipitation rates that the present study will focus on. From the final 10 GCMs chosen by California, four models did not provide the required data variables. Two additional GCMs that did provide these additional variables, from among the models that didn't quite make the 10-model threshold negotiated with DWR, were added for development of a reasonably numerous Water for the Seasons climate-change ensemble. In the interests of time and available personnel and resources, the resulting 8-GCM ensemble is used to project and explore hydrologic futures for the Tahoe Basin.

Downscaling

To use GCM projections as input to a model as detailed as the PRMS model of the Lake Tahoe Basin, one additional step called "downscaling" is generally required. The goal of this step is to interpolate results from the very coarse (order of 100 km) GCM spatial grids (e.g., a scale suggested by Figure 2.3) down to spatial scales relevant to the high-resolution representations of the landscape that the PRMS model encompasses. In the present study, GCM projections downscaled onto the same 12-km grid that was used by the TCAAP (and CCC4A) provided the inputs required.

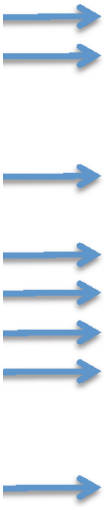

Global Climate Model	Evaluation step where model was removed from consideration. Remaining models are selected for use for California water resources.		
	Global	Regional	California
ACCESS-1.0			
CanESM2			
CCSM4			
CESM1-BGC			
CMCC-CMS			
CNRM-CM5			
GFDL-CM3			
HadGEM2-CC			
HadGEM2-ES			
MIROC5			
BCC-CSM1-1			
CESM1-CAM5			
CMCC-CM			
GFDL-ESM2M			
MPI-ESM-LR			
BNU-ESM			
GFDL-ESM2G			
MRI-CGCM3			
NORESM1-M			
ACCESS-1.3			
BCC-CSM1-1-M			
CSIRO-MK3-6-0			
EC-EARTH			
FGOALS-G2			
INMCM4			
IPSL-CM5A-LR			
IPSL-CM5A-MR			
IPSL-CM5B-LR			
MIROC-ESM			
MIROC-ESM-CHEM			
MPI-ESM-MR			

Figure 2.4. Global climate models evaluated by the California DWR CCTAG (2015) analysis, using performance metrics at three scales (global, regional, and California) with models that were dropped based on various metrics indicated with brown shading, and the 10-model ensemble selected by DWR highlighted in green. GCMs used by the Water for the Seasons study and present study indicated with arrows. (Notice that, in each "scale" category, GCMs are ordered alphabetically, not by relative skill.) Modified from CCTAG (2015).

Figure 2.5 is a cartoon that illustrates the concept of downscaling, and illustrates a particular example of the level of resolution provided by one phase of the downscaling method used here, which is called Multivariate Adaptive Constructed Analogs (MACA; Abatzoglou and Brown, 2012). The cartoon illustrates results when just the constructed-analogs phase (Hidalgo *et al.*, 2008) of the method is applied to GCM projected temperatures for a random day in 2051. This method, developed by John Abatzoglou of UC Merced, is a statistical method that (1) begins by correcting as many initial biases in the GCM simulations (compared to historical observations) so that long-term distributions of the GCM outputs are mimicked by the inputs to the rest of the downscaling process (e.g., Thrasher *et al.*, 2012). Then (2) the corrected GCM outputs are used to develop constructed-analog high-resolution versions of the weather patterns in the coarse-resolution outputs (Figure 2.6), and (3) finally the constructed-analogs versions of the GCM outputs are bias corrected yet again to ensure that, taken as a whole, the high-resolution results are as realistic as possible.

The constructed analogs of step (2) are obtained by statistically finding (through a version of linear regression, least-squares fitting) a set of weights (coefficients) that when applied to the nearest analogs of a given day's (simulated) weather situation found among days in the historical observational record yield a weighted average that is closest to that simulated weather, at the original GCM coarse-scale resolution. Once those coefficients are identified, they

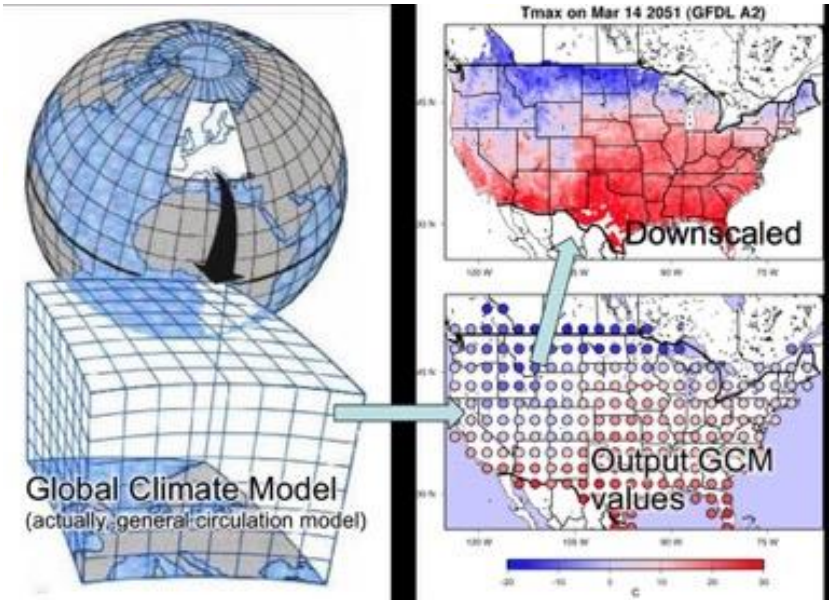

Figure 2.5. Schematic illustrating the central problem requiring "downscaling" before GCM outputs can credibly be input to hydrologic models and local climate-change assessments. Righthand maps illustrate daily maximum temperatures projected by a particular run of the GFDL-CM2 GCM under extreme (A2) greenhouse-gas emissions for March 14 2051, as an example of downscaling from 1-degree latitude-longitude resolution GCM output to the much smaller basin-scale 12-km resolution when downscaled by the original constructed-analogs statistical downscaling method (Dettinger, 2013).

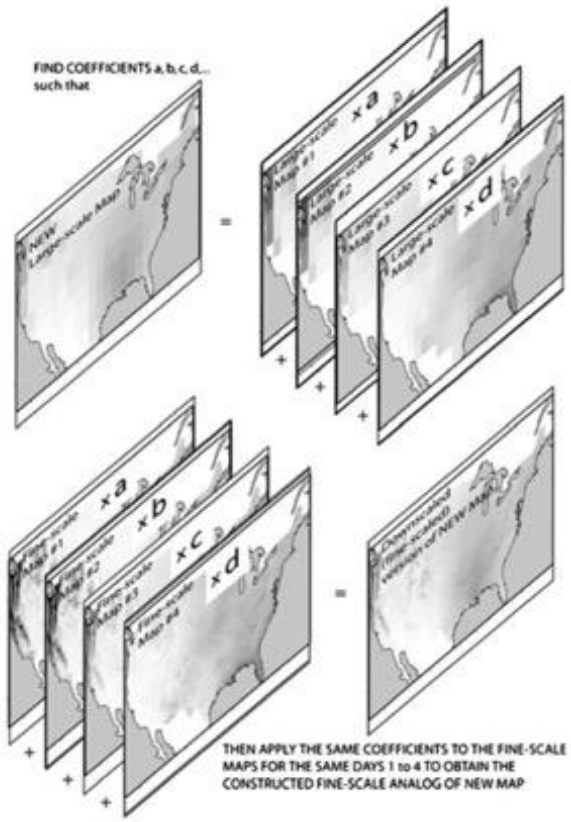

Figure 2.6. Conceptual diagram depicting the core internal process of constructed-analogs downscaling (Dettinger, 2013)

are applied directly to the fine-scale observational record of weather for those same nearest-analog days to obtain a high-resolution 'constructed analog' of the simulated weather. This process is repeated separately for each day in each simulation by each model. In step (2) as applied here, a specialized version of constructed analogs called Localized Constructed Analogs (LOCA; Pierce *et al.*, 2014) is used by MACA, because LOCA is specially designed to reproduce weather extremes that are as realistic as possible. The original constructed-analogs method sketched in Figure 2.6 is related to linear regression--to obtain the coefficients mentioned in that figure—which tends to smooth out extremes because all results are linear mixes of many different days of weather, whereas LOCA is designed to use individual days of weather fitted to various sections of the overall downscaled map to reduce this smoothing and preserve the extremes. By this means, MACA provided statistically downscaled versions of daily GCM outputs on the 12-km grid used by CCC4A and TCAAP.

The PRMS model as configured for the Lake Tahoe Basin uses daily maximum- and minimum-temperatures and daily precipitation at ten weather stations in and around the Basin as its inputs (Figure 2.7). The daily temperatures and precipitation at the MACA (12-km) grid cells containing these stations were extracted for each day, and then those values were used to adjust 300-m-resolution maps of monthly historical 30-yr average (normal) temperature and

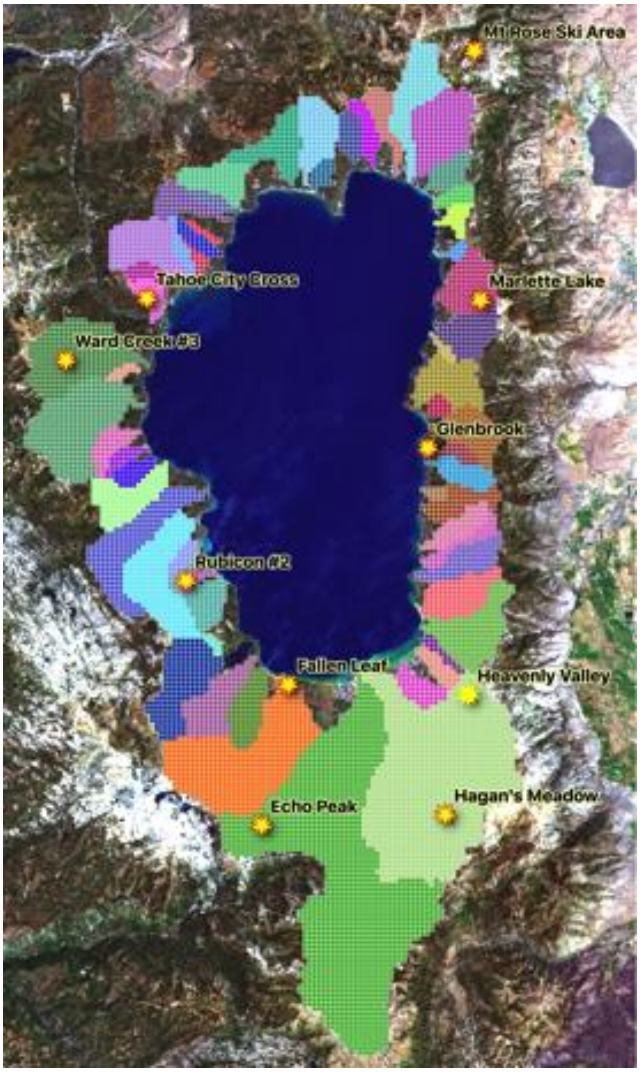

Figure 2.7. PRMS-model subbasins of the Tahoe Basin, as in Figure 1.2, with eleven weather stations used as meteorological inputs indicated with yellow stars, overlain on a real-color representation of data gathered by Landsat 8 on August 11, 2021.

precipitation patterns from the widely-used Parameter-elevation Relationships on Independent Slopes Model (PRISM, Daly *et al.*, 2008; https://prism.oregonstate.edu) to fill in all of the spatial gaps between the ten stations for each day's weather, i.e., to provide individualized inputs for each HRU in the PRMS hydrologic model.

The result is time series of daily temperatures and precipitation for each HRU based on daily historical-era climate simulations from 1950-2005 and for two climate projections, representing two version of future greenhouse-gas concentrations in the atmosphere from 2006-2099, from each of 8 GCMs. These daily meteorological time series are the basis of the hydrologic projections that will be presented and discussed in later sections of this report.

2.2. TAHOE BASIN PROPERTIES

To configure PRMS for a particular basin or subbasin, more than 30 parameters describing land-surface configuration, vegetation cover, soil conditions, and precipitation and temperature conditions need to be specified, and ultimately calibrated, at each HRU (300 m square) of the area modeled. These parameters dictate whether rain or snow (and how much of each) falls on a given area under given meteorological conditions, how much reaches the soil surface, how much sunshine reaches the snow fields, how evapotranspiration is computed, how fast water moves through the subsurface, and many other aspects of the storages and fluxes shown in Figure 2.2.

Figures 2.8 and 2.9 illustrate how just a few of these parameters vary within the Tahoe Basin. Elevations (Figure 2.8) matter because of the climatological tendencies for temperatures to decline with increasing elevation and for precipitation (all other things being equal) to increase with increasing elevation. Some of the highest areas in the Tahoe Basin are along the southeast corner of the Basin, in the Desolation Wilderness area towards the southwest, and in the northernmost reach of the Basin above Incline Village. Broad low areas characterize the Upper Truckee River subbasin extending south of the Lake. Aspects (Figure 2.8) matter because they determine how much sunshine a given area receives which influences evapotranspiration rates and how the snowpack "cold content" (essentially, readiness to melt) evolves as the winter and spring seasons proceed. The eastern edge of the Basin is characterized by west-facing slopes and the western side of the Basin by east-facing slopes. These differences in aspect will affect their relative climate-change sensitivities.

Figure 2.9 shows the distributions of forest-canopy cover and of soil-moisture storage capacity, one of the primary soil properties within the Basin. Canopy density (just one of the parameters used to describe vegetation and cover for hydrologic purposes) influences how much sunshine penetrates to the soil surface, how much snow and rain are intercepted and stored in the trees prior to melting or evaporating, and so on. In the Basin, canopies are densest on the west side of the Basin down near the Lake and at middle elevations, as well above parts of the western Lake shore and at middle elevations in the southernmost Basin. The high, bare-rock expanses of the Desolation Wilderness area in the southwest form the largest contiguous area of very sparse canopy cover. Similarly, soils are thinnest (can hold less soil moisture) in the high bare-rock Desolation area and are thickest along the more heavily forested northwest parts of the Basin, as illustrated in Figure 2.9 (right). The thick soils allow for more subsurface storage of moisture and more of the slower flowpaths for surface and interflow runoff from rainfall and snowmelt to streamflow.

As noted earlier, there are many other parameters and properties that contribute to the simulated hydrologic responses to weather and climate variations, but these few provide a basis for understanding many of the climate-change responses to be reported later in this report.

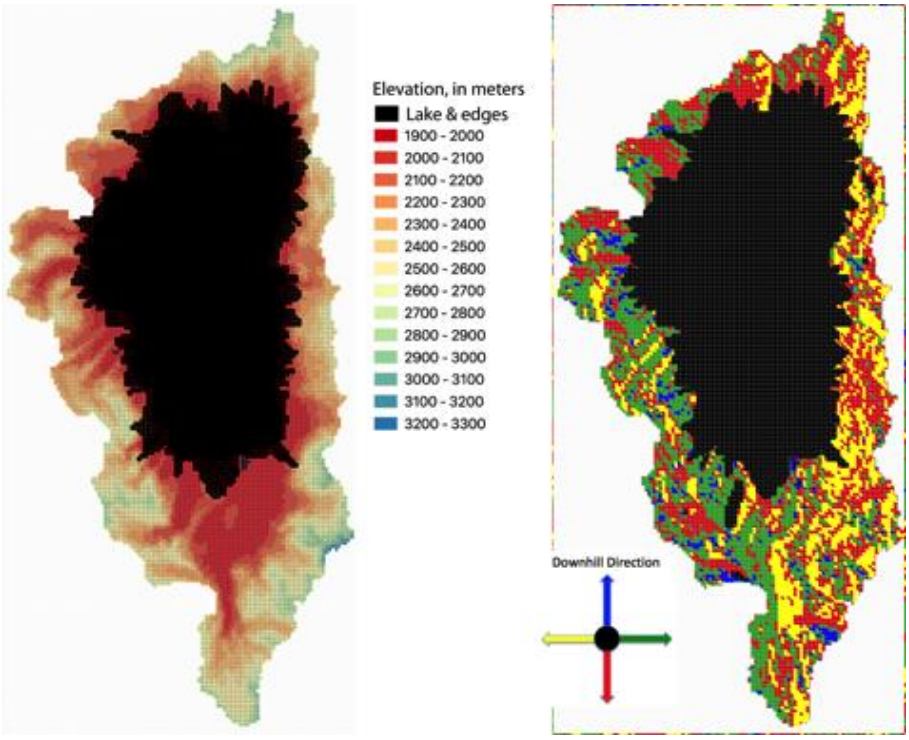

Figure 2.8. Elevations (left) and aspects (right) within the Tahoe Basin on the 300-m grid (of HRUs) that constitute the PRMS model used here.

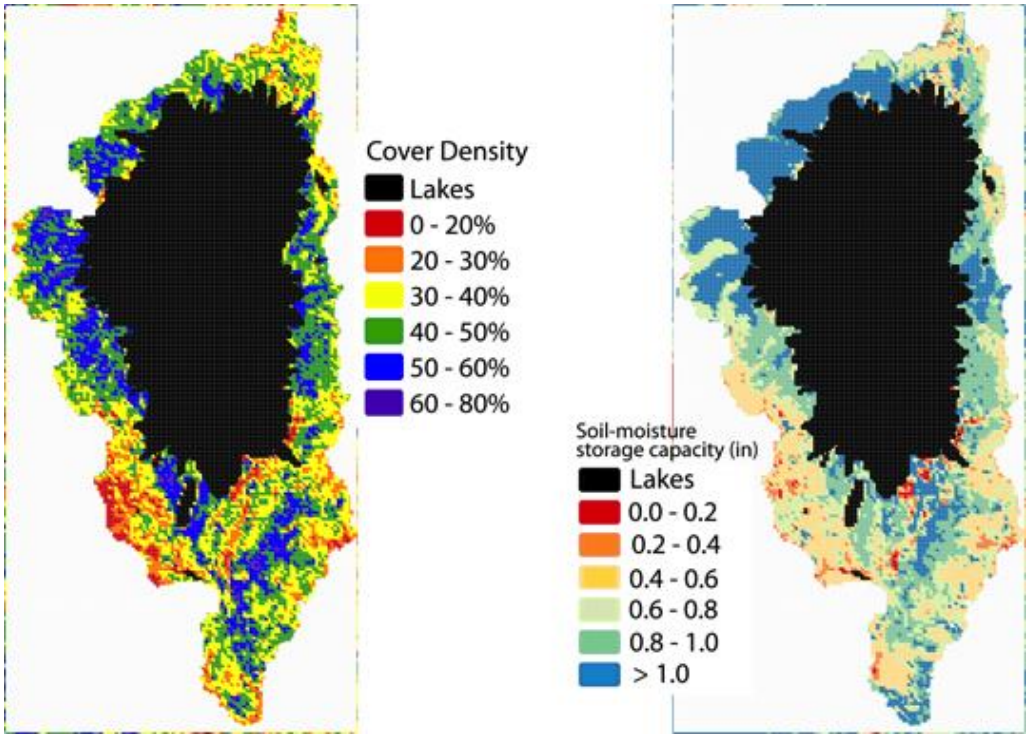

Figure 2.9. Forest-canopy density (left) and soil-moisture storage capacities (right; parameter name: saturated threshold) within the Tahoe Basin on the 300-m grid (of HRUs) that constitute the PRMS model used here.

In addition to the parameters that describe properties that don't change from year to year in the PRMS model, daily temperatures and precipitation totals are input to the model on the same grid. For use in comparisons and interpretations of the subbasin-level hydrologic responses to climate change later in this report, Figure 2.10 shows the 30-yr normal (historical) annual-mean temperatures and precipitation totals at this subbasin scale. The range of annual-mean temperatures within the Basin, at this subbasins scale, it not large historically (Figure 2.10, left), spanning only 40°F to 45°F. The scatter of average temperatures within this range reflects the range of elevations that each subbasin incorporates as well as, secondarily, the distribution of elevations within each subbasin. On the whole, subbasins on the north side of the Lake tend to be somewhat warmer than those elsewhere. Subbasins like Trout, Third, Eagle and Marlette Creeks rise to higher elevations at their upper ends and have cooler subbasin-average temperatures. Subbasins on the west side of the Lake have historically received significantly more precipitation overall than basins on the east side, as storms have tended to "rain out" to a large extent over the western ridgelines, leaving less precipitation to fall into the eastern subbasins.

The PRMS model implementation for the Tahoe Basin is a combination of (a) model equations and routines that have been applied in basins all over the world, with (b) many time-invariant and time-varying inputs specific to the Tahoe Basin. At this point, the most pressing question before turning to climate-change projections is "what can the Tahoe Basin PRMS model simulate well versus what does it fail to capture?"

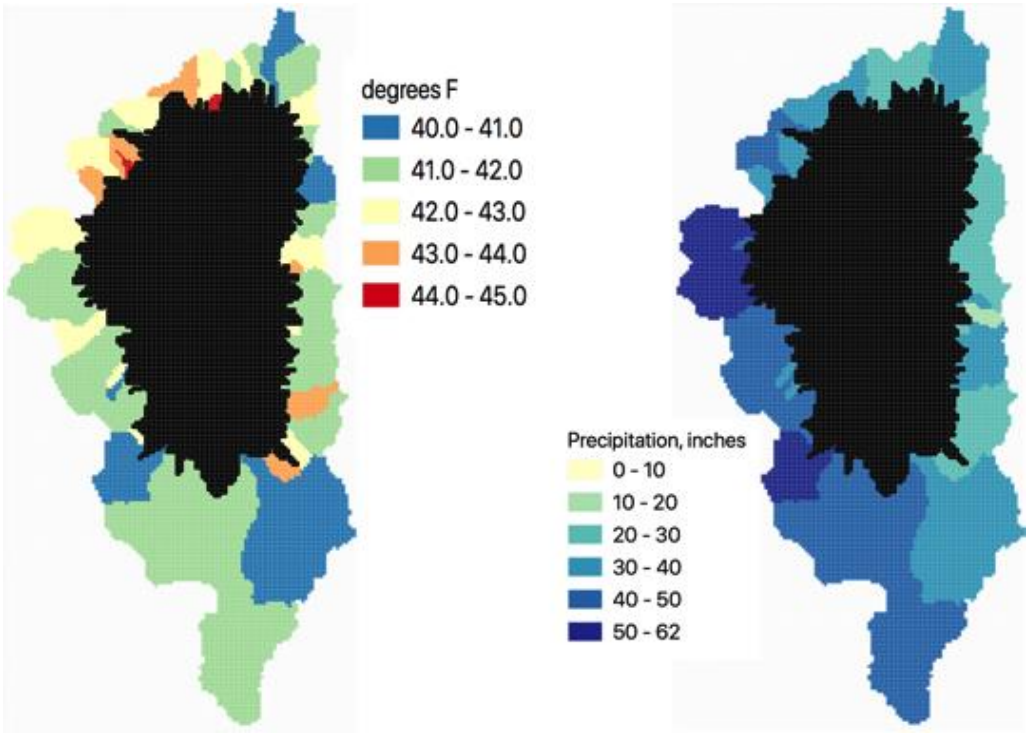

Figure 2.10. Historical normal (30-yr average, 1981-2010) annual temperatures (left) and precipitation (right) within the Tahoe Basin at the scale of PRMS subbasins analyzed in this study.

3. MODEL PERFORMANCE

To evaluate the capacity of this modeling system to predict responses to climate change, its accuracy in reproducing observed historical variations of streamflow and snowpack at available gage sites in the Tahoe Basin must first be evaluated, when the model is forced with observed daily weather variations for the 30 water years between October 1, 1980 and September 30, 2010. This evaluation is indicative of the ability of the hydrologic model to reproduce real-world hydrologic variations on time scales ranging from daily to annual, when it is provided with an observed sequence of daily temperatures and precipitation and its outputs compared to observed snowpack and streamflows. To the extent that the various data and simulations allow, this report focuses on 30-yr averages (or as close as reasonably possible to that averaging length), to mirror the common "normals" used in much meteorology. The particular years averaged over differ in some sections, but are described in each. One consequence of this analytical strategy is that the most extreme events simulated are subject to smoothing, by averaging over 30 yrs and (later, in chapters 4-7) by averaging over the 8 different climate models used here. A variety of time series figures are provided in this and subsequent sections that include simulated annual values from all climate models, separately, wherein the results are not smoothed by this kind of averaging, to provide the reader with a sense of what the rawer simulations look like.

Then the capacity of the model to reproduce the observed distributions of hydrologic responses when forced by climate-model simulated weather variations under the greenhouse-gas conditions that occurred during a similar 30-yr period is evaluated. This second evaluation is indicative of the extent to which the combination of statistically downscaled climate model simulations and projections with the hydrologic model can represent real-world historical hydrologic statistics within the Basin. Notably, the climate-model simulations of weather under historical greenhouse-gas conditions do not reproduce the day-to-day sequencing of weather events, because of the butterfly effect in the global climate system (e.g., Moore *et al.*, 2018). Climate model simulations, unless continually corrected with inputs of observed conditions (as in weather forecast models), are neither expected to, nor able to, follow precisely along with historical day-to-day weather events, and in the future projections no such observed inputs are available. Thus statistical distributions of hydrologic variations, rather than individual hydrologic events, are compared in this second evaluation.

Between these two evaluations, indications of which projected hydrologic responses to projected climate changes are most trustworthy will be garnered. These indications will provide a basis for choosing which hydrologic projections to focus on in later sections of this report.

3.1. COMPARISONS WITH OBSERVED STREAMFLOW VARIATIONS, WATER YEAR 1981-2010

Measured daily streamflow variations from the nine long-term streamflow gaging stations in the Tahoe Basin were obtained and are paired here on a day-to-day basis with a simulation by

the PRMS model forced with corresponding measured daily temperatures and precipitation. The gages measure streamflows in Ward, Third, Incline, Glenbrook, Edgewood, Trout, General, and Blackwood Creeks, and Upper Truckee River, near their outlets to Lake Tahoe.

Simulated and measured streamflows in the Upper Truckee River and Third Creek are compared in Figure 3.1, showing general agreement between timing and fluctuations between 1980-2011. A more complete and direct comparison of day-to-day measured and simulated streamflow rates for each of the nine gages is Figure 3.2, along with gage locations. Notice that, on average (as indicated by the green linear-regression fits), measured and simulated flows closely follow each other (lay close to or on the red one-to-one lines in each graph) for streamflow rates from medium through high flows at all of the gages, excepting perhaps the gage at Edgewood Creek. Correlations between measured and observed flows are a measure of scatter

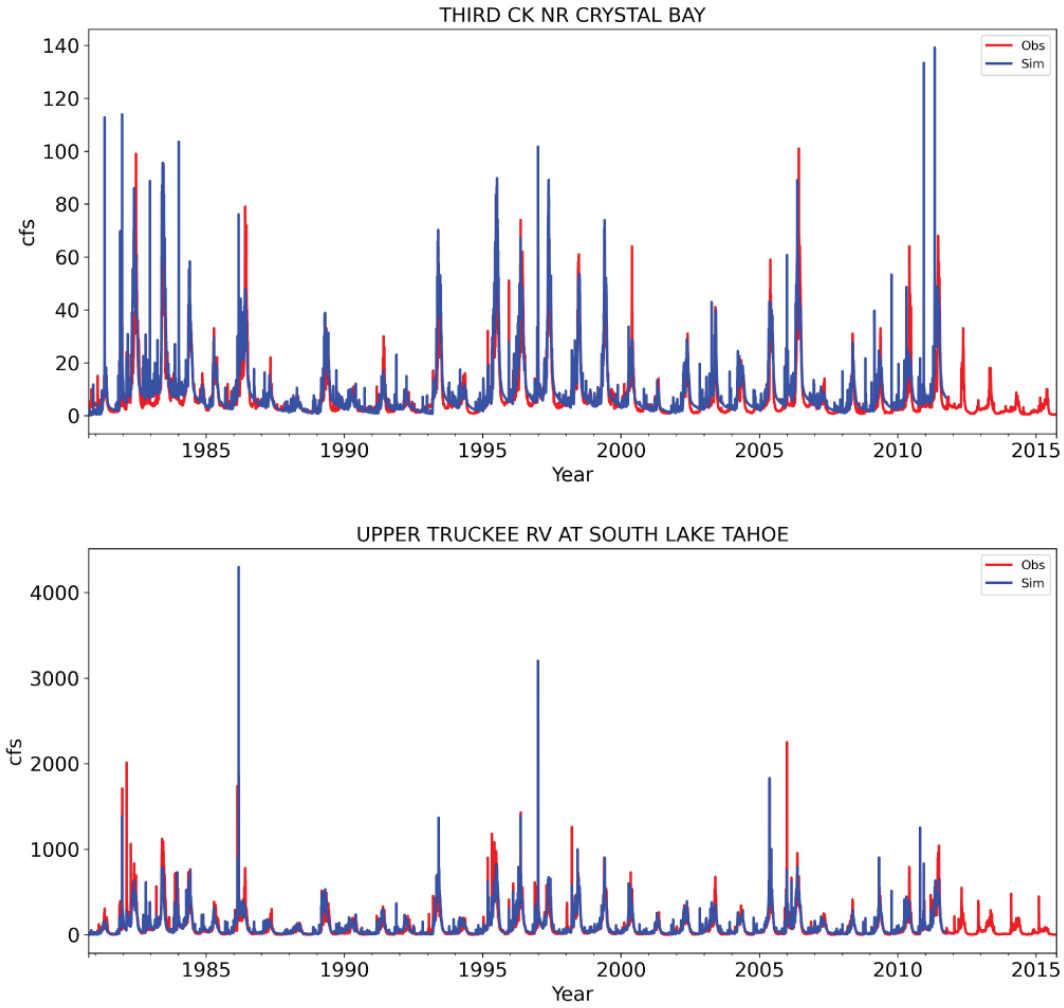

Figure 3.1. Comparisons of daily streamflow rates, water years 1981-2011, from measurements at Third Creek and Upper Truckee River streamflow-gaging stations with streamflow rates simulated by the PRMS model in response to observed daily temperatures and precipitation totals.

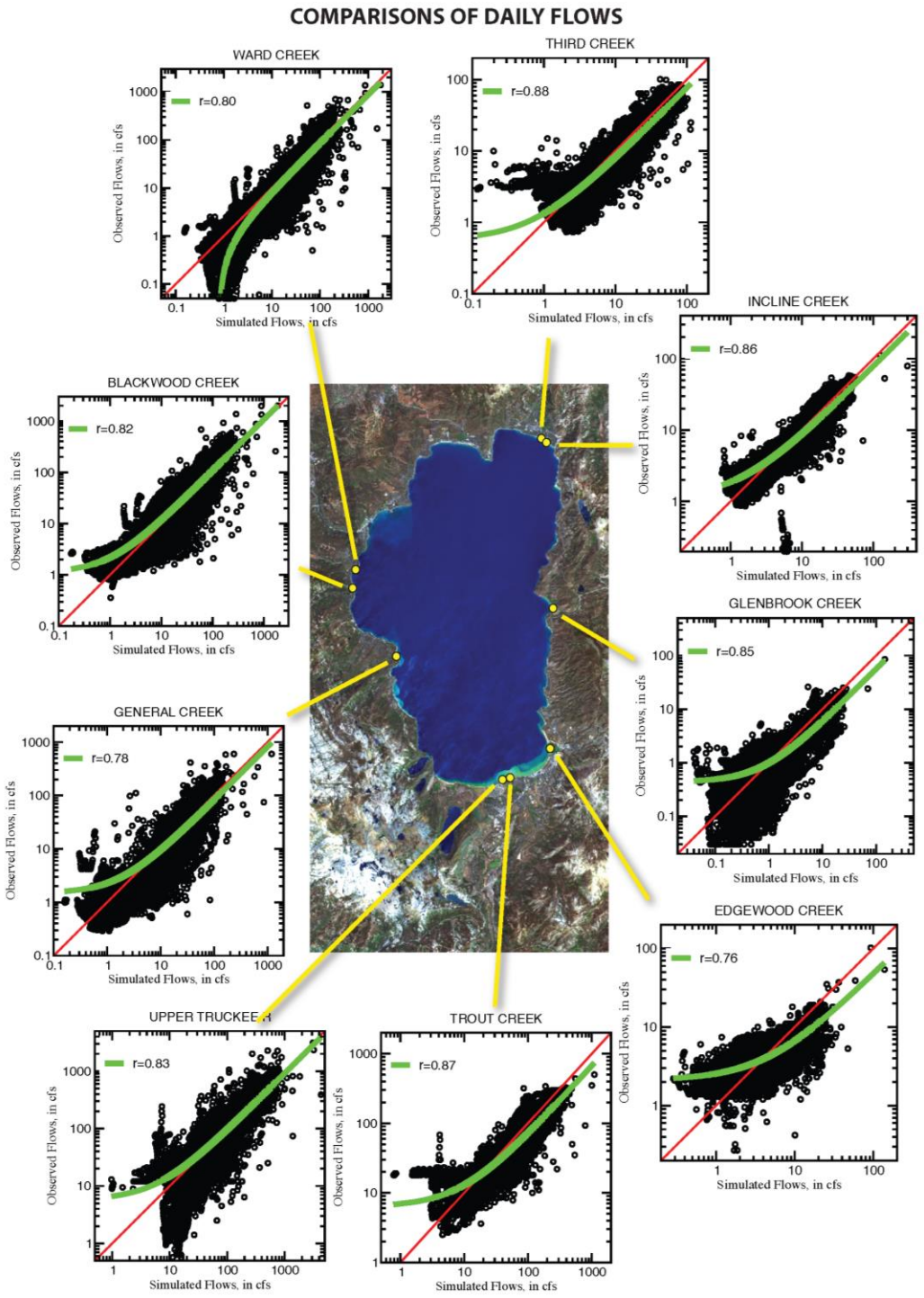

Figure 3.2. Comparisons of daily streamflow rates, water years 1981-2010, from measurements at nine streamflow-gaging stations around Lake Tahoe with streamflow rates simulated by the PRMS model in response to observed daily temperatures and precipitation totals. Red lines in graphs are one-to-one lines where observed and simulated values would be in perfect agreement; green lines are linear-regression fits of observed to simulated flow values, curving here because both axes are logarithmic scales.

around that general average agreement, and the simulated flows capture 60 or more percent of the daily-level variance (r-squared) at all gages except Edgewood. From this initial comparison, we judge that the PRMS model is capable of representing most flow variations with the notable exception of low flows. The deviations at low flows likely reflect the absence of a complete groundwater system in PRMS, where groundwater flow systems might add significant "baseflows" to streams during the low-flow seasons in some places and might route baseflows away from streams in others. A well-calibrated GSFLOW model of the Basin could improve the representations of low-flow conditions in many areas (Huntington and Niswonger, 2012). Thus we will avoid focusing on low-flow responses to climate change in this report, but have some reasonable assurance that the model is capable of reproducing the character, if not always the exact magnitudes, of streamflow under most other conditions, if provided with suitable meteorological forcings.

Lumping the measured and simulated streamflows to monthly and annual levels, Figures 3.3 and 3.4 compare monthly and annual average flows, respectively. On both of these time scales, simulated flows closely reproduce measured variations in most cases, although on the monthly scale, there is again a tendency for greater error at some gages under the lower flow conditions. In general, simulated monthly flows cluster closely along the one-to-one comparison lines in Figure 3.3, indicating only modest model biases. On the other hand, simulated annual flows (Figure 3.4) tend to somewhat overestimate annual flows (fall to the right of the red lines) at most gages, excepting Blackwood Creek where flows are undersimulated. Simulated annual flows at Edgewood Creek are problematic (highly scattered in Figure 3.4), so projections in that subbasin will need to be considered with caution.

Figure 3.5 compares year-by-year simulated and measured daily flow maxima. This is a more difficult comparison than that of the annual or even monthly averages because it requires that both the timing of the yearly extreme and its absolute magnitude by perfectly reproduced. Nonetheless, comparisons are encouraging across the entire range of historical maxima. Still, there is a notable tendency for flow maxima to be oversimulated along the eastern side of the Basin and undersimulated on the western side.

Figure 3.6 is another way to compare simulated and measured flow maxima, in terms of their respective distributions of maxima (probabilities of being exceeded). That is, the inverse of the probabilities on the horizontal axes in Figure 3.6 are estimates of return periods of flood magnitudes. Model performance in Figure 3.6 is more varied among the subbasins, with some gages showing fine agreement (i.e., Ward, Third, Upper Truckee River, and Blackwood Creek) across either the full range of historical maxima or at least the moderate to highest maxima. The distributions at four other gages (Incline, Glenbrook, Edgewood, and Trout) are strongly biased towards oversimulation of flow maxima, with maxima at General Creek tending towards undersimulation.

The "normal" (30-yr averaged) streamflow seasonalities in measurements and simulations are compared in Figure 3.7. As observed and expected, the subbasins of the high-

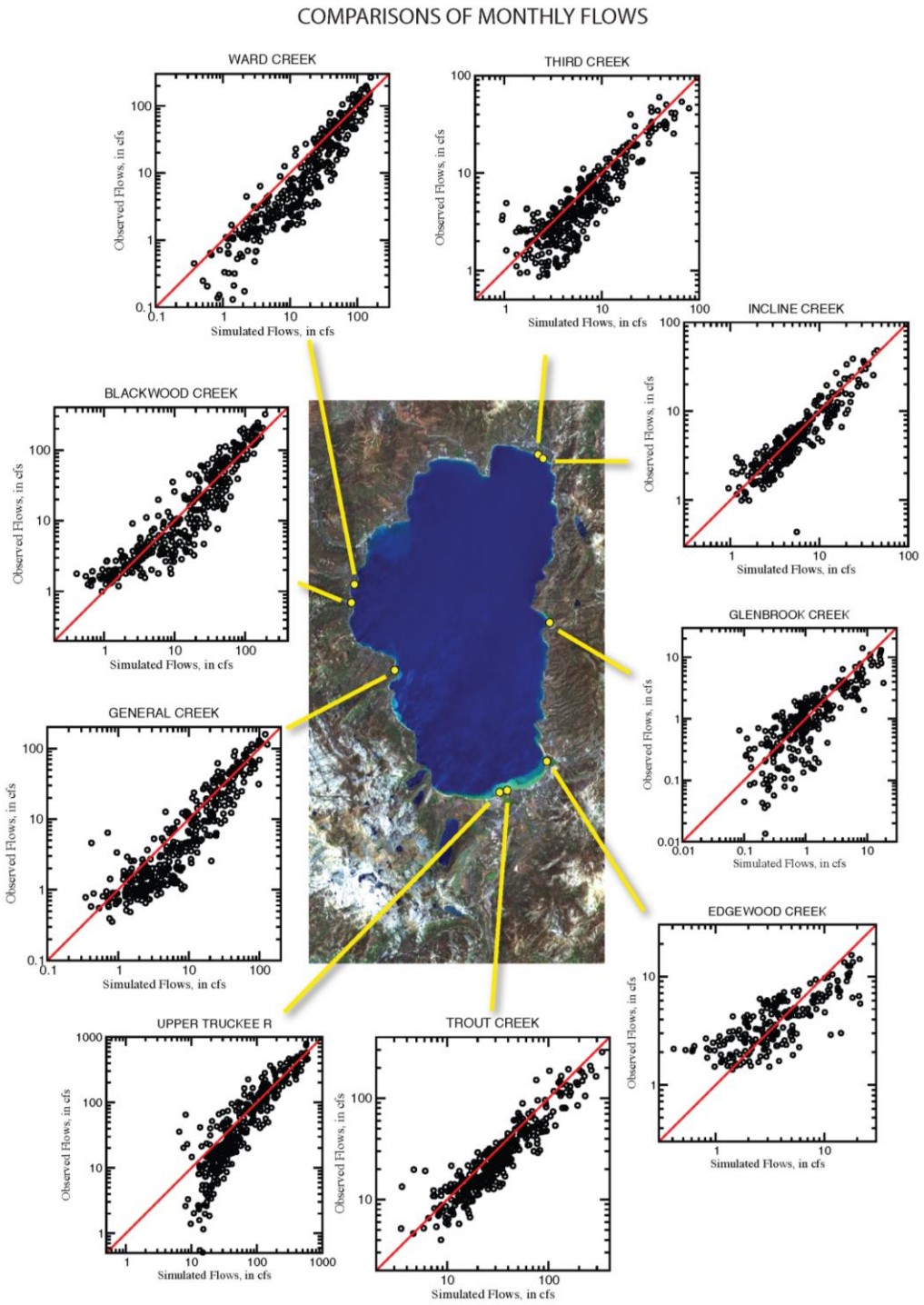

Figure 3.3. Comparisons of monthly streamflow rates, water years 1981-2010, from measurements at nine streamflow-gaging stations around Lake Tahoe with streamflow rates simulated by the PRMS model in response to observed daily temperatures and precipitation totals. See caption of Figure 3.2 for further explanation.

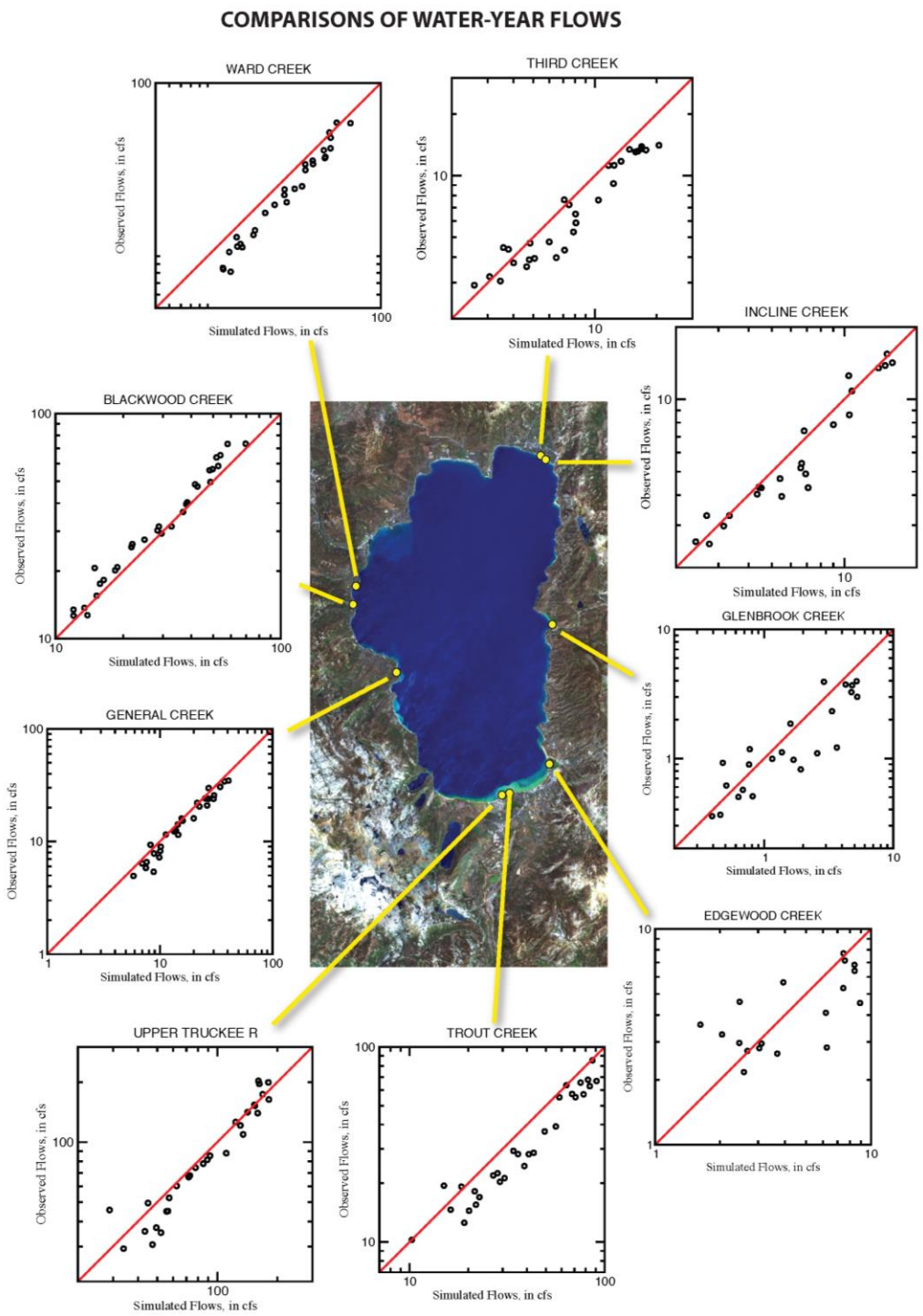

Figure 3.4. Comparisons of annual streamflow totals, water years 1981-2010, from measurements at nine streamflow-gaging stations around Lake Tahoe with streamflow rates simulated by the PRMS model in response to observed daily temperatures and precipitation totals. See caption of Figure 3.2 for further explanation.

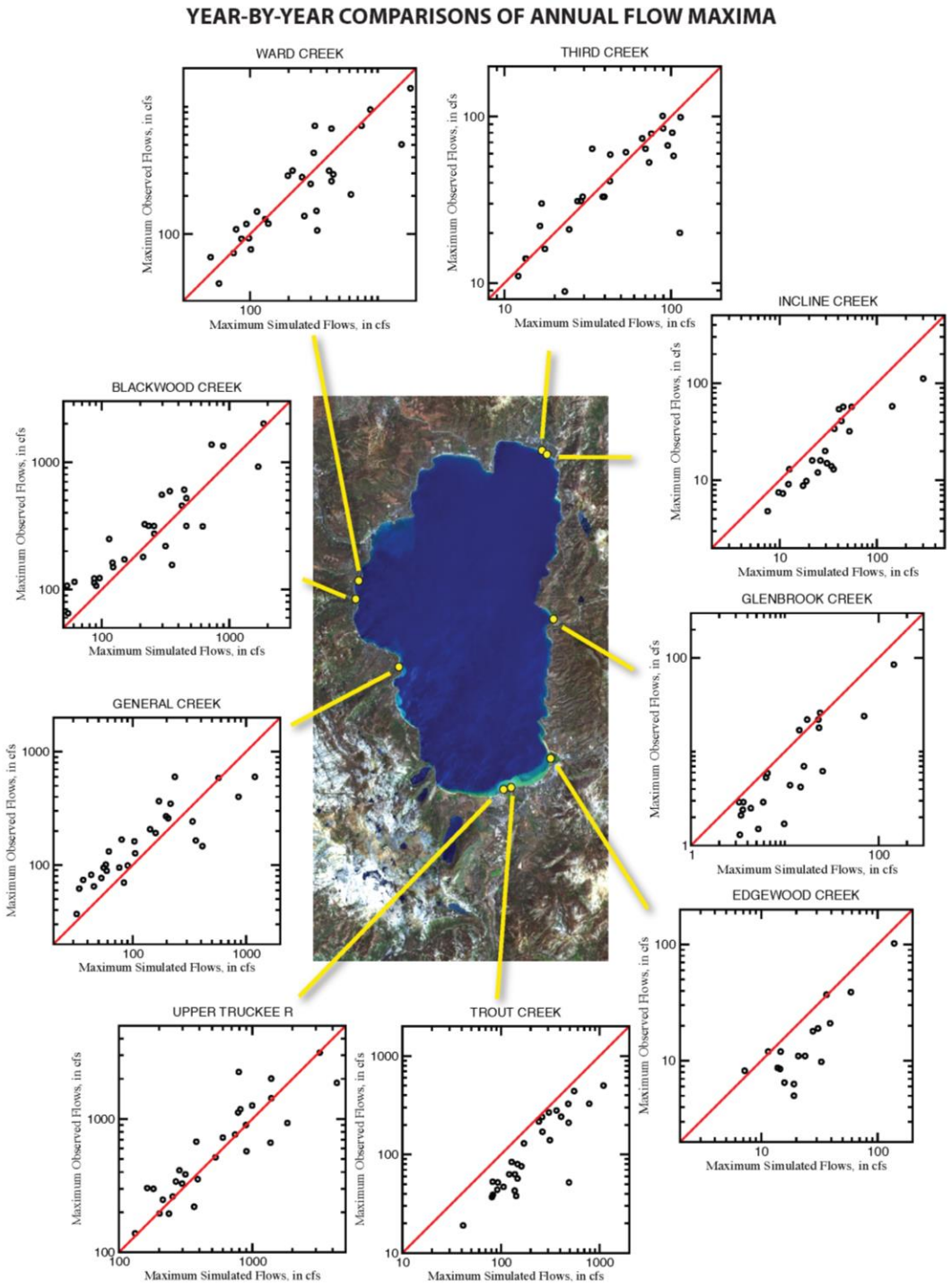

Figure 3.5. Comparisons of daily streamflow maxima, water years 1981-2010, from measurements at nine streamflow-gaging stations around Lake Tahoe with streamflow rates simulated by the PRMS model in response to observed daily temperatures and precipitation totals. See caption of Figure 3.2 for further explanation.

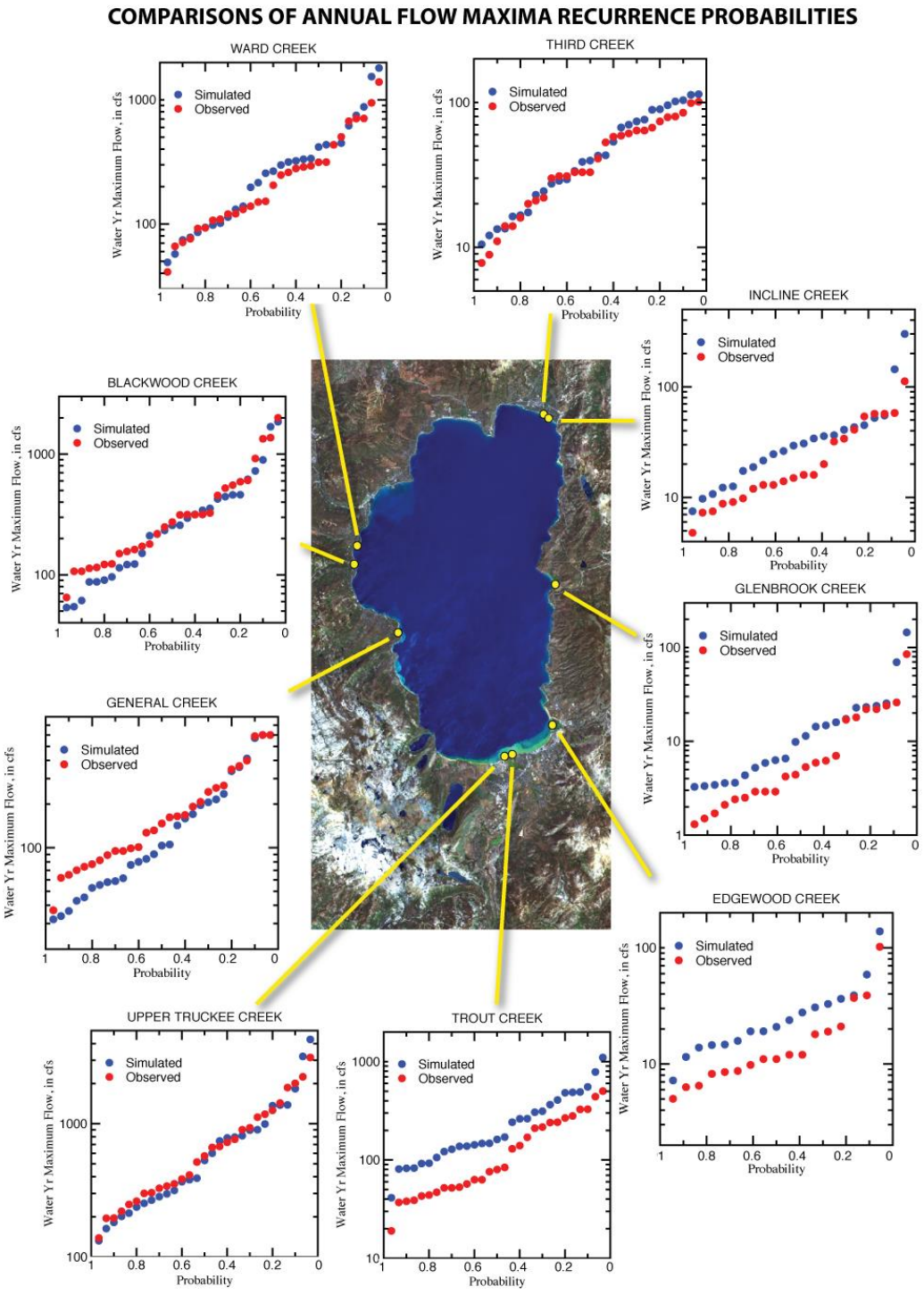

Figure 3.6. Comparisons of distributions of annual maximum flows, water years 1981-2010, from measurements at nine streamflow-gaging stations around Lake Tahoe with streamflow rates simulated by the PRMS model in response to observed daily temperatures and precipitation totals. See caption of Figure 3.2 for further explanation.

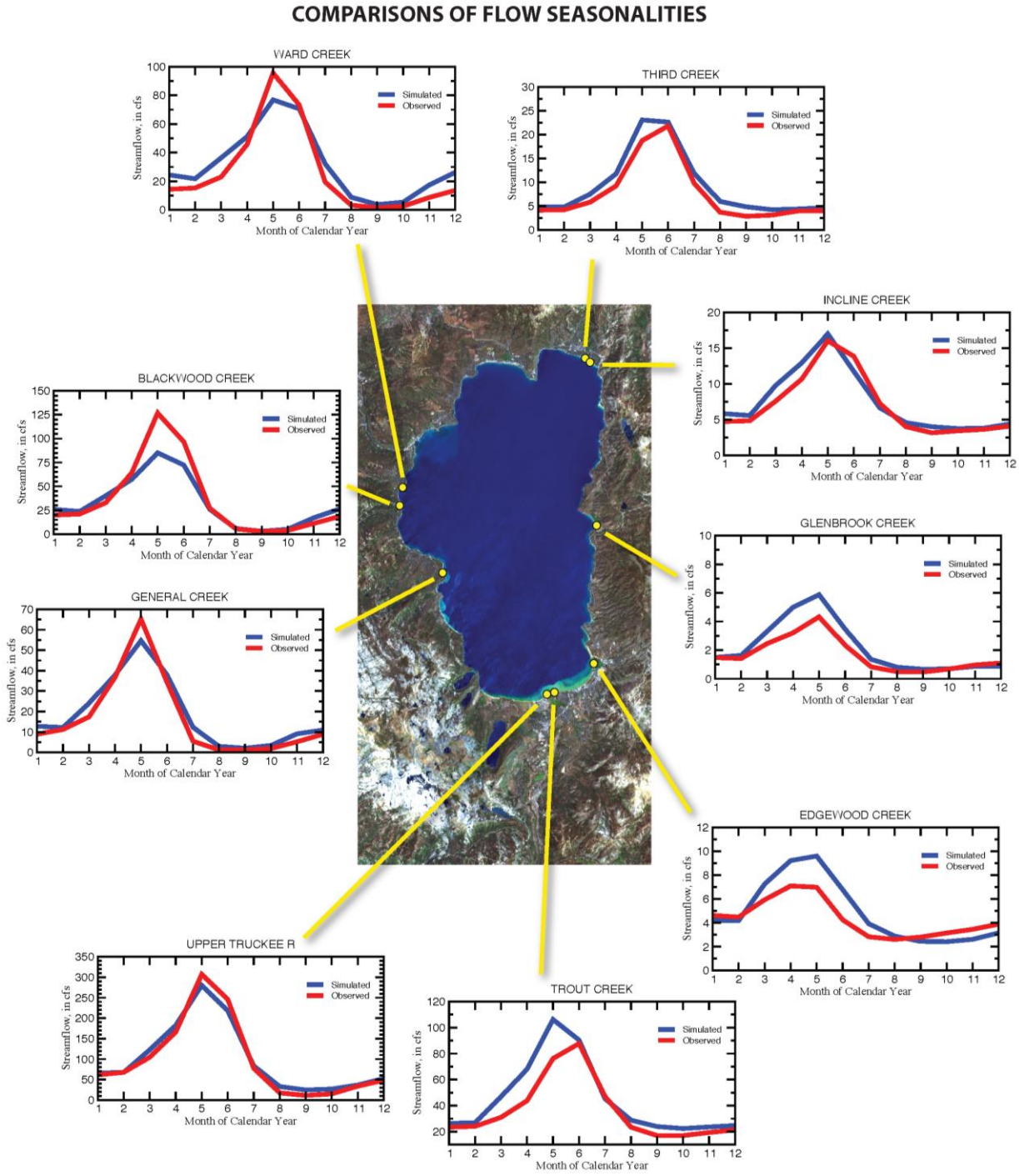

Figure 3.7. Comparisons of 30-yr averaged monthly streamflow rates, water years 1981-2010, from measurements at nine streamflow-gaging stations around Lake Tahoe with streamflow rates simulated by the PRMS model in response to observed daily temperatures and precipitation totals. See caption of Figure 3.2 for further explanation.

altitude Tahoe Basin yield annual hydrographs dominated by primary spring snowmelt-fed flow peaks with low flows in summer and moderate flow increases through the autumn – winter wet season. With the exception of Trout Creek, the month of that maximum average flow is well captured in the simulated time series at each gage. Flows in Trout Creek are simulated, on average, to arrive about a month earlier than observed. As noted in Figures 3.4 - 3.6, flows on the east side of the Basin are oversimulated, and this bias is obvious in the annual hydrographs of Figure 3.7. As in those other figures, flows at Blackwood Creek are underestimated on the whole, but this undersimulation all comes from undersimulation of the spring snowmelt peak.

Despite the broad agreements in Figure 3.7, that general capacity of the PRMS model to reproduce the average snowmelt-driven streamflow timings in Figure 3.6 could presumably arise for the wrong reasons. Thus, it is worth exploring whether the generally "correct" results in Figure 3.7 somehow arise for the wrong reasons. The primary observations-based comparison that provides some insight into this possibility is evaluating whether year-to-year variations of a metric of the timing of flows at each gage is correctly simulated. (If so, then the climatic drivers of the year-to-year differences in the shapes of each year's hydrograph are at least yielding correct flow-timing responses; if not, then we cannot rule out "right timings for wrong reasons"). Figure 3.8 illustrates a center-of-flow timing index that, in date of water year, is measured as

$$CT = \Sigma\, d_i * Q_i \;/\; \Sigma\, Q_i$$

where Σ is summation of all days of the water year, d_i is the day of water year, and Q_i is streamflow rate on that day. CT may be thought of as approximately the day by which half the year's accumulated of streamflows has occurred (Stewart *et al.,* 2004). In fact, CT takes more account of when during the year occurs throughout the year than does a half-flow date; that is, in the end, the precise timing of a half-flow date depends on flow during the handful of days right around the final day estimated. A closer analogy is that the CT is modeled on the process for finding the center of mass of an object, the point in the object where which the object could be balanced without tipping or falling under the pull of gravity. In any event, it is a metric of when in each year the "middle" of the hydrograph arrives.

Figure 3.9 compares center-of-flow timings in observations and simulations. Notice that in the Basin, CT timings have been observed to range by over three months or more from "earliest" to "latest" years. Generally, simulated CTs follow their yearly measured counterparts (follow or parallel the red one-to-one lines) across the whole range of years from years with very early flow timings to years with very late timings. Timings at Edgewood Creek are worst simulated, but mostly because the simulated range is considerably larger than in the observations. (That is, the scatter of simulated timings follows observed timings from highest to lowest in a narrow linear packet, but the scale of the simulated timing variations is just too large along that line.) Simulated timings of flows in General Creek deviate most from observations and will need to be considered skeptically in the projections to come.

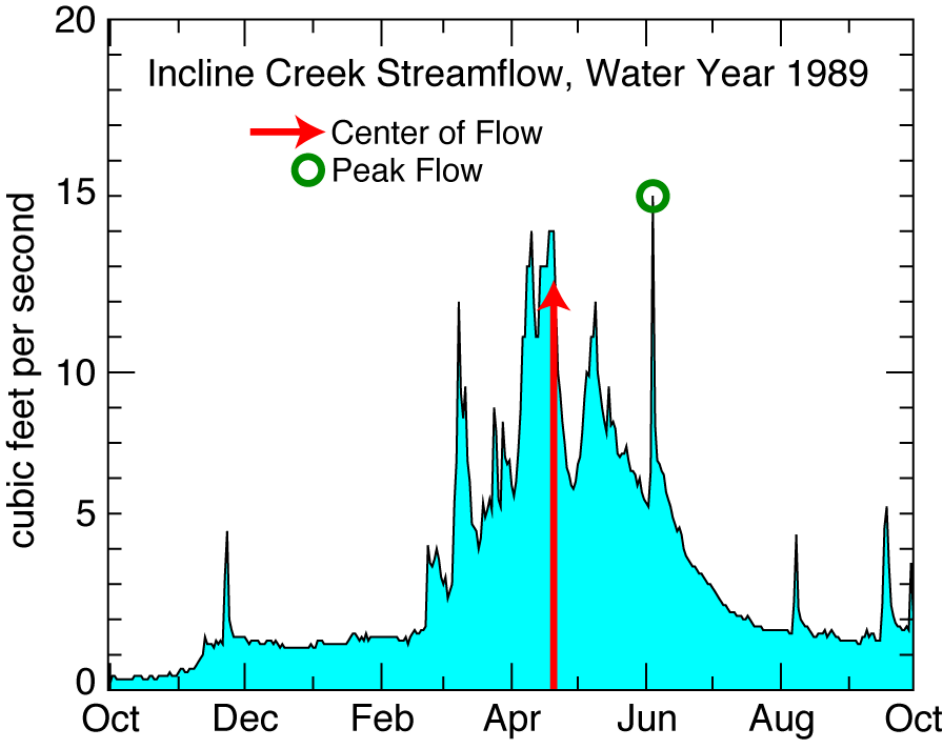

Figure 3.8. Comparison of daily maximum streamflow and center of flow timing at Incline Creek, for water year 1989. Notice that an errant peak flow can occur almost anytime in the annual hydrograph, e.g., when a large storm arrives, so that maximum daily flow can be a nearly random measure of flow timing in many settings, whereas the center-of-flow timing depends on flows throughout the water year and so is a more stable timing index.

Broadly speaking, simulated flows at Edgewood Creek are problematic and, especially considering Figures 3.2, 3.4 and 3.9, simulated responses in that sector of the Basin may need to be considered with some suspicion in results that follow. More generally, low flows are poorly simulated throughout the Tahoe Basin and should not be relied on in climate-change projections.

3.2. Comparisons with Climate-Model-Driven Simulated Streamflow Variations, Water Year 1981-2005

Next, the observed flows are compared to a set of simulations of flows responding to climate-model simulated weather for a 25-yr historical period with the same greenhouse-gas conditions (as in the observed period); the historical climate-model simulations in archived in CMIP5 end in 2005, so that unlike the 30-yr comparisons in section 3.1, here we compare 25-yr periods of observations and simulations. Figure 3.10 provides two examples of how the observed and simulated flows compare to each other. Notably the sequences of simulated flow events do not coincide directly with the observed sequence of flows (nor are they expected to, as discussed above). The comparison here of simulations by the eight models to observations provides a sense of how well the combination of climate models, downscalings, and PRMS model can reproduce observed distributions of flow statistics.

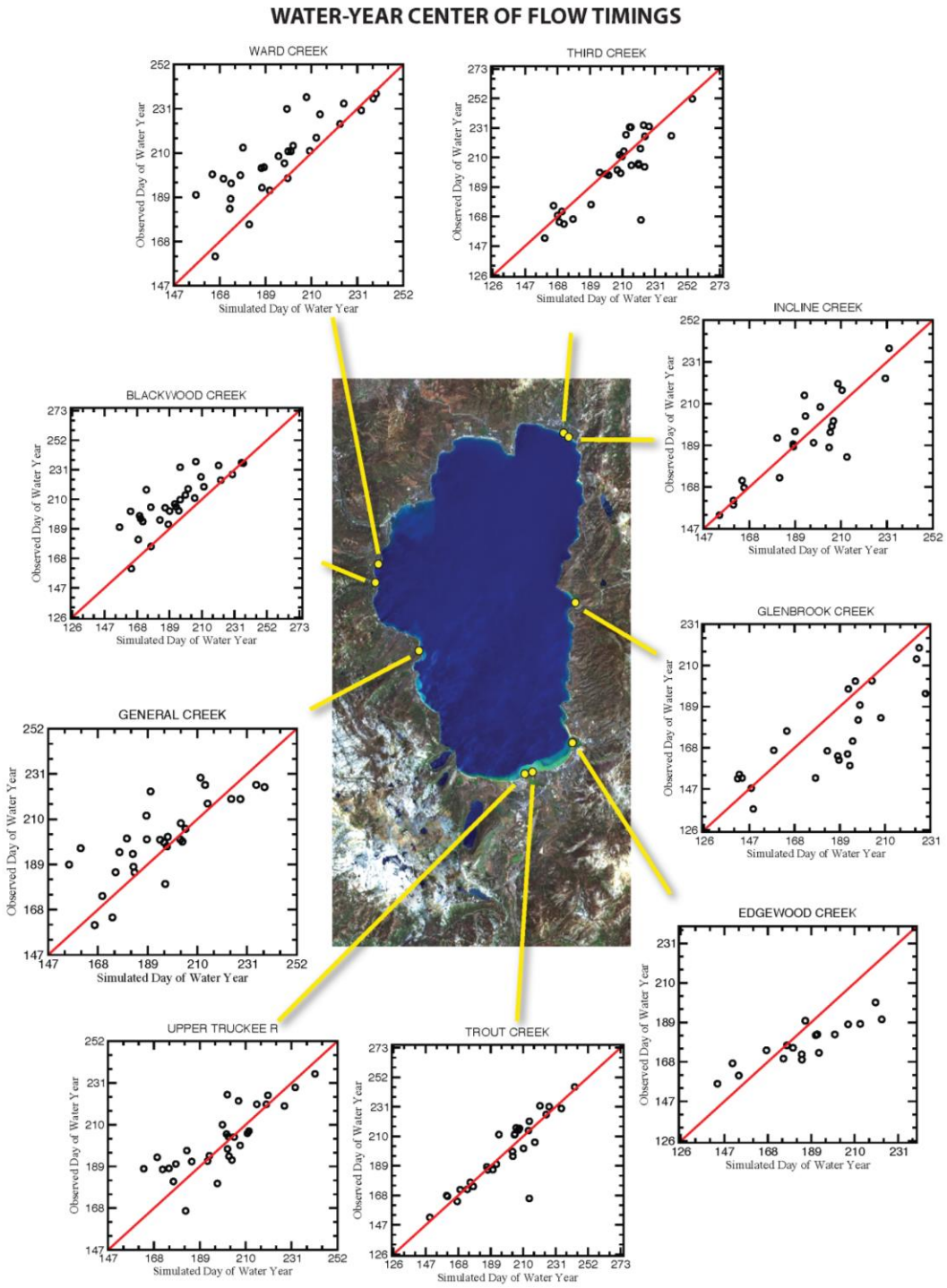

Figure 3.9. Comparisons of center-of-streamflow timings, water years 1981-2010, from measurements at nine streamflow-gaging stations around Lake Tahoe with streamflow rates simulated by the PRMS model in response to observed daily temperatures and precipitation totals. See caption of Figure 3.2 for further explanation.

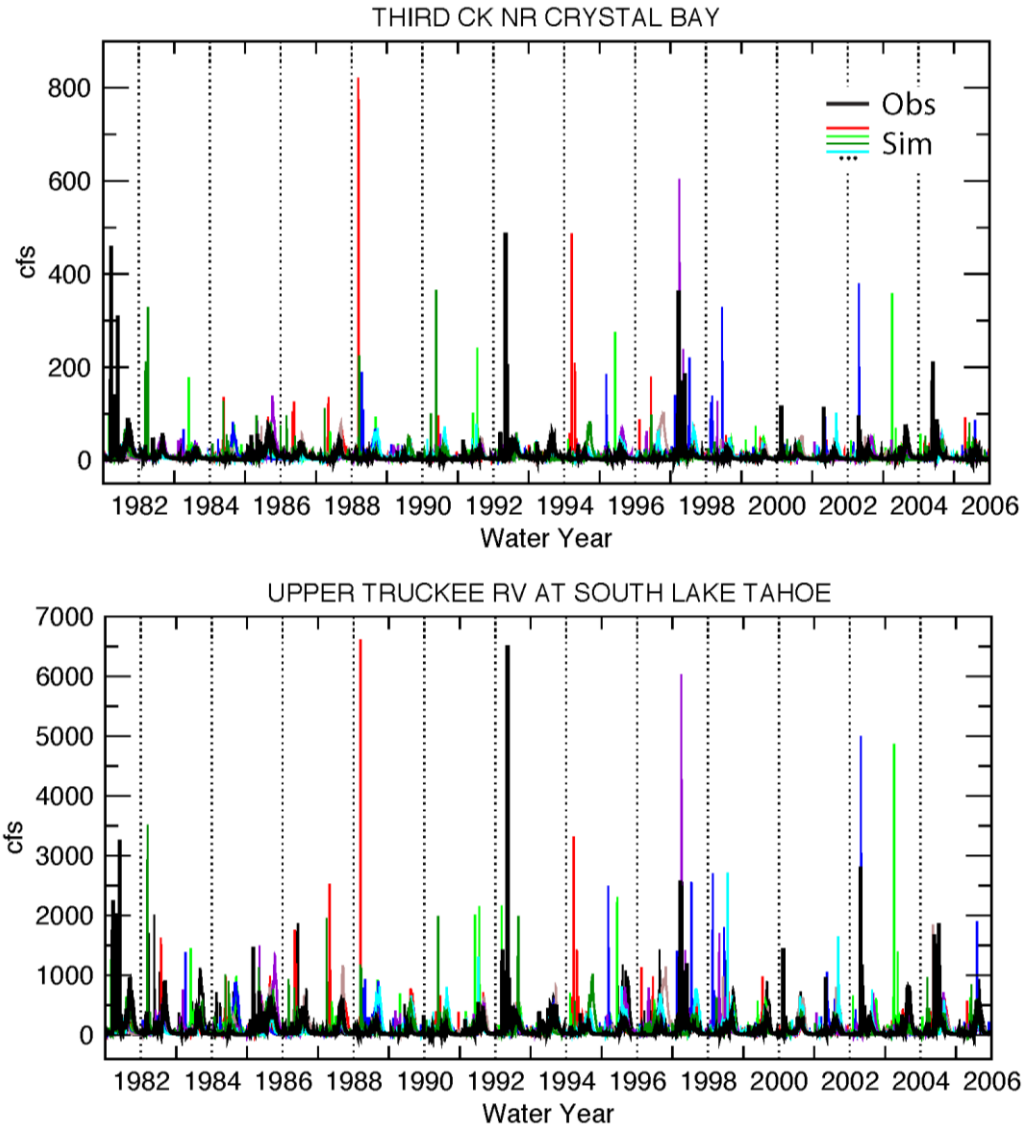

Figure 3.10. Comparisons of daily streamflow rates, water years 1981-2005, from measurements at Third Creek and Upper Truckee River streamflow-gaging stations (black) with streamflow rates simulated by the PRMS model in response to downscaled climate-model simulated daily temperatures and precipitation totals under historical greenhouse-gas conditions from eight climate models (different colors).

In a comparison that is largely analogous to Figure 3.2, the distributions of all daily flow observations and flows simulated under historical greenhouse-gas conditions by the eight climate models are compared in Figure 3.11. Besides the source of simulated flows, the other difference between Figure 3.2 and 3.11 is that—because the flow sequences in the Figure 3.11 climate-model-through-PRMS simulations do not follow the same (observed) weather sequence as in Figure 3.2—both the observed flows and simulated inflows in Figure 3.11 were sorted so that the largest daily flow from each is the upper rightmost dot, the second largest is next upper rightmost dot, and so on down to the lowest values in each series is the lowest leftmost dot. If the statistical

distributions of observed and simulated flows are the same, then the dots should fall close to (or ideally if there was no sampling scatter, on) the red one-to-one lines in each frame.

At essentially all of the gaging stations in Figure 3.11, the dots of all colors (each color representing flows simulated in response to a different climate model) in the midrange of flows during the 1981-2005 period compared are very similar (little vertical scatter and approximately overlying the one-to-one line). This indicates that over the midrange of flows the distribution of climate-model-downscaled-through-PRMS flows are very near the distribution of observed flows. At the Ward, Upper Truckee, Incline, and Glenbrook gages, simulated low flows are too high (fall well to the right of the one-to-one line); at the Blackwood, Third, and Edgewood gages (and less so at Trout and General), low flows are somewhat undersimulated. We have already noted a tendency for the PRMS model to simulate low flows poorly, and have concluded that using the PRMS model to project future low flows may be problematic. When PRMS is driven with the downscaled historical-climate simulations used here, gages on the east side of the Basin tend to be oversimulated for highest flows; elsewhere the distribution of high flows is quite good. Thus we will want to be careful regarding projected changes at the high-flow ends of streamflow distributions on the east side of the Basin as we look to the future.

Aggregating the simulated and observed flows to water-year totals, Figure 3.12 compares the observed and simulated annual flows responding to weather from the various climate models. There is more scatter of points in Figure 3.12 than in Figure 3.11, due to 365 times smaller sample sizes in Figure 3.12. Generally the distributions of observed flows are within or near to the clouds of simulated flows, indicating that the combination of climate and PRMS models reproduces the observed distributions reasonably well. Deviations from one-to-one in Figure 3.12 appear to be much like the deviations in Figure 3.4, presumably deriving from much the same causes.

The distributions of observed and simulated annual flow maxima are compared in Figure 3.13. For most part, the clouds of simulated flow maxima overlie or else are adjacent to the one-to-one lines in each frame, indicating that flow maxima (or, at least, variations thereof) are reasonably well reproduced in the combination of models used here. Notably major deviations are found at Third and Trout Creeks where the highest end of the flow-maxima distributions deviate remarkably from observations (a hint of similar behavior occurs at Incline Creek), and at Glenbrook Creek where almost all flow maxima are oversimulated. In this corner of the Basin, projected highest flows should be considered with some caution, although—with exception of Glenbrook—projected changes in ensemble-average annual flow maxima nearer the long-term average of maxima are reasonable to consider.

Finally Figure 3.14 compares the long-term normal streamflow hydrographs at monthly levels. As in Figure 3.7, simulated seasonal timing of streamflow is similar to observations when the whole ensemble of climate models is considered, plus or minus a month. The average amplitudes of the seasonal peaks are not so universally well simulated, which ultimately bleeds into tendencies for over- and undersimulation of annual totals in Figure 3.12.

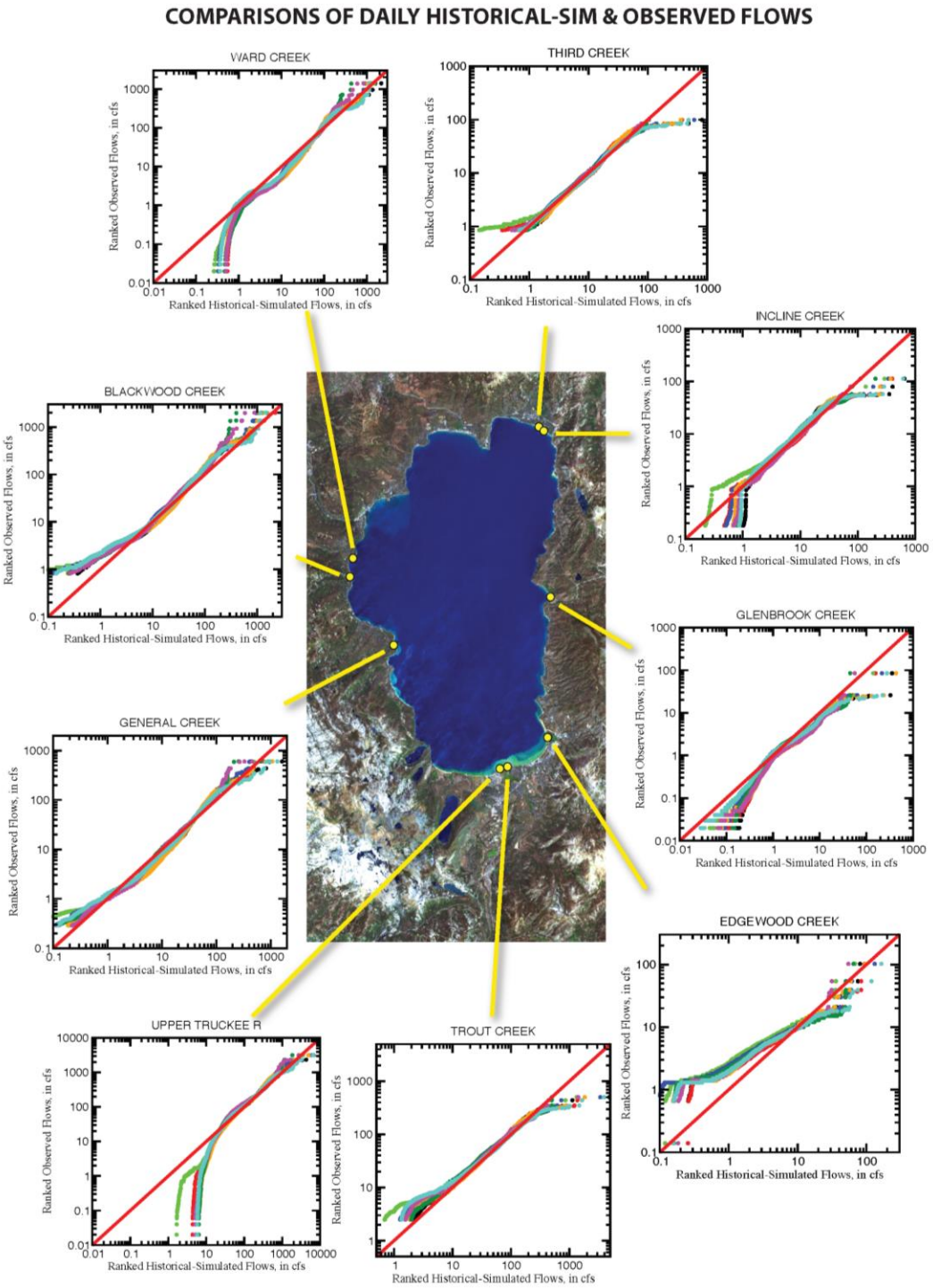

Figure 3.11. Comparisons of distributions of daily streamflow rates, water years 1981-2005, from measurements at nine streamflow-gaging stations around Lake Tahoe with streamflow rates simulated by the PRMS model in response to downscaled climate-model simulated daily temperatures and precipitation totals under historical greenhouse-gas conditions. Dots of difference colors represent the different climate models. See caption of Figure 3.2 for further explanation.

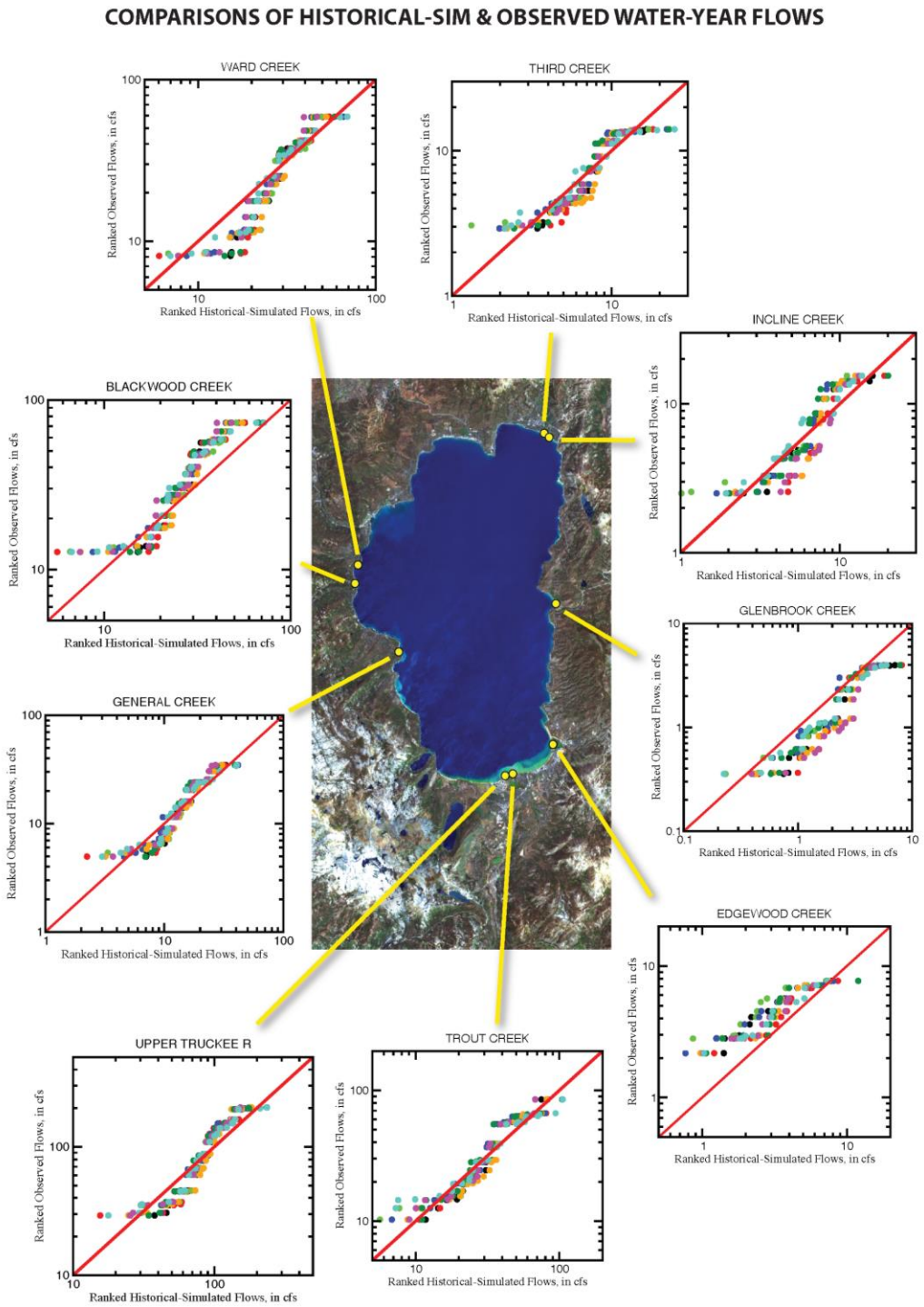

Figure 3.12. Comparisons of distributions of water-year average streamflow rates, water years 1981-2005, from measurements at nine streamflow-gaging stations around Lake Tahoe with streamflow rates simulated by the PRMS model in response to downscaled climate-model simulated daily temperatures and precipitation totals under historical greenhouse-gas conditions. Dots of difference colors represent the different climate models. See caption of Figure 3.2 for further explanation.

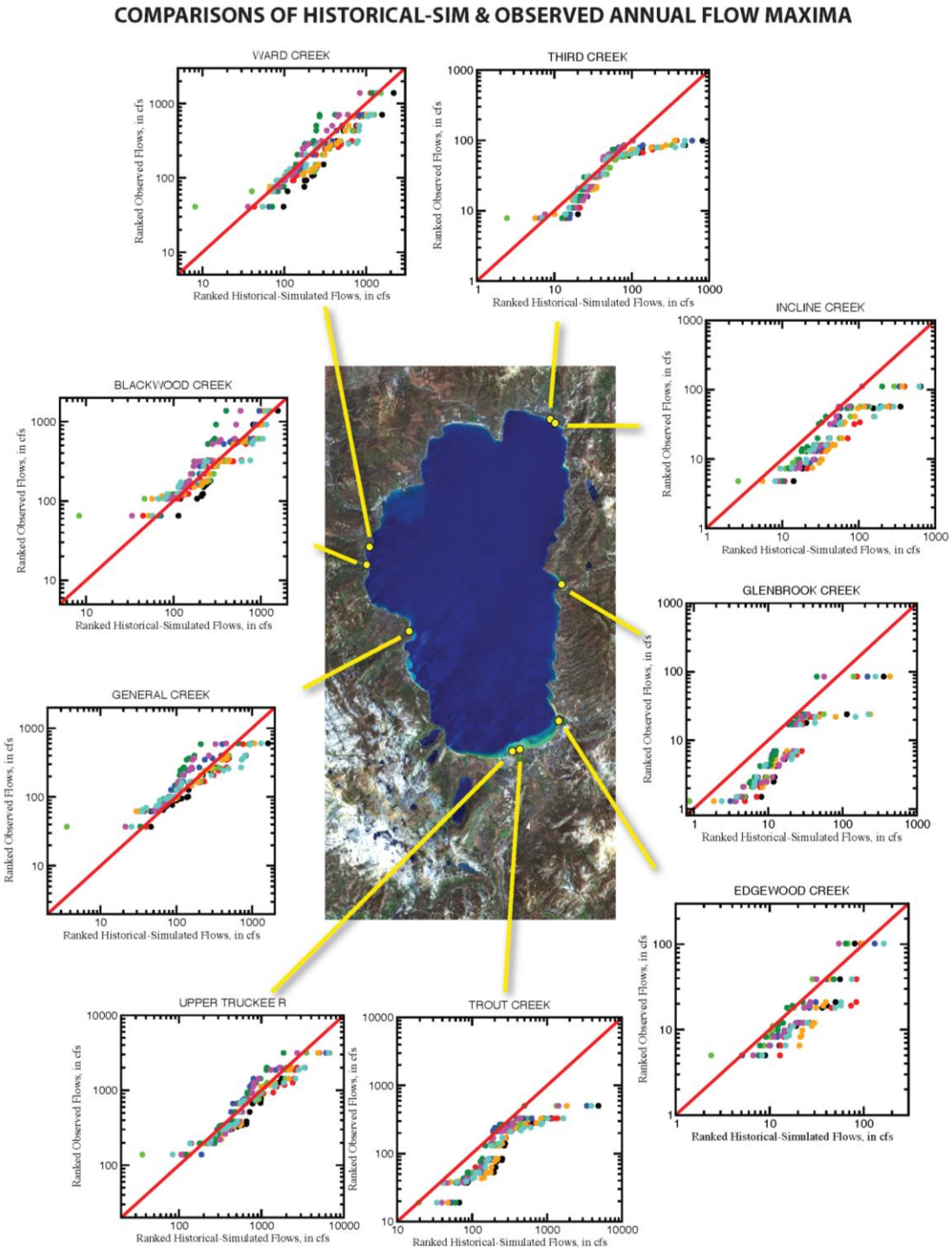

Figure 3.13. Comparisons of distributions of water-year daily maximum streamflows, water years 1981-2005, from measurements at nine streamflow-gaging stations around Lake Tahoe with streamflow rates simulated by the PRMS model in response to downscaled climate-model simulated daily temperatures and precipitation totals under historical greenhouse-gas conditions. Dots of difference colors represent the different climate models. See caption of Figure 3.2 for further explanation.

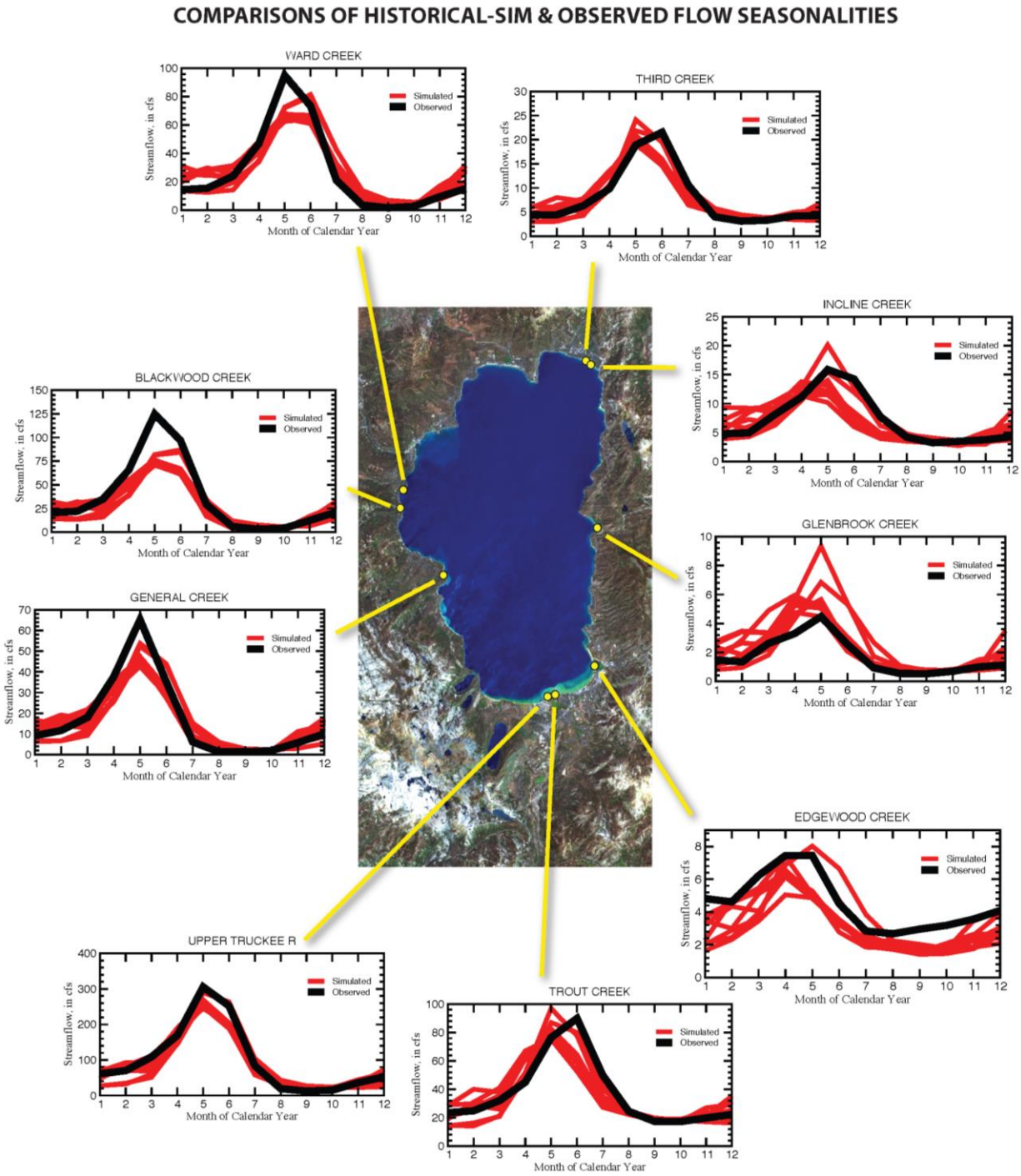

Figure 3.14. Comparisons of average seasonal cycles of streamflow, water years 1981-2005, from measurements at nine streamflow-gaging stations around Lake Tahoe with streamflow rates simulated by the PRMS model in response to downscaled climate-model simulated daily temperatures and precipitation totals under historical greenhouse-gas conditions.

4. PROJECTED CLIMATE CHANGES

Climate projections in this report are responses by a hydrologic model of the Lake Tahoe basin to climate projections from a collection (ensemble) of global-climate models adjusting to two plausible greenhouse futures (California DWR CCTAG, 2015), arising from different ways that humans might manage future greenhouse-gas emissions: One future — labeled RCP4.5, for a "Radiative Concentration Pathway that traps 4.5 W/m^2 of extra heat by 2100"—assumes that extra heat (Figure 4.1a) trapped by greenhouse-gases that humans introduce to the global atmosphere (Figure 4.1b) will grow until midcentury, and then slow rapidly thereafter to stabilize later in the century. This version of global heating will result if we achieve net reductions in emissions by about 2040, going on to stabilize emissions at low levels by about 2080 (figure 4.1b). The other future--labeled RCP8.5, for Radiative Concentration Pathway that traps 8.5 W/m^2 of extra heat by 2100—assumes, on the contrary, that greenhouse-gas concentrations and extra heat continue to increase throughout the century (figure 4.1a). This future would result from greenhouse-gas emissions that aren't stabilized until nearly 2100 and never reduced (figure 4.1b). In response to these two futures, different climate models yield different results. Because of this, modern climate projections are best interpreted in terms of the extent to which ensembles of models agree about likely climate changes in climate. In this report, results are presented from forcing the hydrologic model of the Lake Tahoe basin with climate projections from eight different models responding to the historical and two future greenhouse-gas warming scenarios shown in Figure 4.1.

The range of projected changes in temperatures and precipitation in the 8-model, 2-emissions scenarios ensemble evaluated in this study is illustrated Figure 4.2, using the conditions projected for the Upper Truckee River basin as an example. Temperatures warm rapidly and well above the range of historical year-to-year variations (these long-term changes

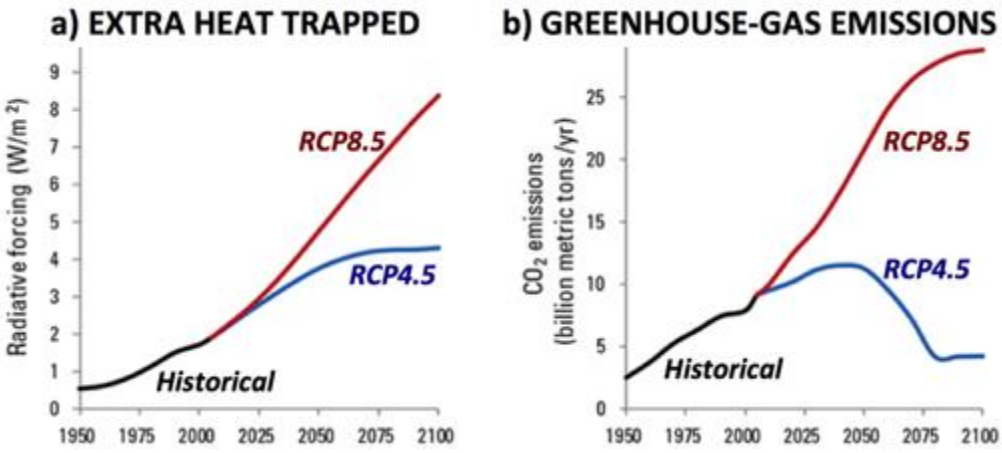

Figure 4.1. a) Extra heat trapped in the earth system (atmosphere, oceans, and land surface) by anthropogenic emissions of greenhouse gases, historically and under two assumptions about future emissions, and b) rates of anthropogenic greenhouse-gas emissions that would result in the extra heat shown in panel a).

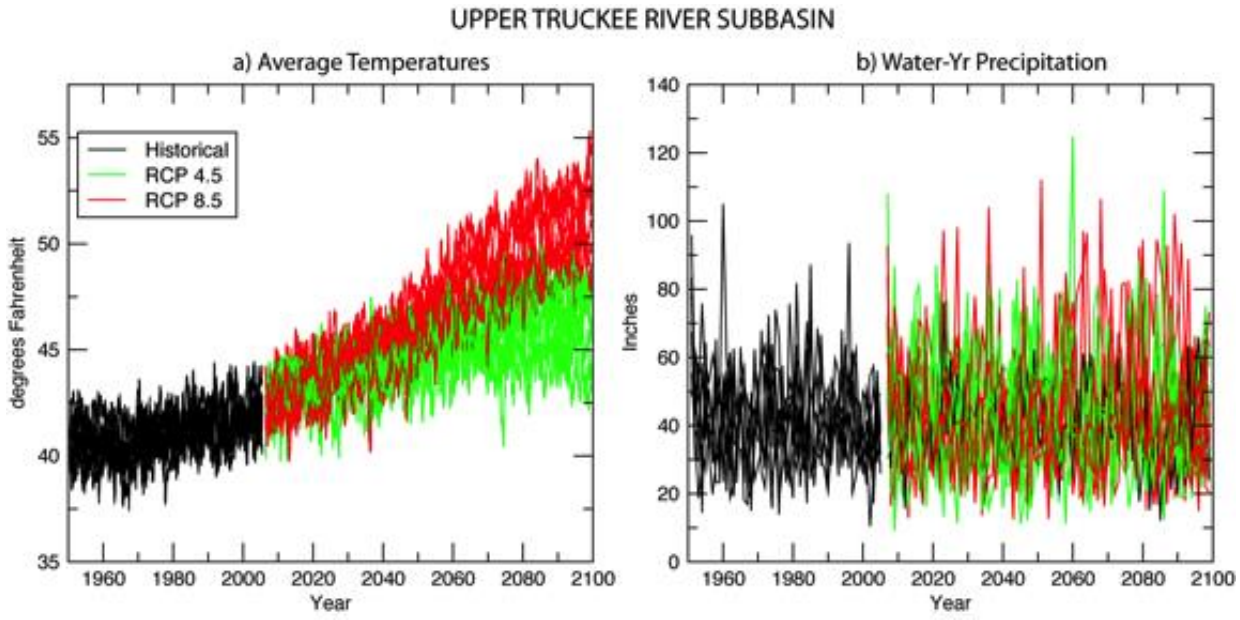

Figure 4.2. Ensemble-projected changes in (a) air temperatures (smoothed with a 365-day running average) and (b) water-year precipitation totals, over the Upper Truckee River subbasin, as an example of the changes projected by eight climate models downscaled and run through the basin PRMS model.

will be mapped quantitatively below). Under the RCP 4.5 emissions (green curves), temperatures warm until midcentury before starting to level off towards end of century. Under the RCP 8.5 emissions, warming continues apace throughout the century, arriving at about 8°F warmer than historical norms by end of century. Changes in long-term averages of precipitation are relatively small compared to the historical and ongoing natural variations, but the upper edge of those year-to-year precipitation variations increase in future decades, indicating that "wet years" get wetter. Less obviously in Figure 4.2, dry years also get drier.

To see how these changes play out within the basin, consider the average (across climate models) projected 30-yr normal temperature, shown in Figure 4.3. This figure illustrates, in four larger maps on the left, average projected changes from the 1971-2000 historical-simulation normal to two future 30-yr periods (2036-2065 and 2071-2100) representing midcentury and late-century temperature changes. Two smaller maps on right show the standard-deviations of the projected normals from the eight climate models to give a sense of whether the projected ensemble-mean changes are large compared to model-to-model differences. That is, the standard-deviation maps give a sense of how much agreement there is concerning the ensemble-mean changes among the different climate models in the ensemble. If the projected mean changes are larger than these standard deviations then the models are in good agreement regarding the character of the coming climate. If the standard deviation among climate models are larger than the mean changes, then there is less agreement and confidence in the character of the future climate.

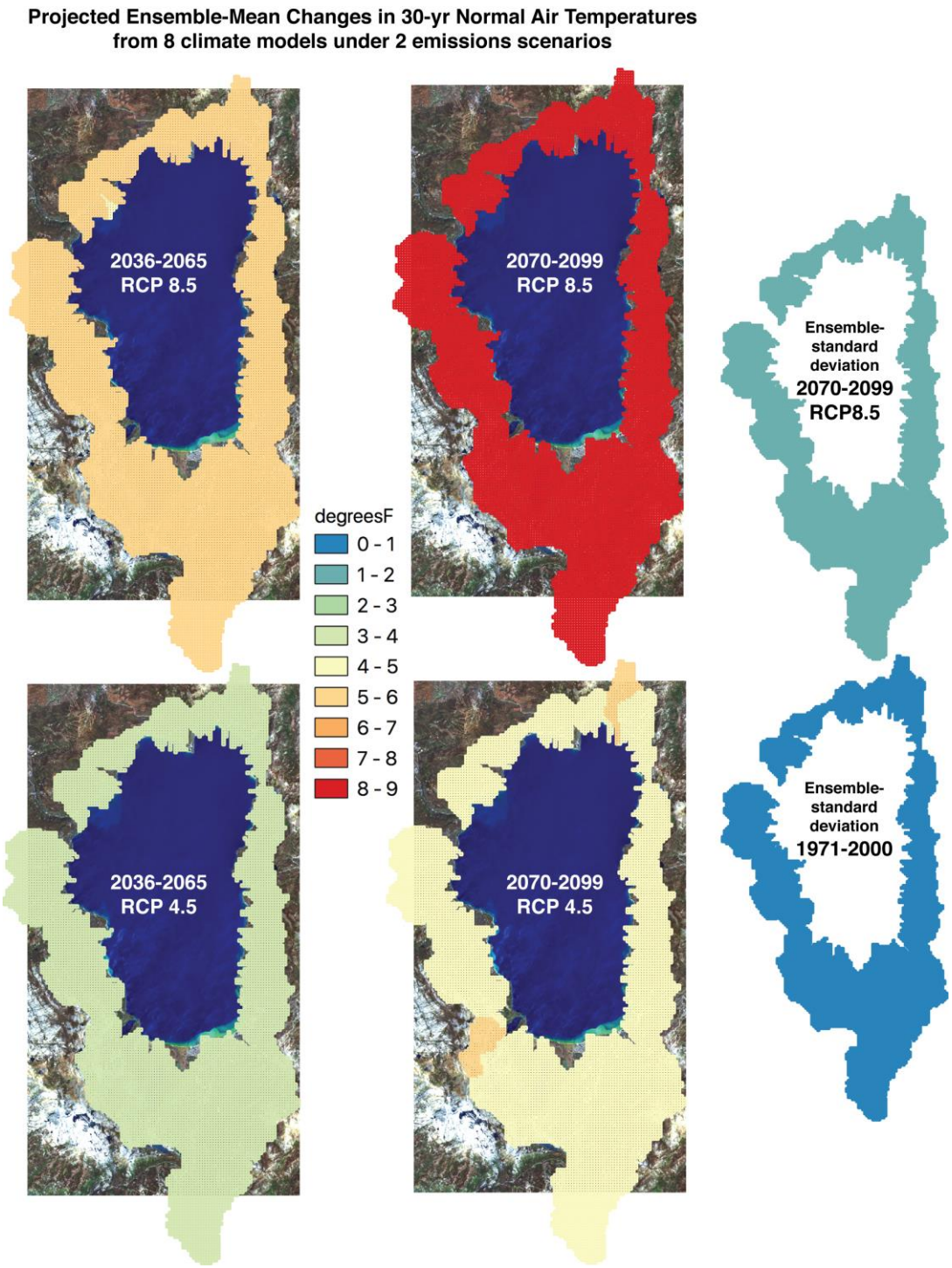

Figure 4.3. Ensemble-mean increases in 30-yr (1971-2000) normal air temperatures over the Lake Tahoe basin (large maps), as projected by eight climate models downscaled and run through the basin PRMS model. Small maps show standard deviations of the projected normals from the eight different climate models. Results here are mapped at the scale of 60 subbasins that encompass the entire basin excepting the lake surface and various lake-front areas too small to be reliably represented by the PRMS model.

Most notably, the ensemble-mean temperature changes (all in the form of warming) differ very little among the subbasins. Generally speaking, this uniform-looking pattern reflects the fact that global warming is a phenomenon that affects areas as "small" (by global standards) as the Tahoe basin almost uniformly rather than at the scale of high-resolution micrometeorological conditions that are so notable in this mountain setting. That is, weather and climate normals within the basin vary markedly from place to place with altitude, aspect, proximity to the lake, and geographic location, but the greenhouse-gas climate changes in temperature happen on much larger spatial scales. Beyond this broad near-uniformity of warming within the Basin, Figure 4.3 indicates that warming amounts to about +3ºF by midcentury under the RCP4.5 scenario and increases only about a degree or two more by late-century, due to the flattening of the greenhouse effect shown in Figure 4.1a. However, under RCP8.5 the temperatures rise by an average of about +5ºF by midcentury and continue their rapid rise to over +8ºF by late century. As late as 2050, the warming is quite similar between the RCP 4.5 and 8.5 projections—as suggested also in Figure 4.2. But the 30-yr normals mapped in Figure 4.3 and many figures to come in this report include another 15 years of change within which time RCP 8.5 continues to warm quickly while temperatures under RCP 4.5 are already leveling off. All of these changes are considerably larger than the ensemble standard deviations, which indicates that the ensemble members are in agreement about the general magnitude of the warming. Notice also that the ensemble-standard deviations by late century are somewhat larger than in the historical period, indicating that the models are not in perfect agreement as to how much warming will occur.

Before turning to the projections of precipitation, in the interests of human-health, quality-of-life, and other nonhydrologic purposes, we consider here the projected changes in occurrence of heat waves associated with the general warming mapped in Figure 4.3. Specifically, Figure 4.4 shows projected changes in daytime heat-wave occurrences in the Basin. Daily maximum temperatures rise above 90ºF more often by late-century in most of the basin under both greenhouse scenarios. The RCP4.5 increases are small or comparable to the historical and future ensemble-standard deviations, indicating that the increases are small and uncertain. Under the RCP8.5 scenario, however, the increases are mostly large compared to the ensemble-standard deviations so these increases are more confidently projected, yielding up to 15 additional days above 90ºF annually. Subbasin-level differences in these projected changes reflect differences in how much of each subbasin is historically near to the threshold for daytime heatwaves as defined here. Notably the Tahoe basin is, by and large, considerably less vulnerable to daytime heat-wave increases compared to many other lower parts of the range and especially in other areas in the same counties but in the foothills or below. Figure 4.5 shows California Department of Public Health heatwave thresholds (left panels) and the projected increases in occurrence of heat waves (middle and right panels) at the 12-km resolution used in the California Fourth Climate Assessment studies (http://cal-adapt.com) under the RCP8.5 scenario. The lavender areas in the change maps are areas where these very hot temperatures are rarely reached even under the warming trends, and much of the Tahoe basin is in that clement zone.

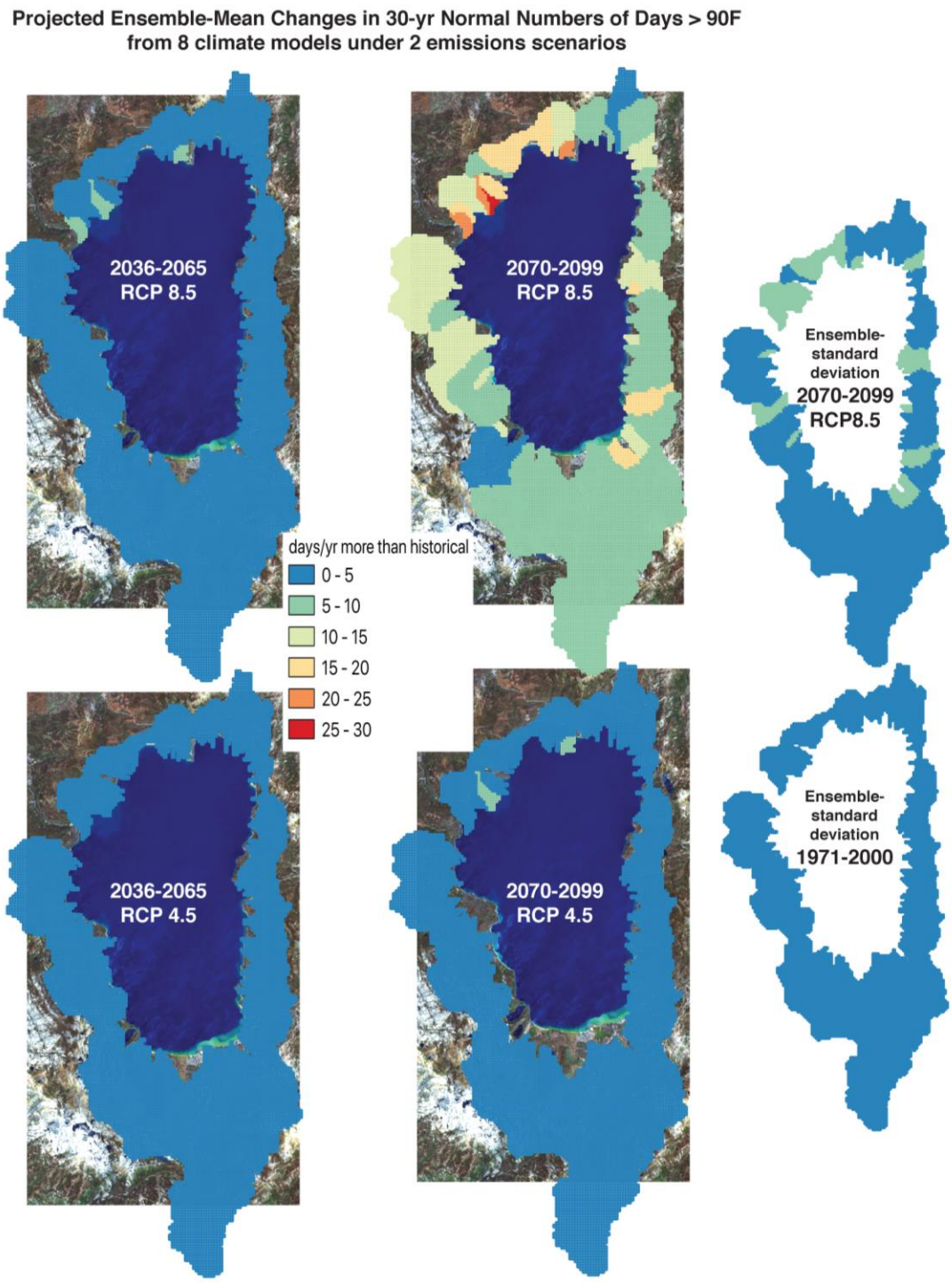

Figure 4.4. Ensemble-mean projections of additional numbers of days with temperatures above 90F over the Lake Tahoe basin, as projected by eight climate models, with ensemble-standard deviations indicated in rightmost panels.

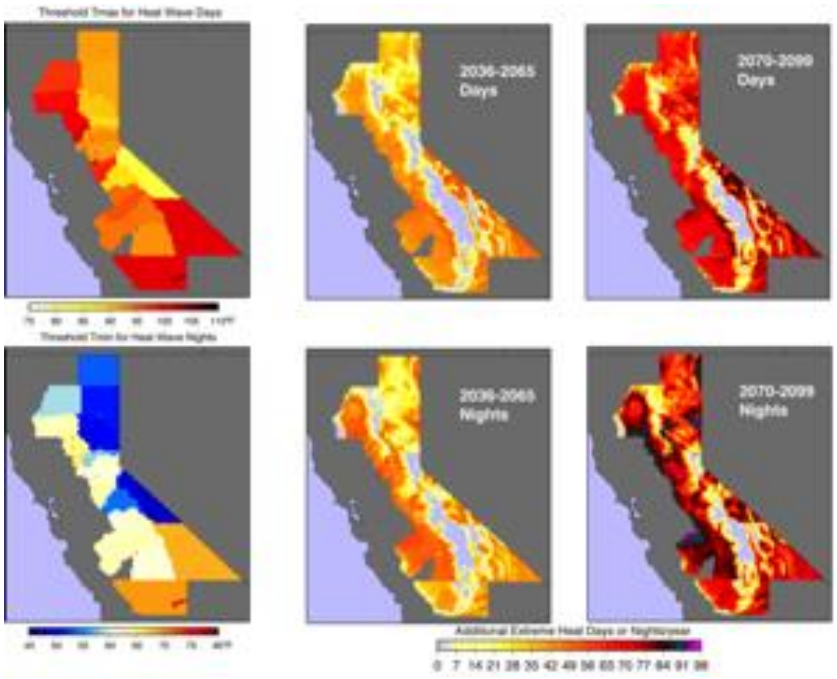

Figure 4.5. Ensemble-mean projections of increases in numbers of heat wave days and nights under the RCP8.5 scenario, with county scale heat-wave thresholds indicated in leftmost panels. Calculations produced for Sierra Business Council's ongoing (as of April 2022) Climate Vulnerability Assessment.

Similar patterns are present in the projections of changes in numbers of nights with temperatures above 60ºF, in Figure 4.6.

The ensemble-mean projected changes in normal total-annual precipitation are shown in Figure 4.7. Notice that there is more subbasin-to-subbasin variations in these ensemble-mean changes than was indicated in Figure 4.3, which reflects the greater influence of local weather, and changes in that local weather, when it comes to precipitation than for temperatures in the current downscaled-projection ensembles. Broadly speaking, under the largest greenhouse-gas increases (RCP8.5 by the 30-yr period centered on 2085, top-center panel), precipitation increases somewhat more in the northeast corner of the Basin than elsewhere. However, also, notice that the ensemble-standard deviations by late-century (upper rightmost small map) are everywhere larger than the projected mean changes, indicating that there is little agreement among the eight climate models as to even the direction (more precipitation vs less) of the change. Thus, the change in total precipitation remains an uncertain feature of the future climate, albeit a change that is relatively small, on the order of perhaps -10% to +15% by late century. Very likely, much of the change indicated in Figure 4.7 reflects long-term precipitation fluctuations of the sort that historically characterize California's hydroclimate, together with—and embedded within—mostly modest climate-change driven trends. The upshot is that precipitation changes may vary within the Basin, but these projections overall lack confidence.

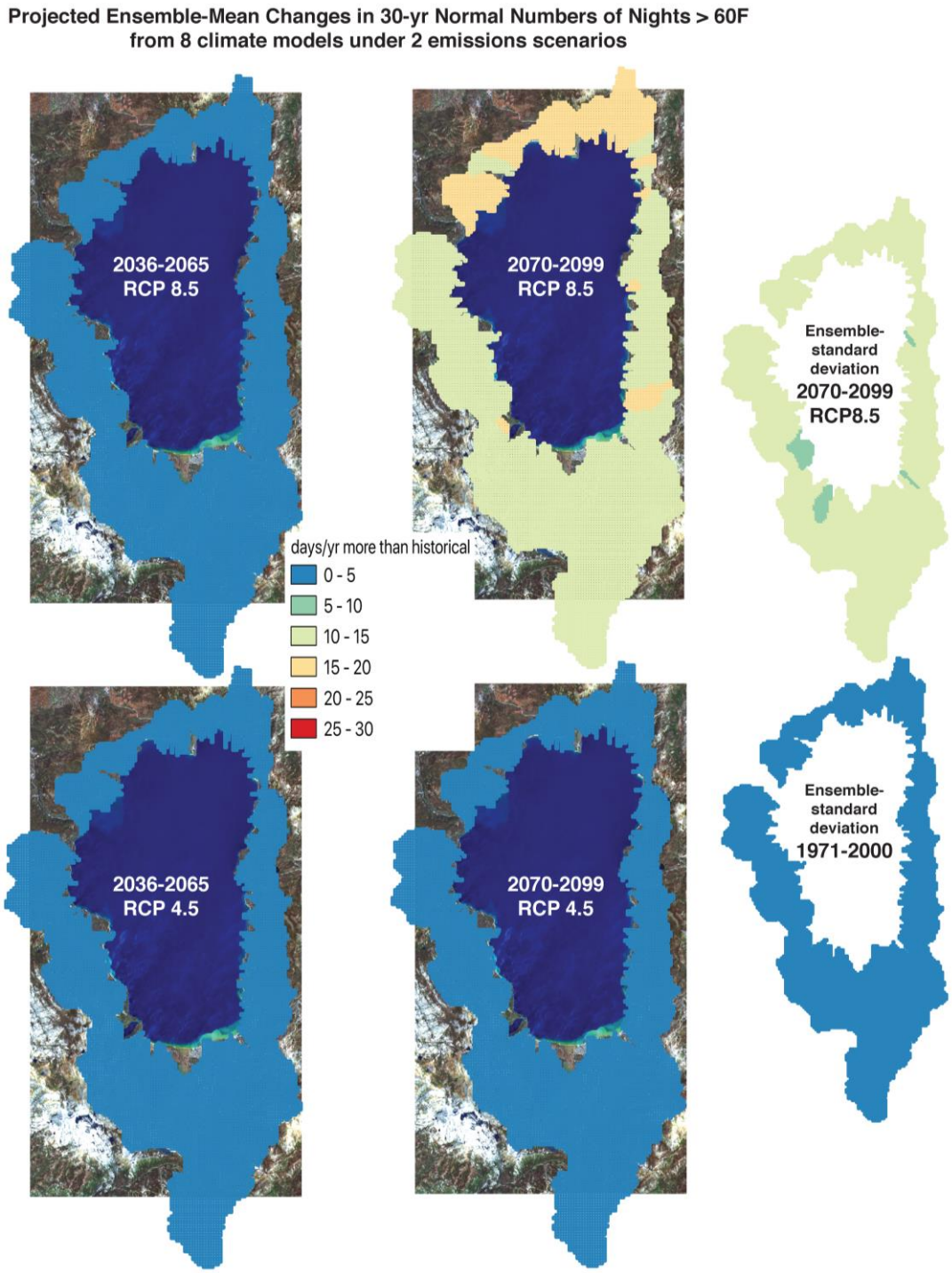

Figure 4.6. Ensemble-mean projections of additional numbers of nights with temperatures above 60ºF over the Lake Tahoe basin, as projected by eight climate models, with ensemble-standard deviations indicated in rightmost panels.

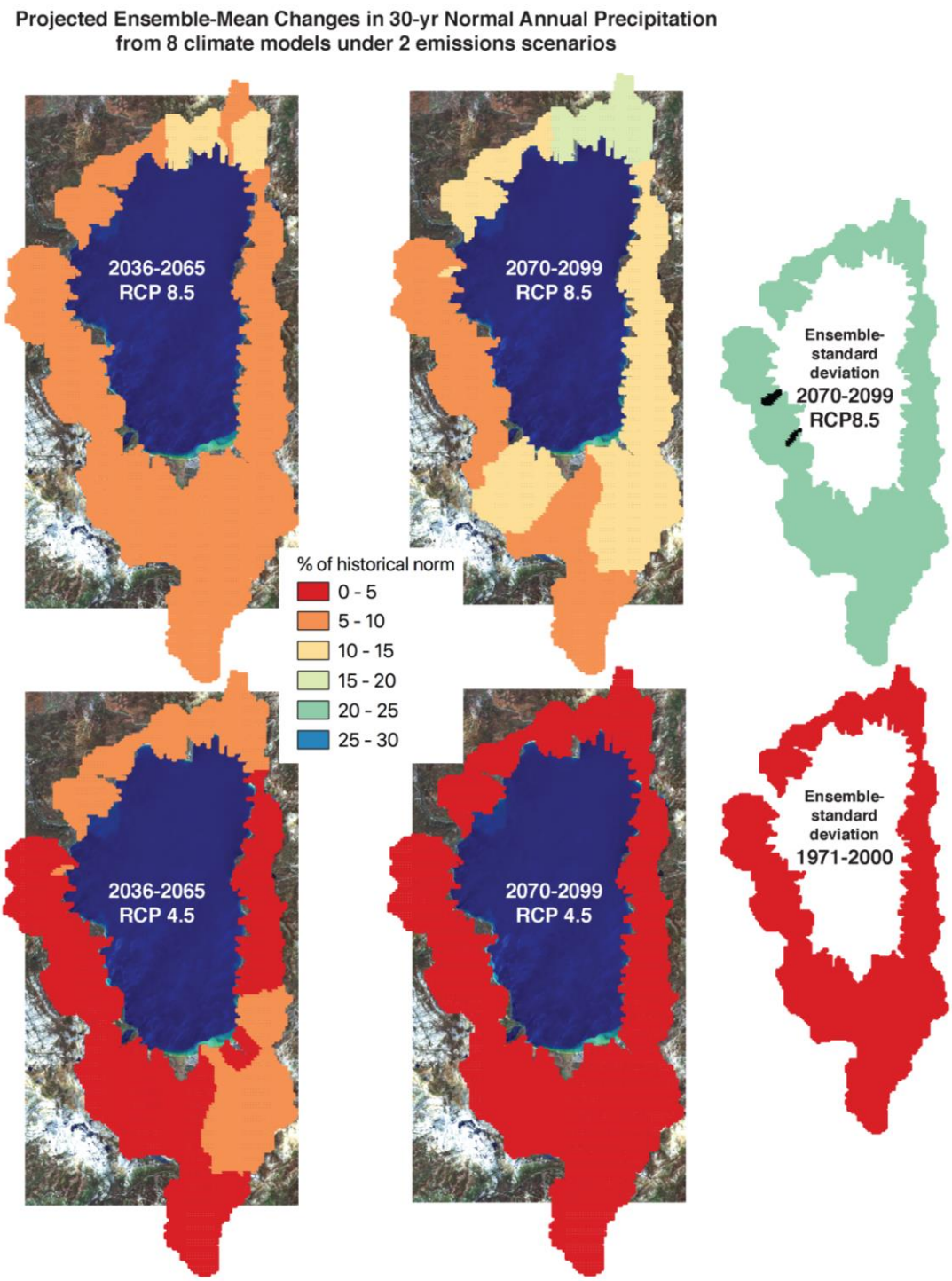

Figure 4.7. Ensemble-mean changes increases in 30-yr normal annual precipitation totals over the Lake Tahoe basin, as projected by eight climate models downscaled and run through the basin PRMS model. See caption of Figure 4.3 for further description.

But, why are all these ensemble-mean changes in precipitation normals i*ncreases*? This moistening reflects the large-scale pattern in the ensemble of GCM projections prior to downscaling, and is a feature that has been present in the past two generations of climate projections explored in past IPCC assessments and the past two National Climate Assessments (NCA3 and NCA4; Walsh *et al.*, 2014, and Hayhoe *et al.*, 2018, respectively). In these NCAs, somewhat more climate models yielded wetter futures for northern California than drier, but there were a fair number of models in both categories. There is still considerable model-to-model uncertainty, and there is no guarantee that the next generation of climate projections will not switch to including more models that are drier than wetter, but the results shown here reflect the projections available at the time of the present study. Notice that in Figure 4.8, for each NCA (and generation of climate projections), the Tahoe Basin has been either on the edge between regions that are projected to become wetter versus drier, or else in the region projected to get wetter (as in NCA3 and NCA4 used in the present study). But also notice that in NCA2 (Karl *et al.*, 2009), the Basin lay in the region of general drying, and indications from the upcoming NCA5 are that the Basin lies in an area projected to straddle the line between wetter and drier. Thus our uncertainties as to the future of total precipitation amounts in the Basin are still large after the past dozen years of research on this topic.

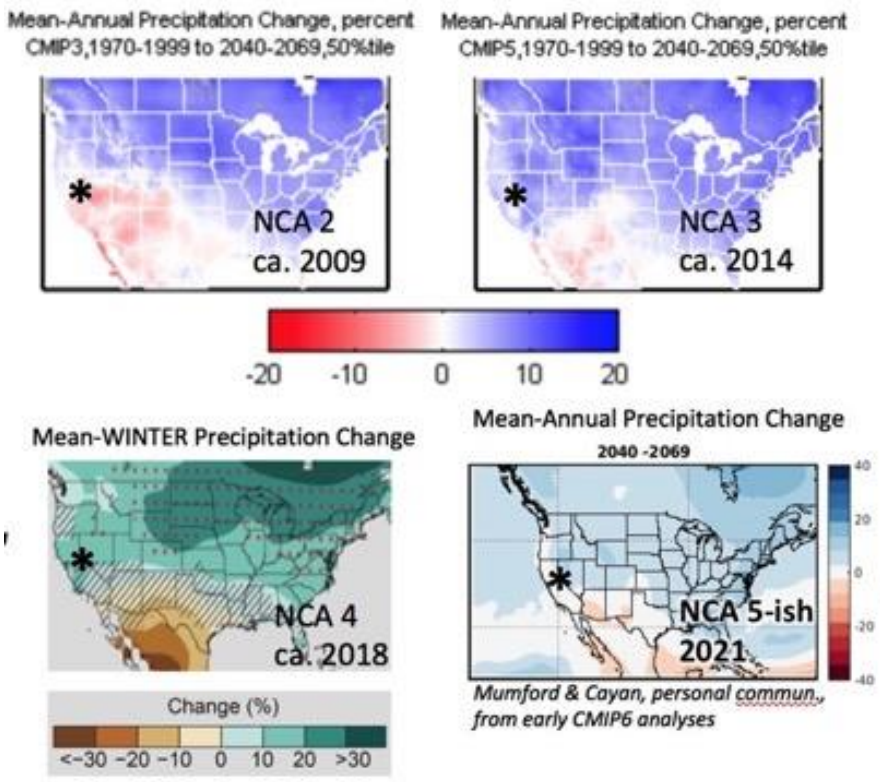

Figure 4.8. Ensemble-mean projections of precipitation change from the second, third and fourth US National Climate Assessments (NCAs), as well as an early indication of the ensemble-mean projections for the upcoming fifth NCA. Each panel presents results from a different ensemble of climate models and projections. Asterisks indicate Tahoe Basin.

Although annual precipitation totals do not change much *on average*, the year-to-year fluctuations of annual precipitation are projected to increase in amplitude as the century passes, as suggested in Figure 4.2. This pattern of increasing year-to-year variations describes a future with more extreme wet years and more extreme dry years, and what Daniel Swain has described as "climate whiplash" (Swain *et al.*, 2018). Generally speaking, it is a future that is mostly droughtier interrupted by occasional very wet years, not unlike an enhanced version of the dry-wet-dry annual-precipitation fluctuations of the past decade, wherein water year 2011 was very wet, 2012-2016 were a major drought, 2017 was extremely wet, 2018 dry, 2019 wet, and now 2020-2022 another major drought. Figure 4.9 shows the projected changes in the standard deviations of year-to-year precipitation fluctuations. In this figure, in contrast to the small maps in Figure 4.7, the "30-yr standard deviations" mapped are the average over the eight climate models of the year-to-year standard deviations of annual precipitation; that is, rather than being an indication of how well the models agree, this figure shows how much the year-to-year precipitation variability is projected to increase (on average over the eight models).

Although the projected total-precipitation changes are relatively small, it is worth evaluating whether there are major changes in either the timing of precipitation or the largest precipitation extremes in the projections because snowpack and streamflow timing will play important roles in the next chapter and they could be influenced by changes in when precipitation arrives. Figure 4.10 shows projected changes in the timing of the "center of mass" of precipitation timing within the Basin (see the discussion in section 3 and Figure 3.8 for an explanation of this particular metric for streamflow timing). Figure 4.10 shows that the normal overall distribution of precipitation timing within the year shifts to somewhat later in the year by late-century, by about a week. However, this shift is smaller than the ensemble-standard deviations, indicating that—like the projected changes in precipitation totals—the timing of precipitation does not change much nor consistently in the ensemble of precipitation projections considered here.

Although neither the precipitation totals nor the precipitation timing are projected to change much or consistently among the climate models used here, the magnitude of precipitation extremes are projected to increase. Figure 4.11 shows the projected increases in the 30-yr normal 3-day maximum precipitation totals under the two emissions scenarios. By late-century under the RCP4.5 scenario, the normal annual 3-day maximum precipitation maxima increase by an average of about 15-20% across most of the basin, compared to ensemble-standard deviations less than 10%, with some less confident suggestions of less increase near Meyers and along the eastern edge of the basin. Under the more extreme RCP8.5 scenario, these precipitation extremes increase by 15-25%, with indications of maximum increases around the Stateline and Incline Village corners of the Basin.

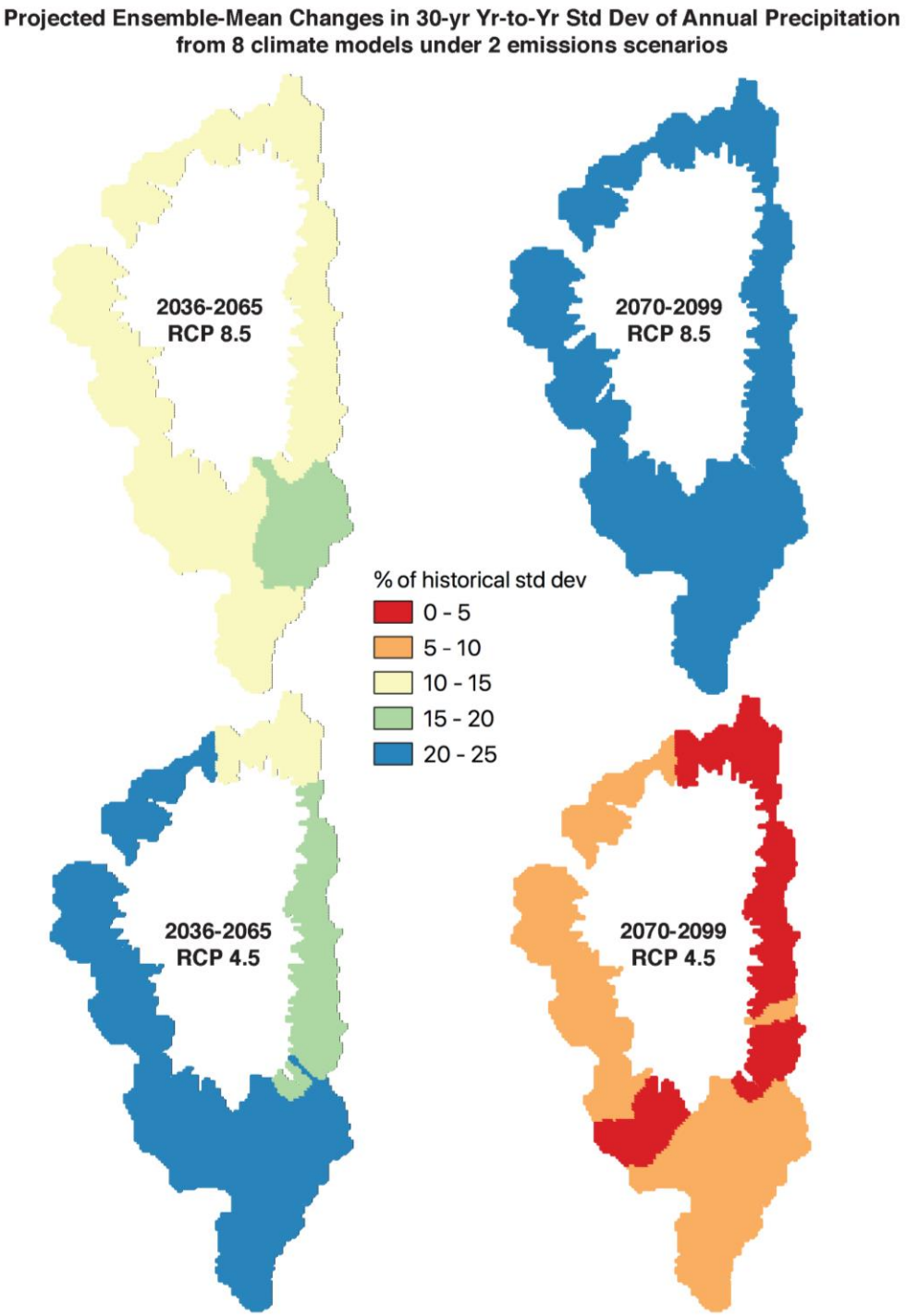

Figure 4.9. Ensemble-mean increases in 30-yr standard deviations of year-to-year annual-precipitation totals over the Lake Tahoe basin, as projected by eight climate models downscaled and run through the basin PRMS model. See caption of Figure 4.3 for further description.

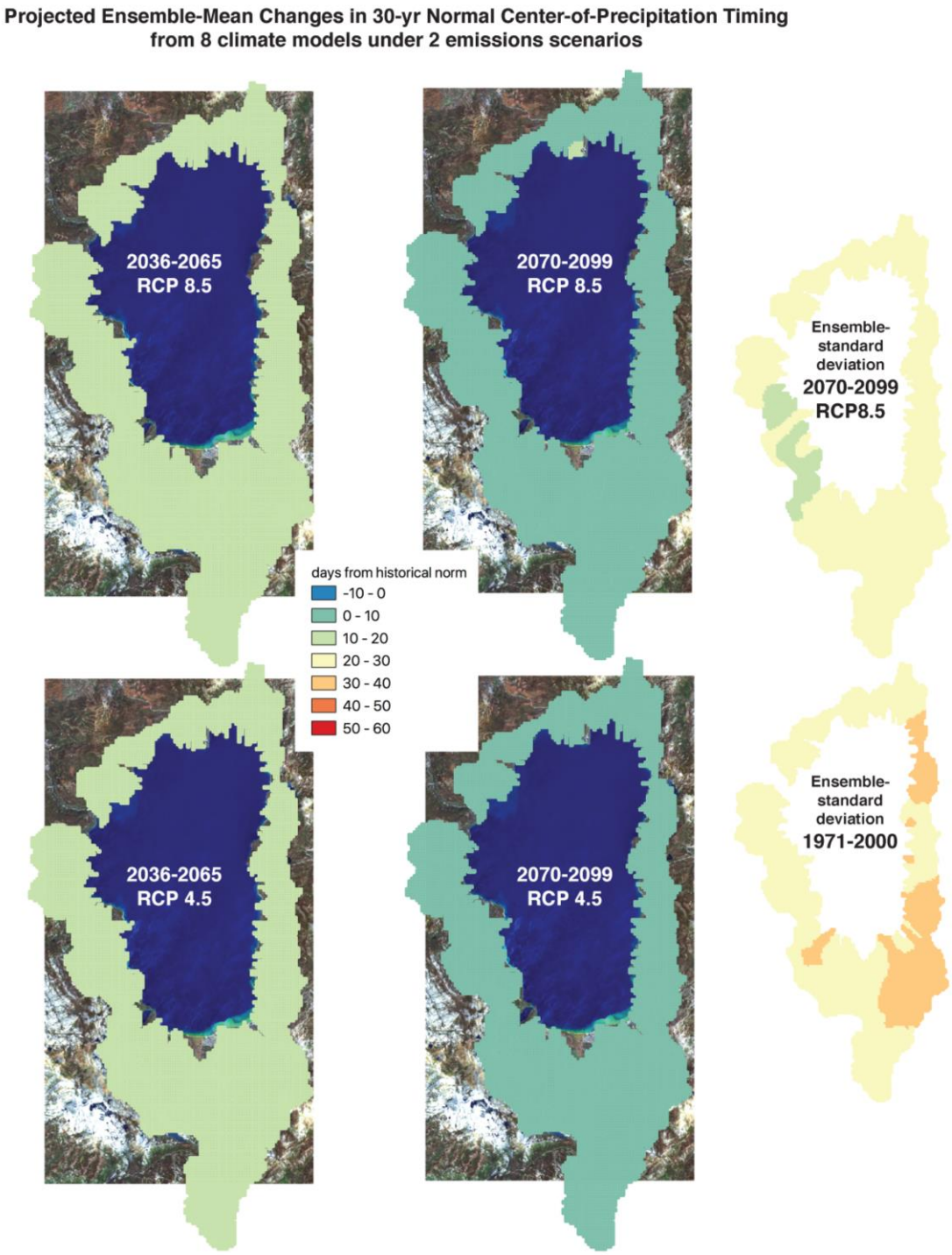

Figure 4.10. Ensemble-mean changes in 30-yr normal center-of-precipitation-mass timing over the Lake Tahoe basin, as projected by eight climate models downscaled and run through the basin PRMS model. See caption of Figure 4.3 for further description. The color bar here is extended to allow comparisons, later, with much larger changes in the center-of-streamflow timing.

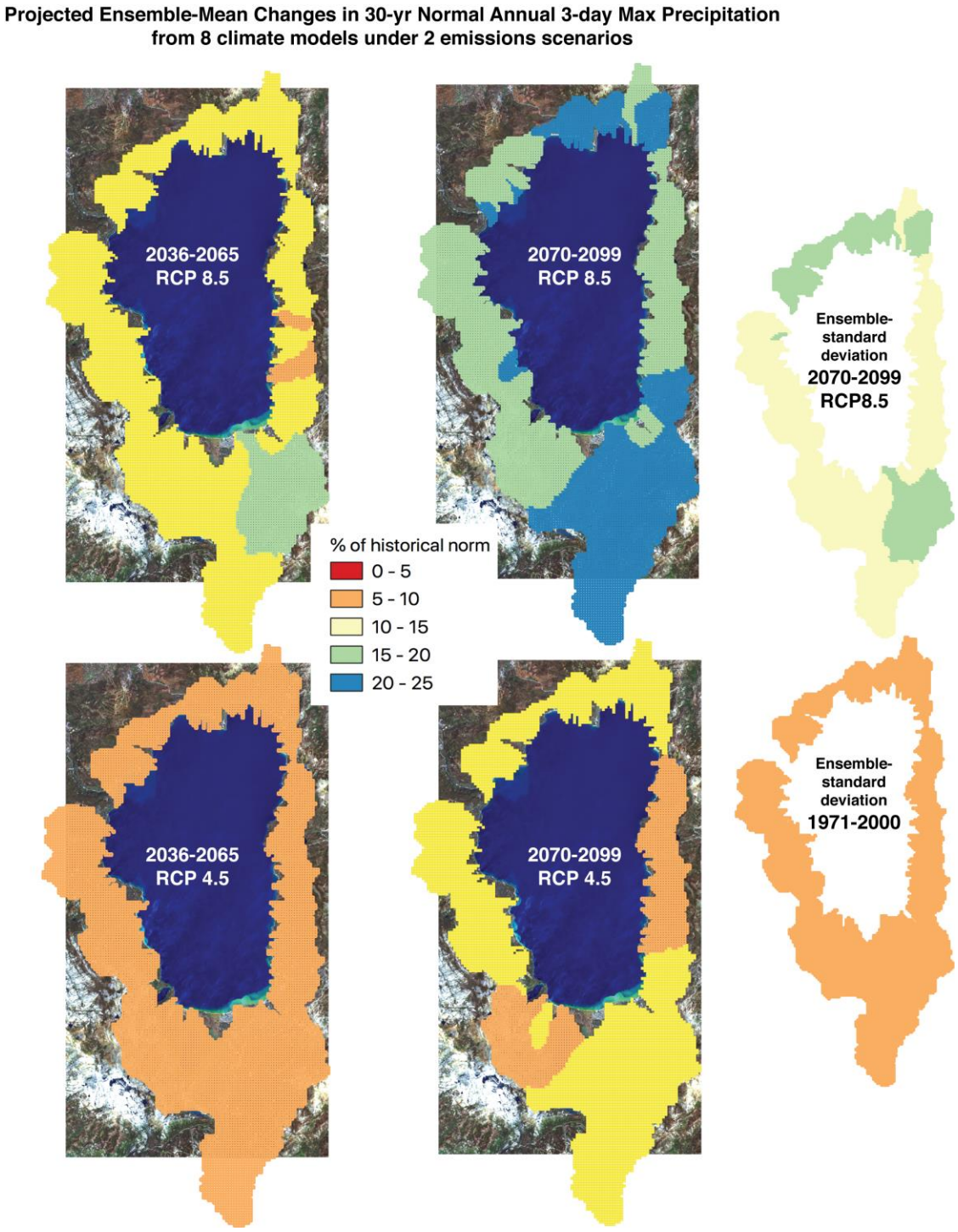

Figure 4.11. Ensemble-mean increases in 30-yr normal annual 3-day maximum precipitation amounts over the Lake Tahoe basin, as projected by eight climate models downscaled and run through the basin PRMS model. See caption of Figure 4.3 for further description.

Thus, broadly speaking, the ensemble of climate projections that will be used to drive the hydrologic model of the Basin include (1) large, confident, emisisons-dependent, spatially nearly-uniform levels of warming up to 5–8ºF by late century, (2) modest (compared to historical and future natural variability) increases in total precipitation with small if any changes in overall precipitation timing, and (3) notable increases in the precipitation magnitude of the largest storms by as much as 25% of their historical norms. Next we will present and explore the simulated hydrologic consequences of these changes.

5. PROJECTED SNOW AND STREAMFLOW RESPONSES

With significant warming and modest changes in precipitation, the most obvious hydrologic changes that emerge from the hydrologic simulations of the Tahoe Basin are changes in snowpack and snowmelt runoff. Historically, a particularly important metric of year-to-year snowpack variation is the amount of water stored in snow on April 1 of any given year. April 1 snow-water equivalent (SWE) is the amount of liquid water that would be obtained by capturing and melting all the snow stored on a given patch of land on that date, represented as a depth of water (e.g., in inches of liquid water) spread evenly over the patch. April 1 SWE gives an idea how much (and how long) an area's snow is present at this set time of year that historically has been considered roughly when the maximum amount of water availability is present in most years across the Western US. It is used to forecast how much snowmelt-dominated streamflow is to be expected through the remainder of spring and summer by agencies like California Department of Water Resources, the NOAA California-Nevada River Forecast Center, USDA Natural Resources Conservation Service, and Los Angeles Department of Water and Power.

An example of the simulated historical and future April 1 SWEs for the Third Creek subbasin is shown in Figure 5.1, illustrating the rapid and inevitable (if warming continues) decline in beginning-of-spring snowpack in the Tahoe Basin. The projected 30-yr average changes in April 1 SWE across the Basin are mapped in Figure 5.2. The projected changes are considerably larger than the ensemble-standard deviations throughout the basin, indicating a high level of confidence in the direction and magnitude of the changes. On the whole, April 1 SWE amounts decline by 60-80% or 80-100% of historical norms by late century, depending on the greenhouse-gas emissions that occur. Within the basin, losses of April 1 SWE are projected to be more severe on the drier and more south- and west-facing northern and eastern subbasins (Figures 2.8 and 2.10), with smaller fractional declines on the opposite (southern and western) ramparts of the Basin.

These April 1 SWE changes are part of, and in part reflect, changes in the overall amount of time that snow covers the landscape. Figure 5.3 shows projected declines in length of "snow seasons" (the definition used here is in the figure and caption), and illustrates some very large reductions in the length of time each year when subbasin-averaged snow depths more than about 10 inches will be present. This matters for how streamflow will evolve as well as for future winter-season tourism. Depending on the emissions scenario, Tahoe snow seasons may decline

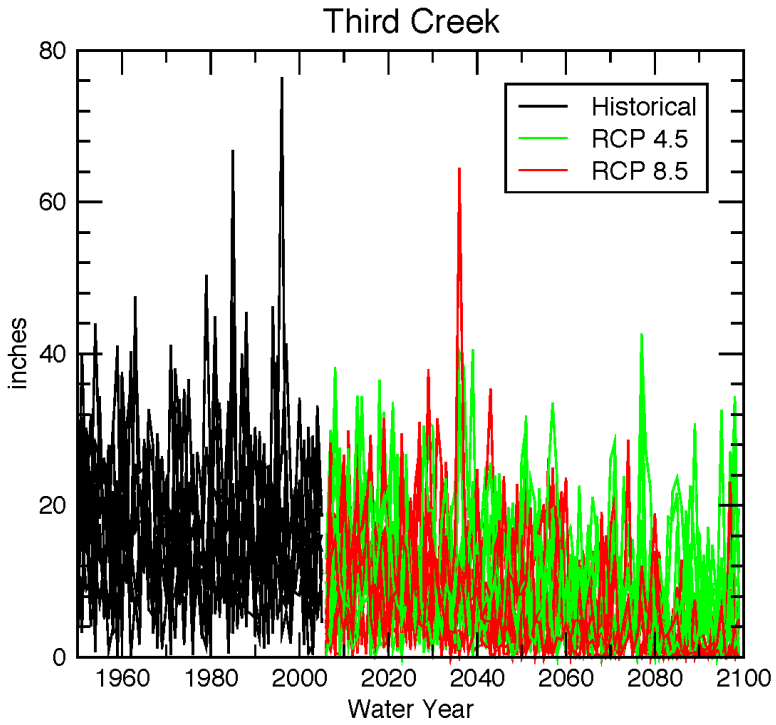

Figure 5.1. Ensemble of April 1 snow-water equivalents in the Third Creek subbasin, as projected by eight climate models downscaled and run through the basin PRMS model.

by more than four months to become nonexistent in some places, on 30-yr average. Generally, snow-season length declines more in the western subbasins, in part because they are longer there in the historical period (so there is more "length" to be lost), and losses can be as much as 80 days more than in some subbasins on the east side.

Another metric of when the "best" snow will cover the Tahoe Basin is the center of mass of snowmelt timing (Figure 5.4), recalling the center of mass of precipitation considered in Figure 4.9. Once snowmelt is well underway, snow conditions for winter sports can be dismal, and the center of snowmelt timing provides a metric of how much earlier snowmelt will come overall. Although the center of precipitation timing did not change significantly in the projections, snowmelt is projected to arrive about one to two months earlier in response to the future warming trends. This change reflects multiple influences of warming: Warming causes precipitation to fall more often overall as rainfall (rather than snowfall), it leads to more winter-time warm-weather or rainy episodes when midwinter melting occurs (intermittently), and it accelerates the arrival of (historical levels of) spring-time warmup and hastens the arrival of the final snowmelts. As with snow-season length, the largest changes (towards earlier snowmelt overall) are projected for the western subbasins. Recall that, if anything, precipitation timing was projected to come later overall (albeit only slightly) so that these large changes in snowmelt timing are entirely a consequence of warming rather than precipitation changes.

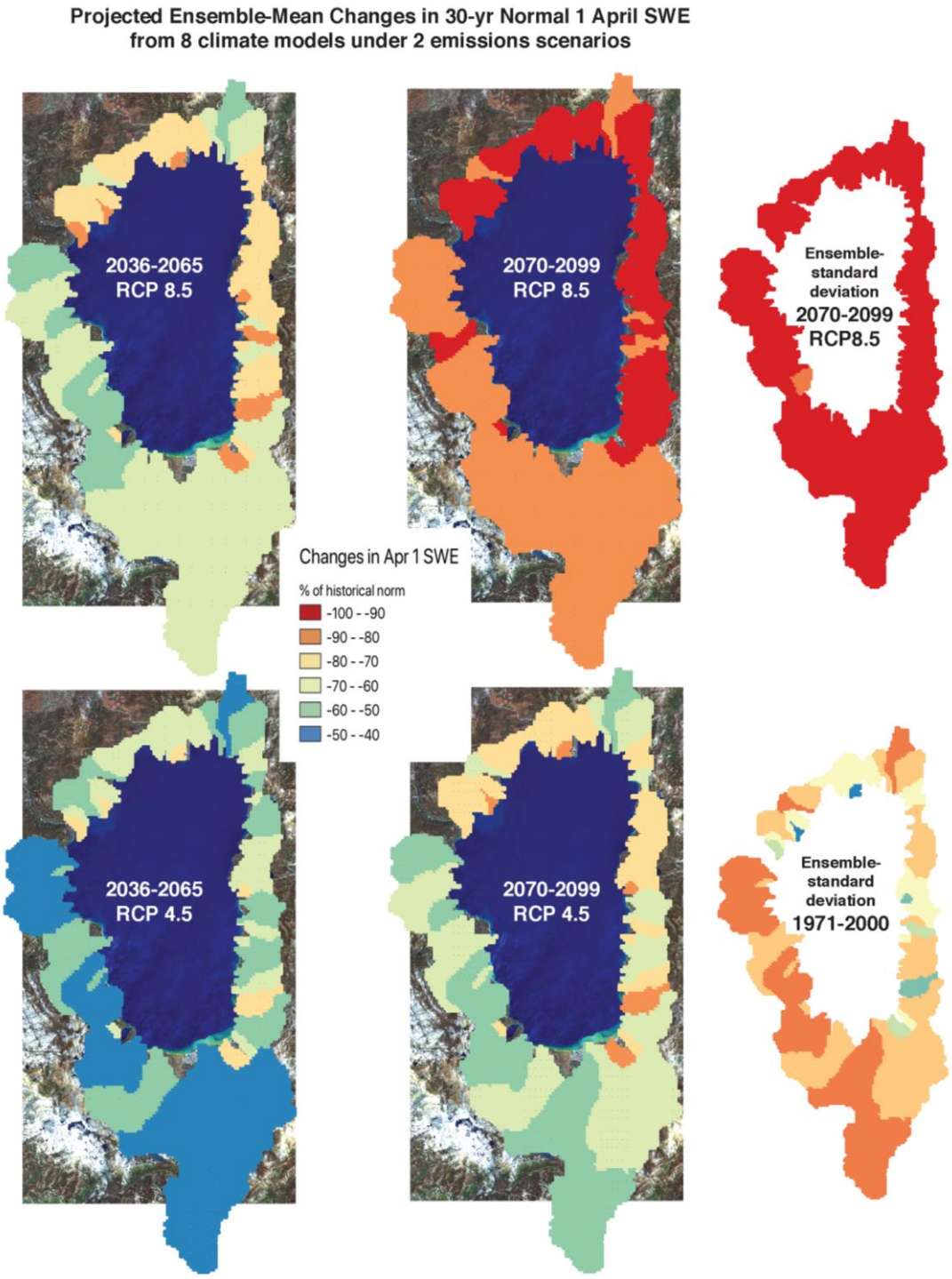

Figure 5.2. Ensemble-mean declines in 30-yr normal April 1 snow-water equivalents (SWE) over the Lake Tahoe basin, as projected by eight climate models downscaled and run through the basin PRMS model. See caption of Figure 4.3 for further description.

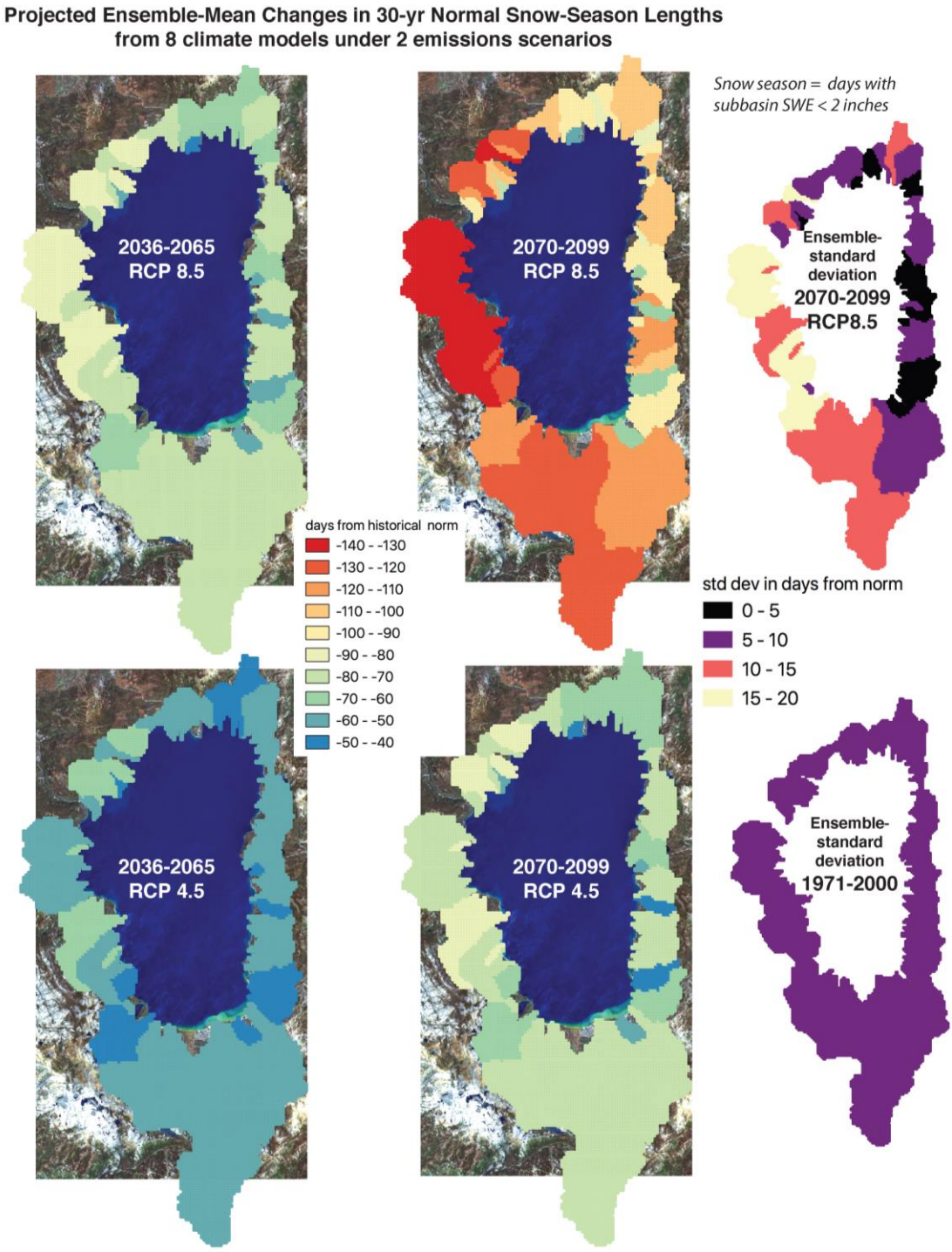

Figure 5.3. Ensemble-mean declines in 30-yr normal "snow-season lengths" over the Lake Tahoe basin, as projected by eight climate models downscaled and run through the basin PRMS model. Snow-season length is defined here as the longest period during which the subbasin-average SWE is more than 2 inches (suggesting subbasin snow depths of greater than 10 inches), in days per year. See caption of Figure 4.2 for further description.

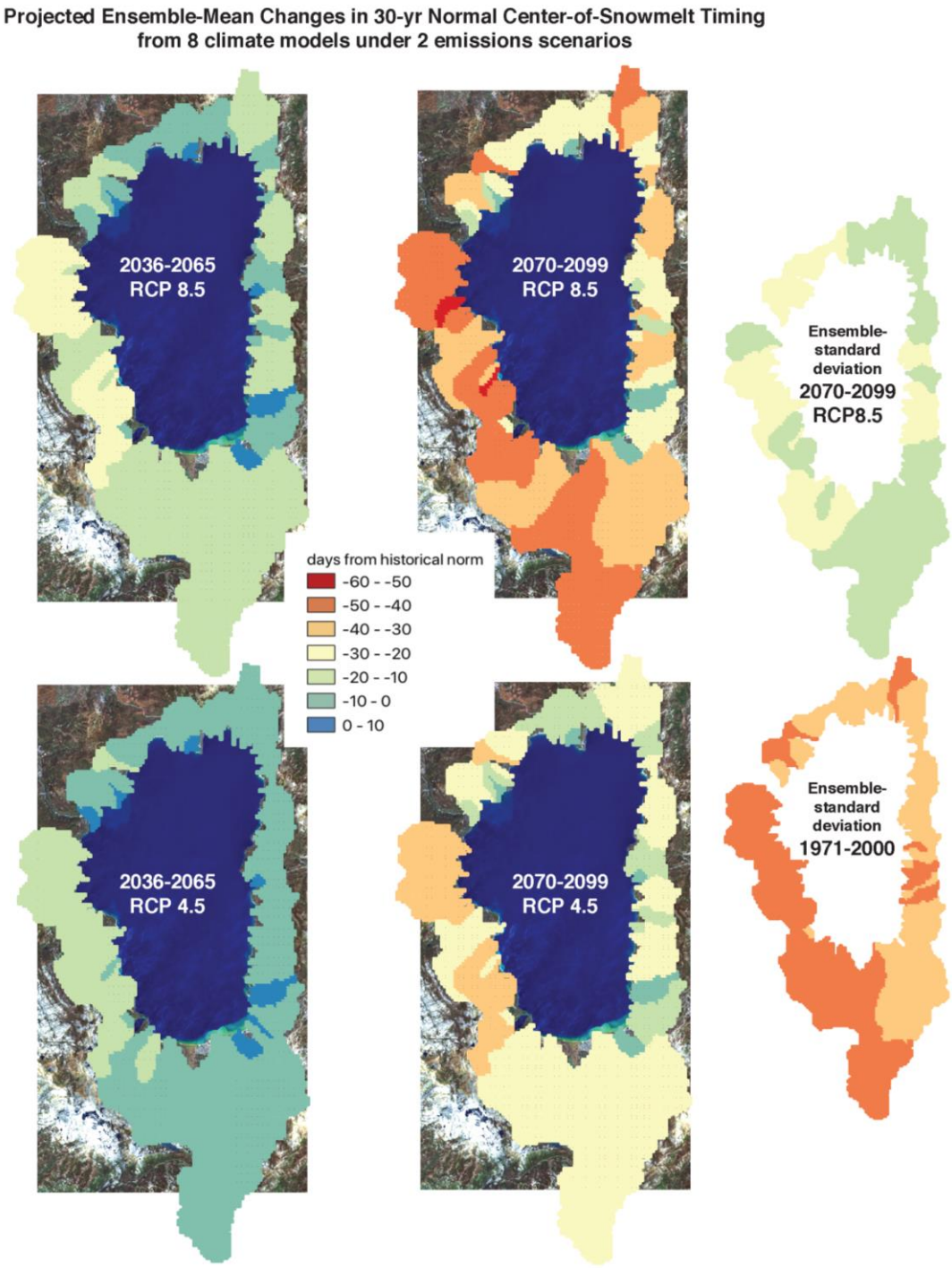

Figure 5.4. Ensemble-mean changes in 30-yr normal center of snowmelt timing over the Lake Tahoe basin, as projected by eight climate models downscaled and run through the basin PRMS model. See caption of Figure 4.3 for further description.

Each year in the Tahoe Basin essentially all snow has melted by summer's end, so the total of all snowmelt over the course of a full year is the same as the overall total amount of water that has accumulated in snowpacks over the course of that year. Therefore one way of answering the question "how much snow is there around the Basin as the century passes" is to consider the annual totals of snowmelt. Figure 5.5 shows the ensemble-mean declines in 30-yr normal snowmelt under the two emissions scenarios. Under the severe RCP8.5 emissions scenario, total snowmelt declines by between about -25 to -50% by late century, with the largest percentage reductions occurring mostly in the west-facing and drier northern and eastern subbasins. Under the less severe RCP4.5 scenario, reductions are mostly in the -10 to -20% range, with less differentiation between the various sectors of the Basin.

Figure 5.6 shows the changes in year-to-year standard deviations of total-snowmelt fluctuations (in parallel with Figure 4.9). As the 30-yr average total amount of snow (and thus snowmelt) in the Basin declines in these projections, the year-to-year fluctuations are also inclined to decline in amplitude. However, where (and when) the declines in total snowmelt are small, the increased volatility of annual precipitation amounts (Figure 4.9) result in small increases in year-to-year snowmelt variability. Thus, on the west side of the Basin, year-to-year snow-amount fluctuations actually increase, whereas along the northern and eastern subbasins, year-to-year fluctuations decline more or less along with average snowmelt amounts.

Snowmelt has historically been a particularly important contributor to streamflow in the Basin, so it is relevant to finally consider projections of streamflow change. As with snow, one of the most important outcomes of warming in the Basin will be changes in streamflow timing. As the snowfall transitions into rainfall, streamflow arising from snowmelt will decline in favor of more (winter) rainfall runoff. Snowmelt also will occur earlier. Figure 5.7 shows the projected changes in streamflow center-of-mass timing, paralleling again the center-of-mass timing metric used in Figure 4.9. Because the west subbasins are generally wetter and snowier, the largest shifts in runoff timing are projected for the western (and increasingly the southwestern subbasins) where center-of-streamflow timing comes between about 30 and 50 days earlier by late century, compared to 10 to 30 days earlier in the eastern and northern subbasins. These numbers are in broad agreement with projected streamflow-timing changes in Dettinger *et al.* (2018) for the northern Sierra subregion, as well as from numerous studies since at least Stewart *et al.* (2004).

Figure 5.8 shows projected water-year totals of streamflow at Upper Truckee River and Third Creek, as examples of how streamflow totals evolve under the projected climate changes. Various aspects of the changes shown will be discussed below. In particular, although warming is projected to increase atmospheric demands for evapotranspiration (potential evapotranspiration; McEvoy *et al.*, 2020), and thus might be expected to reduce runoff, annual total streamflow is projected to increase around the Basin (Figure 5.9). The modest increases in precipitation (only up to about 20% of historical normal, Figure 4.6) that characterize this particular ensemble of projections contribute to some of these increased streamflow amounts. But, in addition, projections of streamflow from the Sierra Nevada under warming scenarios

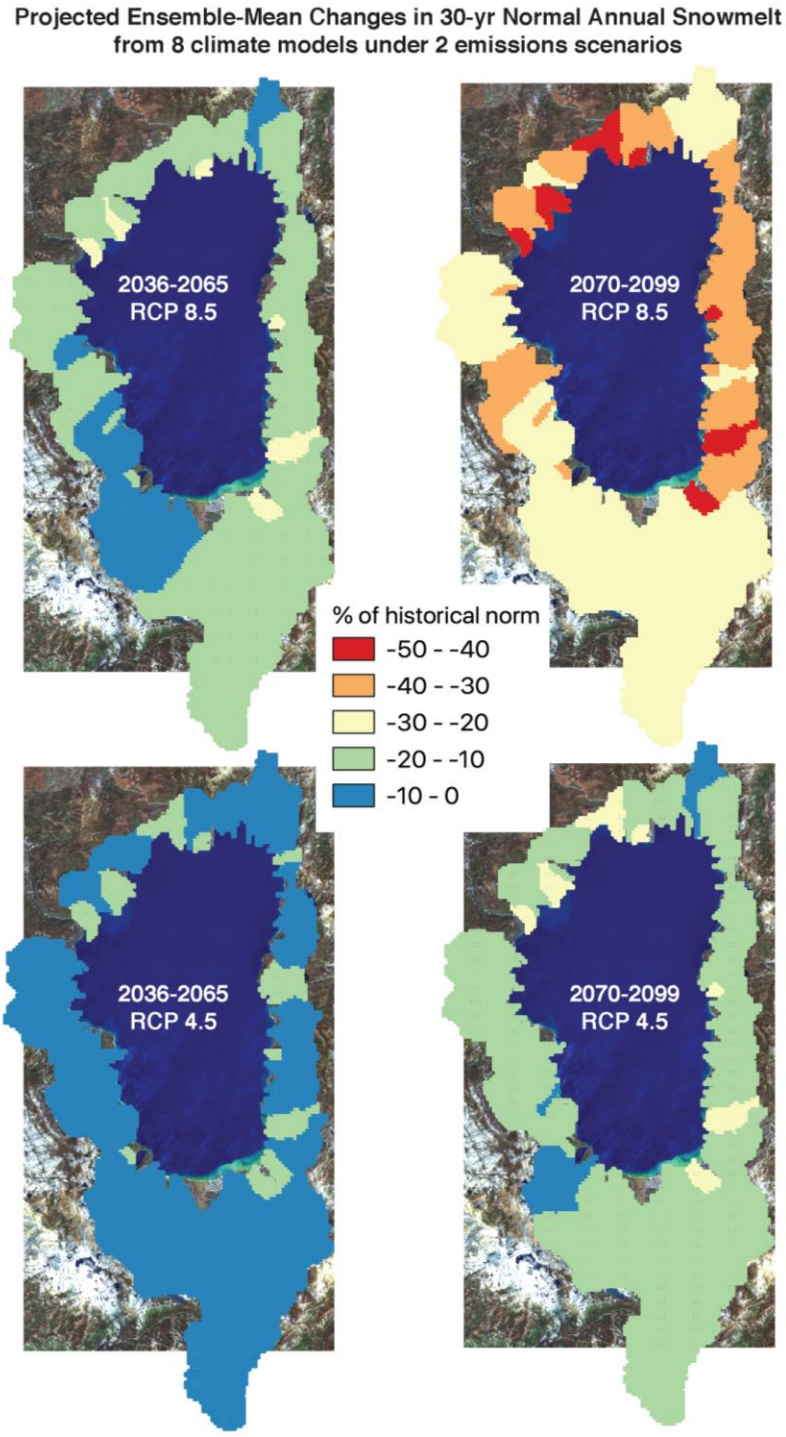

Figure 5.5. Ensemble-mean declines in 30-yr normal annual snowmelt totals over the Lake Tahoe basin, as projected by eight climate models downscaled and run through the basin PRMS model. See caption of Figure 4.3 for further description.

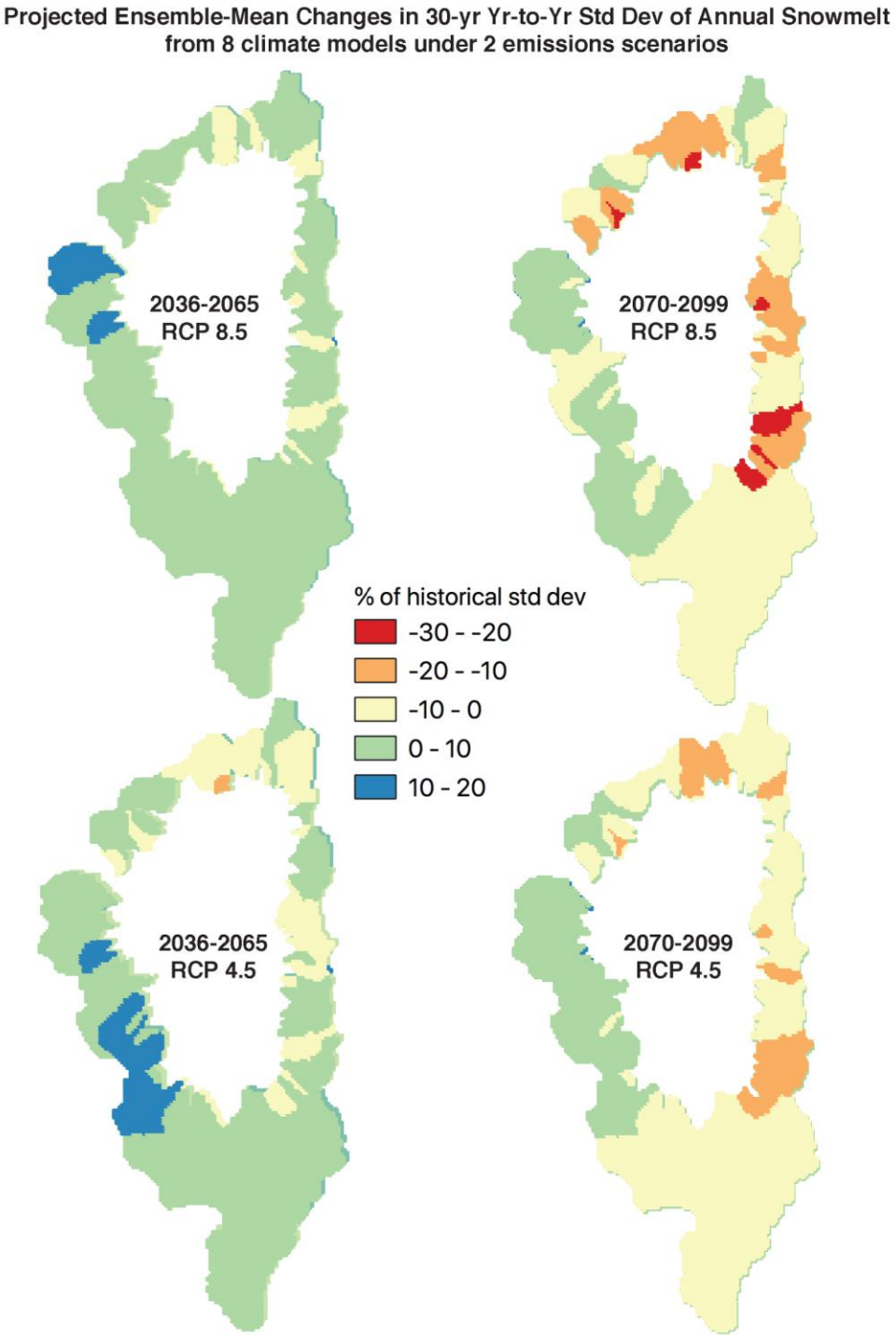

Figure 5.6. Ensemble-mean changes in 30-yr standard deviations of year-to-year annual-snowmelt totals over the Lake Tahoe basin, as projected by eight climate models downscaled and run through the basin PRMS model. See caption of Figure 4.3 for further description.

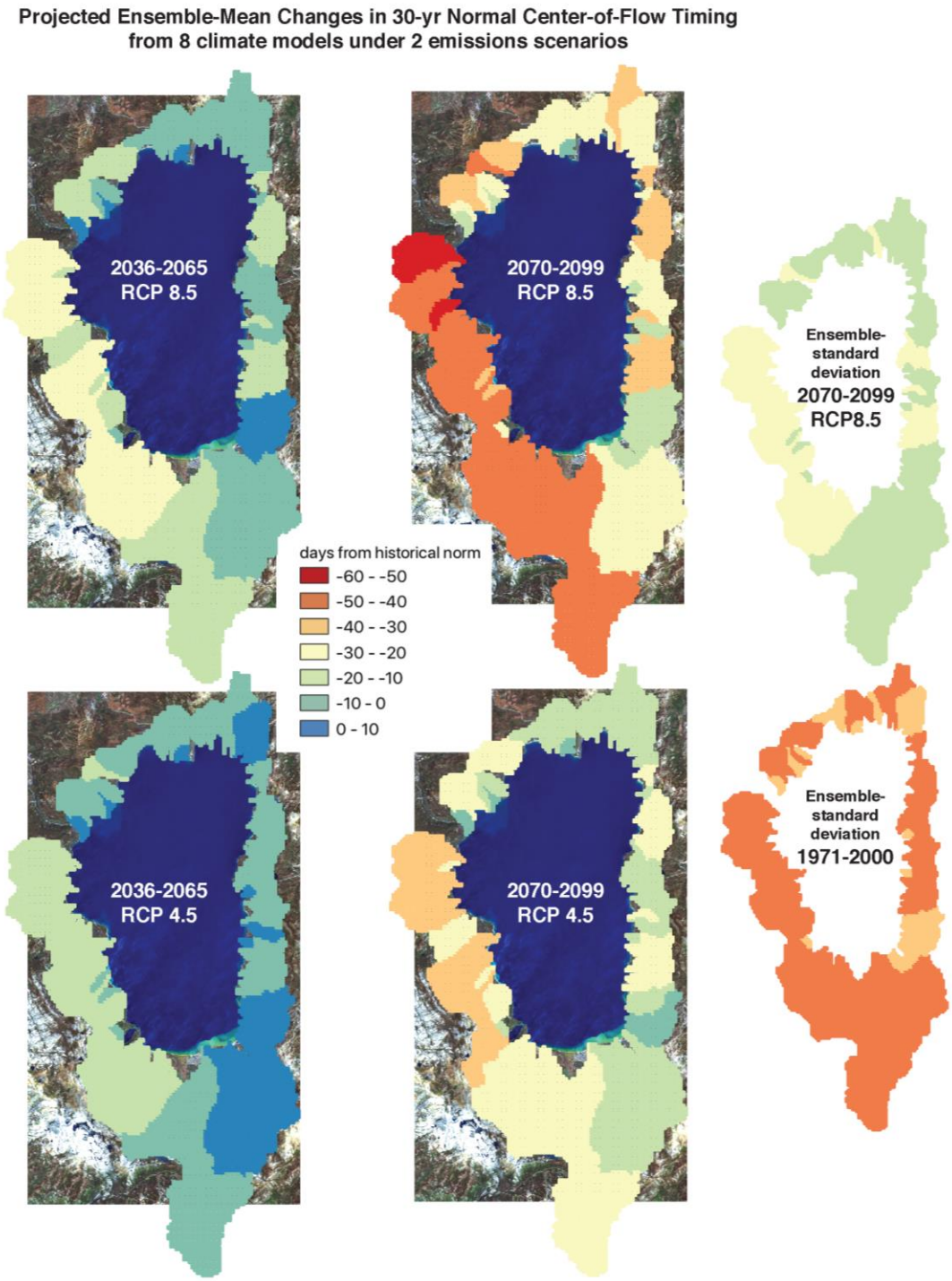

Figure 5.7. Ensemble-mean changes in 30-yr normal center of streamflow timing over the Lake Tahoe basin, as projected by eight climate models downscaled and run through the basin PRMS model. See caption of Figure 4.3 for further description.

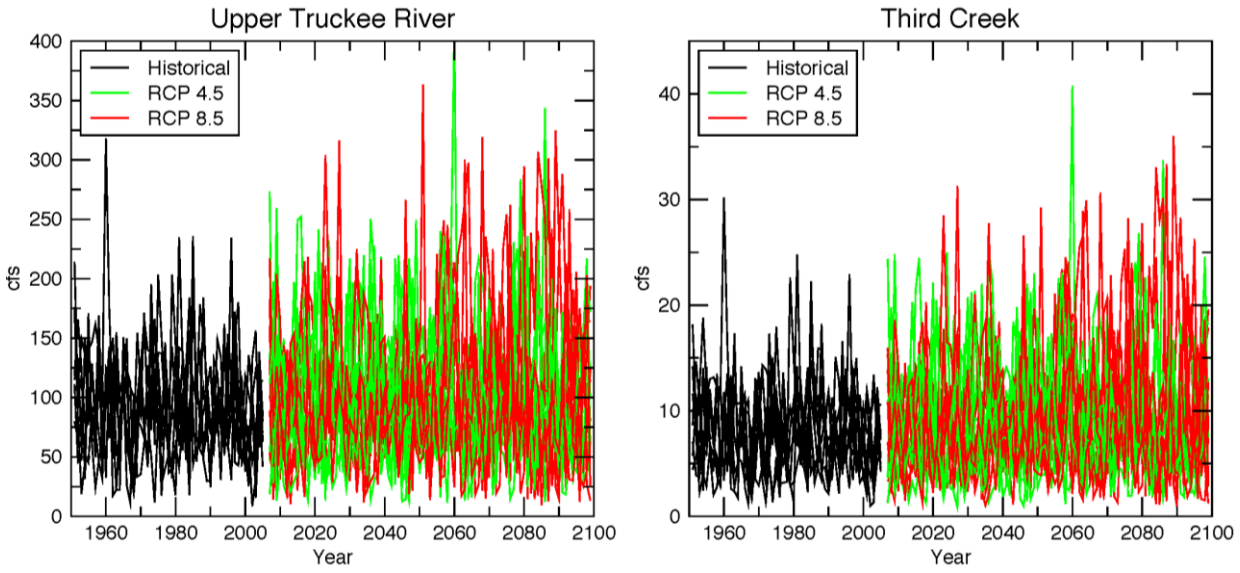

Figure 5.8. Ensemble of water-year streamflow totals in Upper Truckee River and Third Creek, as projected by eight climate models downscaled and run through the basin PRMS model.

have long been notable for the fact that total runoff responds weakly to warming alone (Jeton *et al.*, 1996, and Dettinger *et al.*, 2004, using PRMS models near—but not at--Tahoe; Das *et al.*, 2011 using a different model). Most recently, Ban and Lettenmaier (2022) have found (using different hydrologic models in different basins) that the trends toward earlier snowmelt and thus earlier runoff from Sierra Nevada basins tends to "shelter" the much increased cool-season streamflows from the large summertime increases in potential evaporation that would otherwise tend to reduce warm-season runoff and streamflow enough to reduce overall outflows. This "sheltering" is accomplished by the tendency for more of the runoff to leave the subbasins during future cool seasons when potential evapotranspiration is low for seasonal reasons, and more of that runoff shows up at the Lake than would be the case if the runoff was occurring during the warm season when potential evapotranspiration in the catchments is even more rampant than historically. By the time the warm season has arrived, more of the water has already left the subbasins, depleting soil-moisture reserves, and less of the year's water (precipitation) is still around to be depleted by enhanced summertime evapotranspiration within the watersheds. (Once the water reaches the Lake, it is of course still subjected to enhanced evaporative demands, which are already rising (Albano *et al.*, 2022) and increasing evaporation totals.) The Ban-Lettenmaier (2022) sheltering is most common in western basins that have wet winters that hover closer to freezing than many other basins farther inland than the Sierra Nevada. Because of this sheltering, the moderate precipitation increases in the ensemble of projections used here end up being "magnified" somewhat in the ensemble-mean streamflow projections.

As with several other responses documented above, total streamflow from the northern and eastern subbasins are projected to respond differently from the southern and western subbasins. On the whole, the total-streamflow changes are modestly larger than the ensemble-

standard deviations in most areas (rightmost panels of Figure 5.9) but with larger ensemble-mean increases in the north and east than in south and west. Year-to-year fluctuations in total streamflow (Figures 5.8 and 5.10) increase throughout the basin, so that wet and dry excursions from the new "normals" (Figure 5.9) increase. In some subbasins, due to greater precipitation volatility, together with effects of the uneven (in time and space) transitions from snow-dominated to rain-dominated conditions, the year-to-year scale of fluctuations around the new normal streamflow amounts increase by as much as 60-70% of normal fluctuations. It is perhaps notable that these enhancements in streamflow variability—coming as they do from a mixture of ongoing hydrologic changes in the subbasins—are not as geographically smoothly varying around the Basin as other hydrologic responses illustrated above, and instead are seemingly more randomly distributed among the subbasins.

Changes in the distribution of streamflow extremes are to be expected larger than changes in annual totals. Figure 5.11 shows examples of the projected histories and futures of 3-day maximum flows in Upper Truckee River and Third Creek, and, to clarify the changes, Figure 5.12 shows the statistical distributions (essentially, histograms) of these simulated and projected 3-day maximum flows for the Upper Truckee River during the historical era and end of 21st Century (recalling that simulated Third Creek maxima are a bit suspect, as indicated by Figure 3.12). Historically most 3-day maxima are less than 1000 cfs, and under climate change, many more maxima are much larger than that threshold. Under the more severe RCP 8.5 scenario, maxima two to three times this historical "threshold" become relatively common (~1/20 years) by end of century with outliers up to 7500 cfs. Under the moderate RCP 4.5 scenario, maxima up to about 2.5 times that historical range become relatively common with outliers almost as high as in the RCP 8.5 case.

Figure 5.13 maps the projected changes in the 30-yr normal annual 3-day maximum streamflows around the Basin. By midcentury (and even in late century under the moderate RCP4.5 emissions scenario), these annual maxima increase by about 40-80% of the historical norms more or less throughout the Basin. Under the more severe emissions (RCP8.5), the annual maxima rise to about 120-160% of the historical norms. Trout Creek and streams in the northeast corner of the Basin are simulated to be "hot spots" for increase flow maxima under this more extreme scenario.

Although simulations of single-day flow maxima with the models used in this study have some weaknesses (Figure 3.12), for a variety of uses, projections of flow maxima at the finest time scales available have been a matter of great interest for stakeholders in the Basin. Thus Figure 5.14 shows projections of future one-day flow maxima around the Basin as percentages of the historical 30-yr mean maxima. Expressed in these relative terms, the patterns indicated are not so different from the changes in 3-day maxima (Figure 5.13), but the magnitudes of the increases are somewhat greater throughout the Basin.

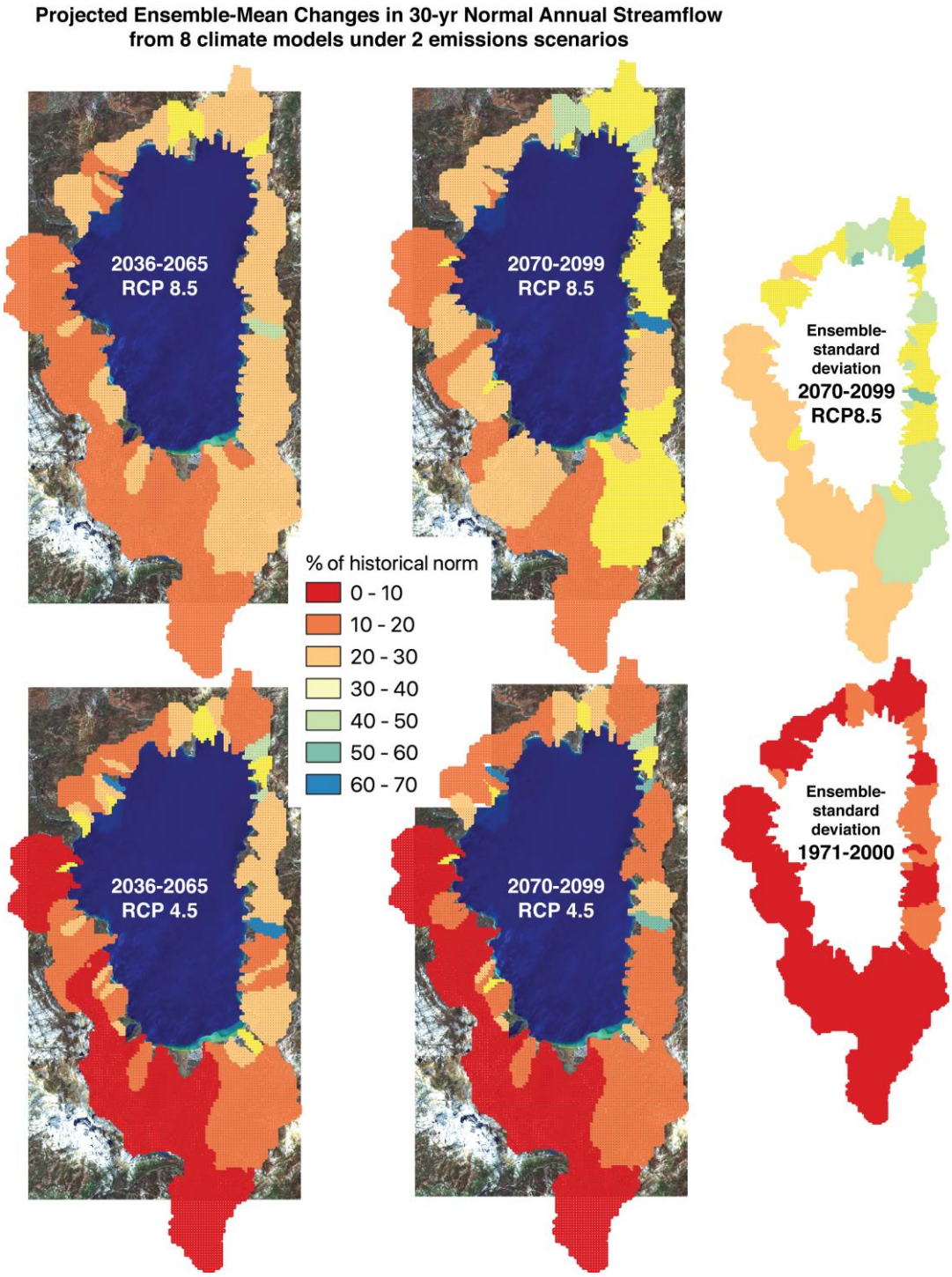

Figure 5.9. Ensemble-mean increases in 30-yr normal annual streamflow totals around the Lake Tahoe basin, as projected by eight climate models downscaled and run through the basin PRMS model. See caption of Figure 4.3 for further description.

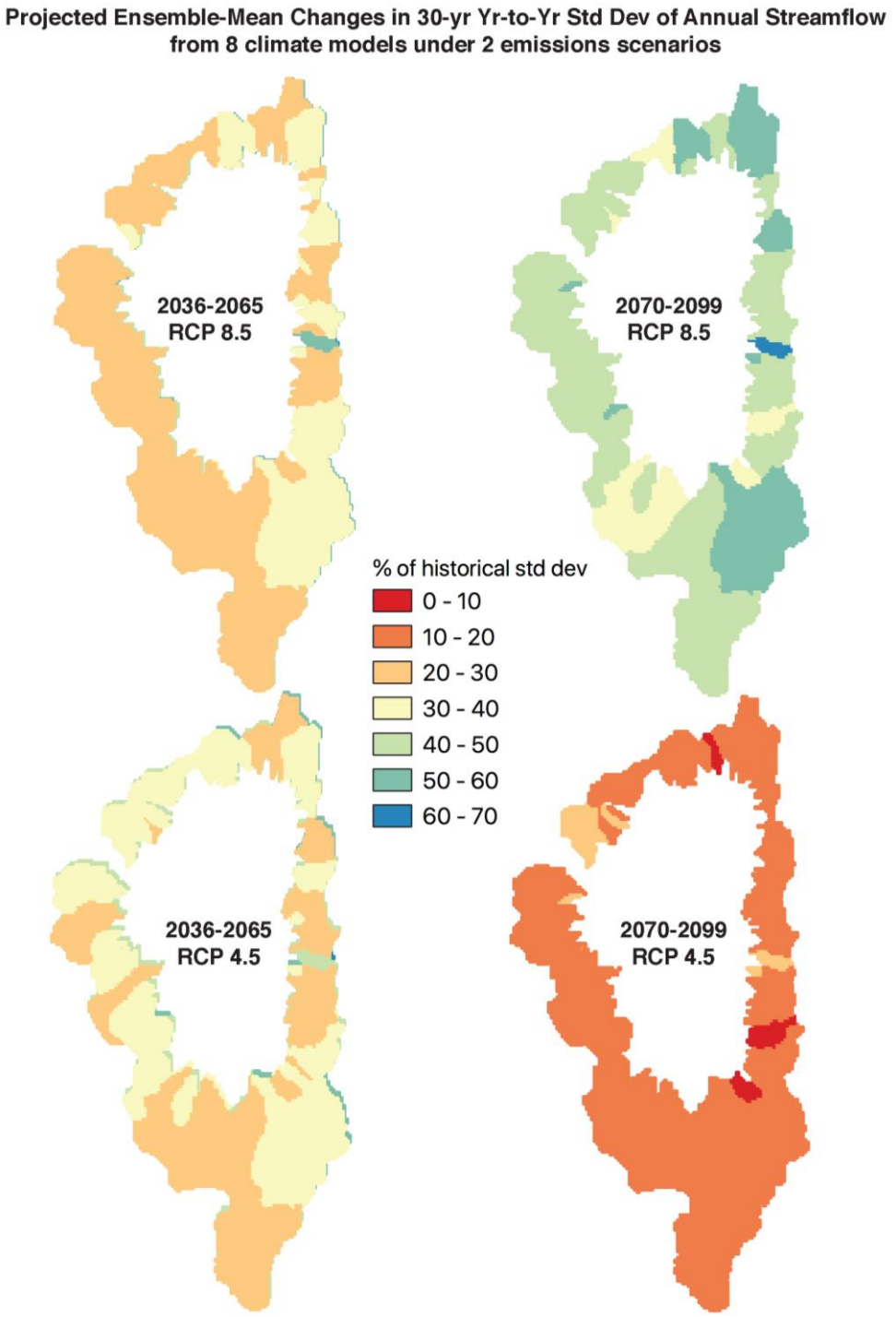

Figure 5.10. Ensemble-mean increases in 30-yr standard deviations of year-to-year annual-streamflow totals over the Lake Tahoe basin, as projected by eight climate models downscaled and run through the basin PRMS model.

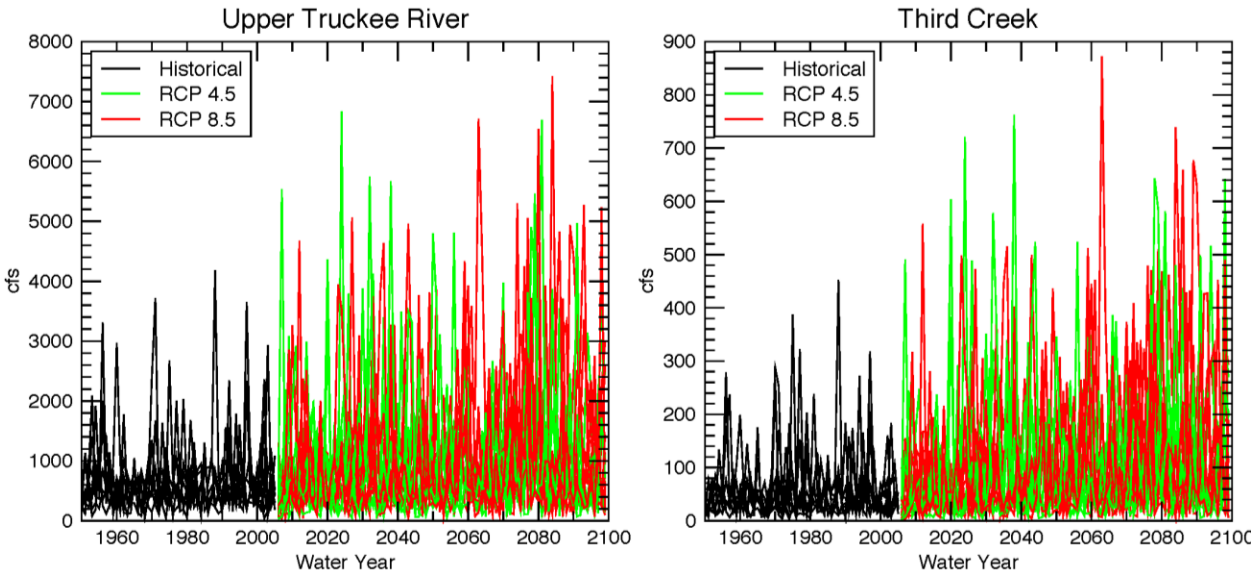

Figure 5.11. Ensemble of water-year 3-day maximum streamflows in Upper Truckee River and Third Creek, as projected by eight climate models downscaled and run through the basin PRMS model.

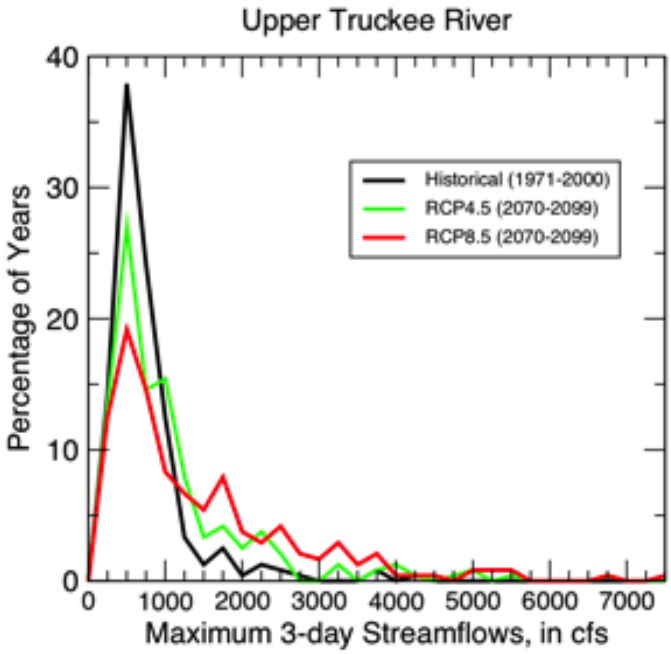

Figure 5.12. Distributions of water-year 3-day maximum streamflows in Upper Truckee River, as projected by eight climate models downscaled and run through the basin PRMS model.

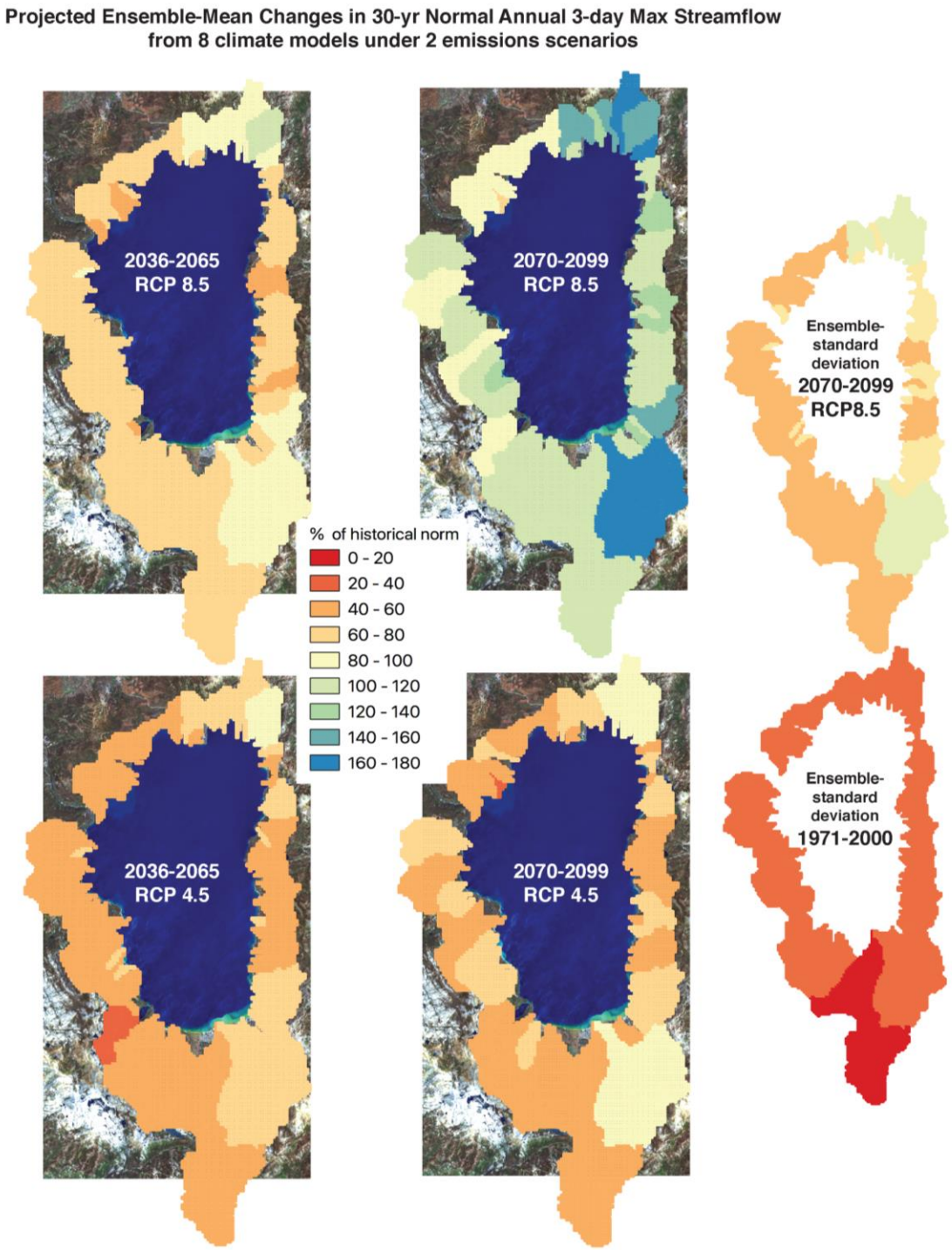

Figure 5.13. Ensemble-mean increases in 30-yr normals of 3-day maximum streamflows over the Lake Tahoe basin, as projected by eight climate models downscaled and run through the basin PRMS model. See caption of Figure 4.3 for further description.

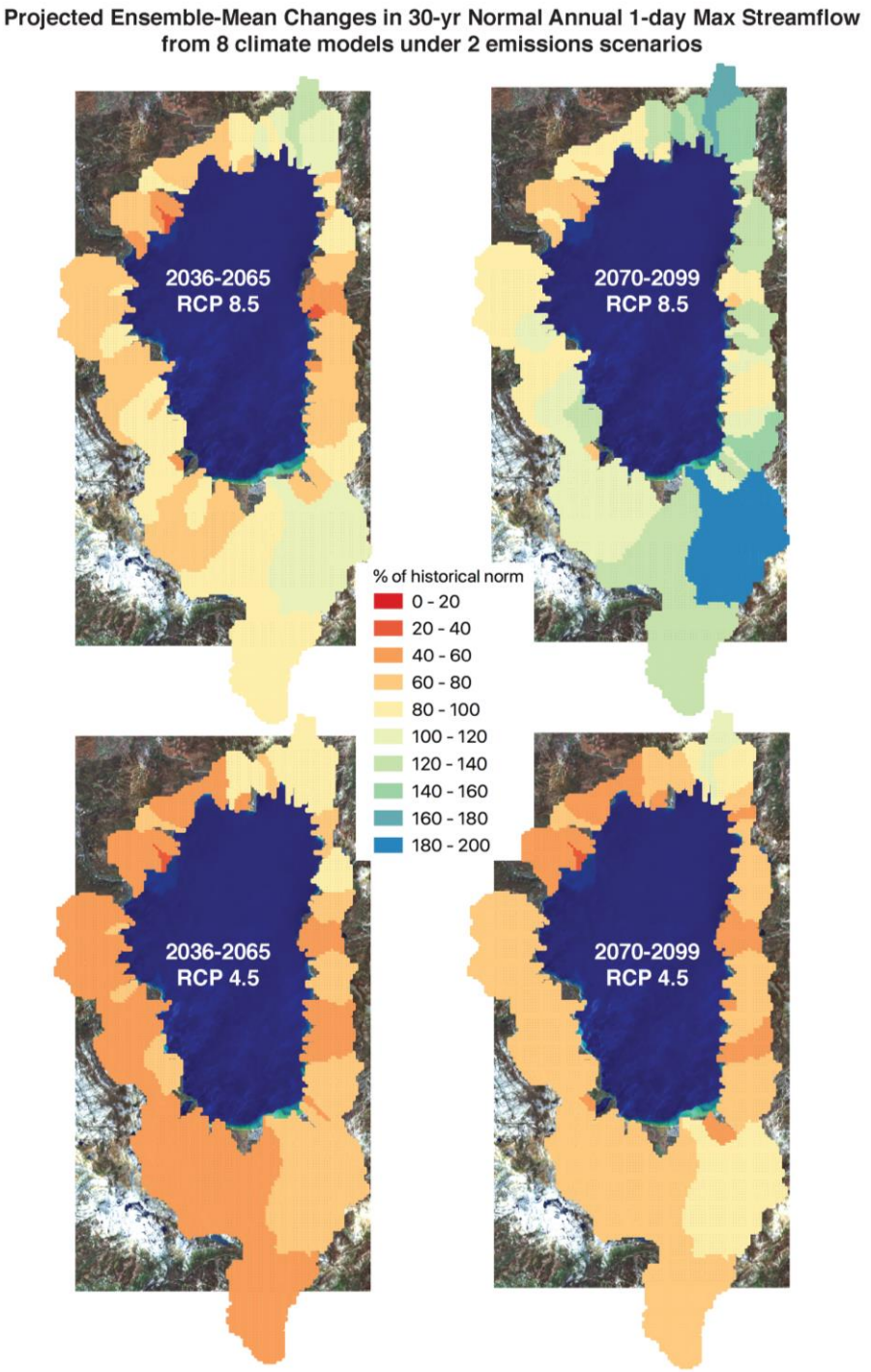

Figure 5.14. Ensemble-mean changes in 30-yr normals of one-day maximum streamflows over the Lake Tahoe basin, as projected by eight climate models downscaled and run through the basin PRMS model. See caption of Figure 4.3 for further description.

These flood flows are of particular interest regarding potential erosion, and sediment and nutrient transports, into Lake Tahoe. Shifts towards greater annual flow maxima will contribute to an overall shift towards having more of the annual streamflow totals into the Lake come from episodes of higher flows at the expense of the long intervening periods with lower flows. Figure 5.15 shows the average percentages of the historical flow totals coming from the highest-flow day (lower left corner), the two highest-flow days (not necessarily two days in a row), three highest-flow days, and so on. As indicated by the black curve of historical conditions, 37% of the total simulated streamflow from all subbasins into the Lake occurs during an average of 36 (10%) days per year. In the climate-changed projections, the same amount of inflow (37% of the historical normal total inflow) will occurs in only 14-25 4-7% of days per year on average. That is, the same amount of high inflows occurs in 30-60% LESS time, requiring that the flows and potentials for erosion and transports during that those days are correspondingly much higher. Notice that total annual inflows to the Lake (values along the right edge of the figure) increase under all climate-change scenarios and periods, as suggested previously by Figure 5.8. Taking these greater annual inflow amounts into account, in the late century under extreme RCP 8.5 emissions the wettest 10% of days contribute 48% of total inflow (rather than the historical 37% in the same number of days).

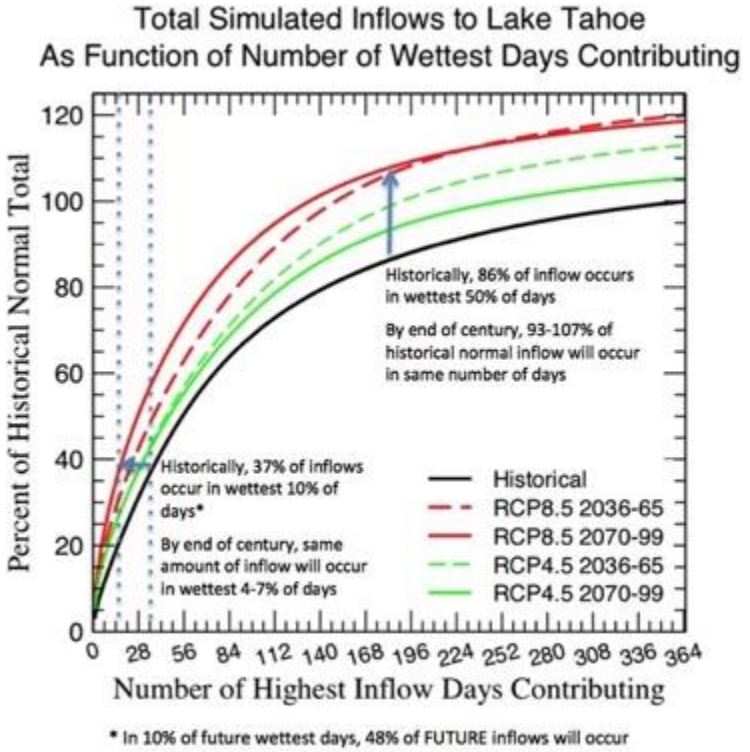

Figure 5.15. Ensemble-mean changes in 30-yr normals of contributions of total inflow to Lake Tahoe during various numbers of highest-flow days per year, as projected by eight climate models downscaled and run through the basin PRMS model.

If we turn to a broader range of inflow rates, Figure 5.15 shows that about 86% of all simulated Lake inflow is simulated to have occurred historically during the wettest half of all days. Under projected climate changes by late century, inflows on the same number of days (183) yield 93-107% of the historical norm. Thus more and more of the total inflows will arrive in the Lake during fewer and fewer days.

One particularly pernicious cause of high flows (read, flooding) in the Sierra Nevada are rain-on-snow (ROS) events. The conditions under which rain falling on snow generate large floods are complex and actually poorly understood, but include factors such as how much rain falls on how much snow and how "warm" (close to freezing) the snowpack is when the rain arrives. PRMS represents these conditions fairly simply, and more complete models are being developed by other researchers. So, rather than rely on PRMS to provide actual ROS streamflow amounts, in this study we instead project how often and especially how much rain falls overall onto pre-existing snowpacks. Figure 5.16 shows projected changes in the annual amounts of rain that falls on snow. By mid-century, the amount of ROS per year increases by about 20-60% across much of the basin but is declining in some subbasins dotted along the eastern and northern sides of the Lake. By late century (especially in the more severe scenario) the ROS amounts decline substantially around almost the entire Lake. These patterns of increasing ROS and decreasing ROS reflect trade offs between the tendency for more storms to yield rainfall rather than snowfall (increasing the occurrence and overall magnitudes of rain for ROS episodes, in those places where snowpacks still occur) versus the loss of snowpack (which decreases the opportunities for rain to have snow to fall on). McCabe *et al.* (2007) observed that this tradeoff is already occurring across the western US, reflected in elevation-dependent changes in ROS historically (with ROS increases at high-altitude sites and ROS decreases at low-altitude sites). In the Tahoe Basin, elevation ranges are not as broad as at the "western US" scale of McCabe *et al.* (2007) so that these tradeoffs are expressed more across time than space in the Tahoe Basin projections. That is, initially (as warming begins and snow loss has not progressed too much) most of the basin is projected to receive more ROS, and then later (as conditions warm even more) most of the basin is projected to have less snow for rain to fall on and thus less ROS.

6. HYDROLOGIC RESPONSES AS FUNCTIONS OF TEMPERATURE CHANGE

The hydrologic responses displayed in section 5 reflect the many different climate projections in the eight-model ensemble studied here. As predictions, they reflect GCM-to-GCM differences, differences between the two emissions scenarios (and how likely each is), and the natural climate variations simulated in the various projections. These various sources of prediction uncertainty mean that the exact rates of climate change during the 21st Century are uncertain. What has been shown in section 5, for the most part, is the average (over the ensemble of projections) rates of climate and hydrologic change. Adaptation based on these average timings implicitly or explicitly assumes that the ensemble average of the climate projections correctly represents the most likely rates of climate change at a function of time.

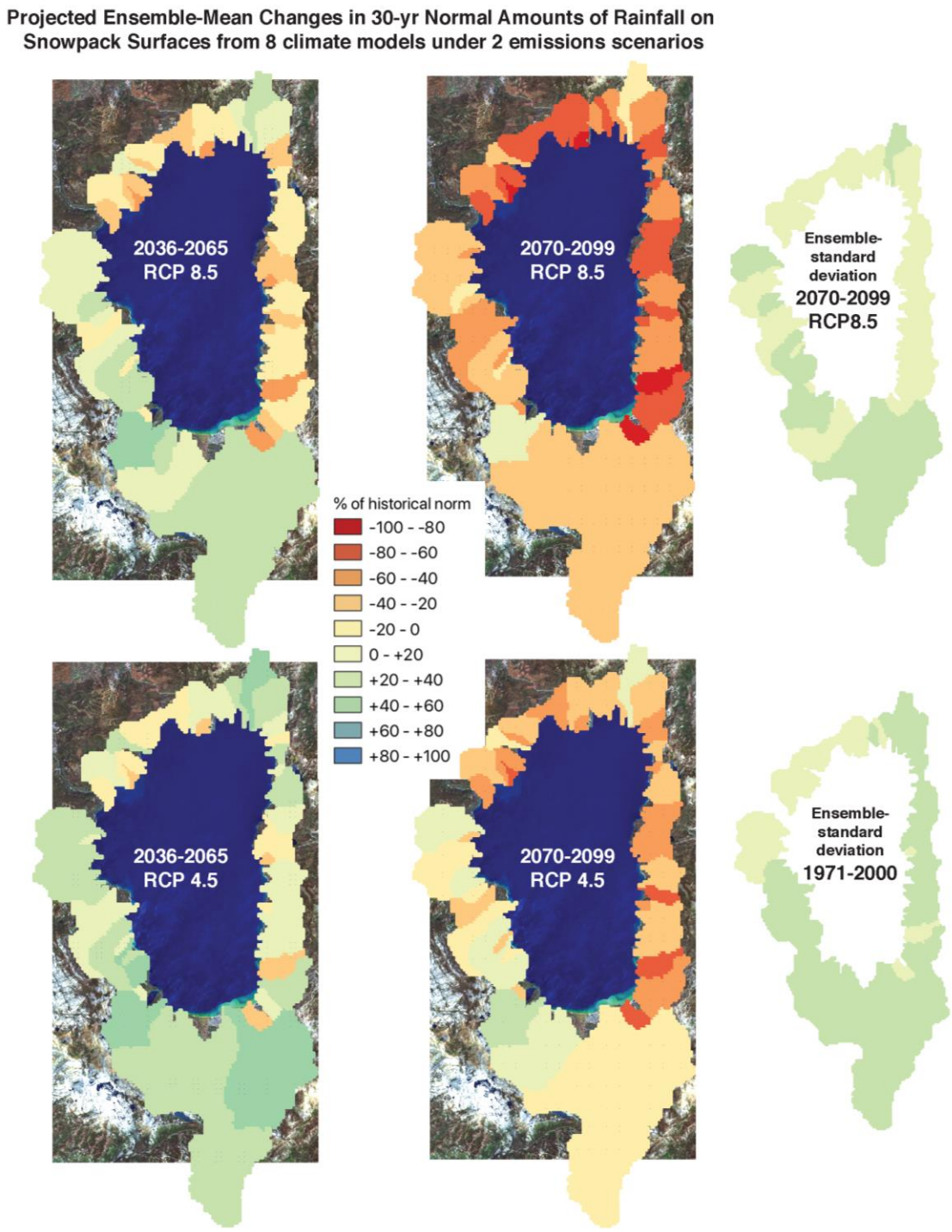

Figure 5.16. Ensemble-mean changes in 30-yr normals of total amounts of rainfall on snow, defined here as precipitation on days with average temperature above freezing and greater than 0.5 inches of precipitation falling onto existing snowpacks that have >2 inches of snow-water equivalent, over the Lake Tahoe subbasins, as projected by eight climate models downscaled and run through the basin PRMS model.

An alternative approach to interpreting the projections and to incorporating the ensemble into planning entails evaluating the hydrologic responses to various user-specified levels of climate change, regardless of which model, which emissions scenario, and when in the century those levels of change arrive. Handled this way, the projections are summarized in terms of how the basin responds to specified levels of climate change (like a local version of the impacts-by-degree-of-global-warming strategy used by https://climatenexus.org/international/ipcc/comparing-climate-impacts-at-1-5c-2c-3c-and-4c/). In this section, some key hydrologic projections will be summarized according to how much hydrologic change results in response to various levels of overall warming. (Other combinations of climate changes could be used, but the level of warming drives many aspects of the hydrologic changes in the previous section and is useful for our purposes here).

Figure 6.1 is a reprise of Figure 4.2a, with three 1-degree temperature bands indicated. Some key projected hydrologic responses to nonoverlapping 30-yr segments from the 8-GCM, 2-emissions scenarios climate-projection ensemble that have 30-yr mean temperatures falling in these bands are summarized below. The 30-yr segments of daily climate that the hydrology is responding to include both the temperatures that identified the segments for inclusion and the corresponding simulated precipitation series. Some of those corresponding precipitation series will be wetter than historical, some drier, and the result of this diversity averages out about as much as it does in the 30-yr time-banded averages shown in sections 4 and 5.

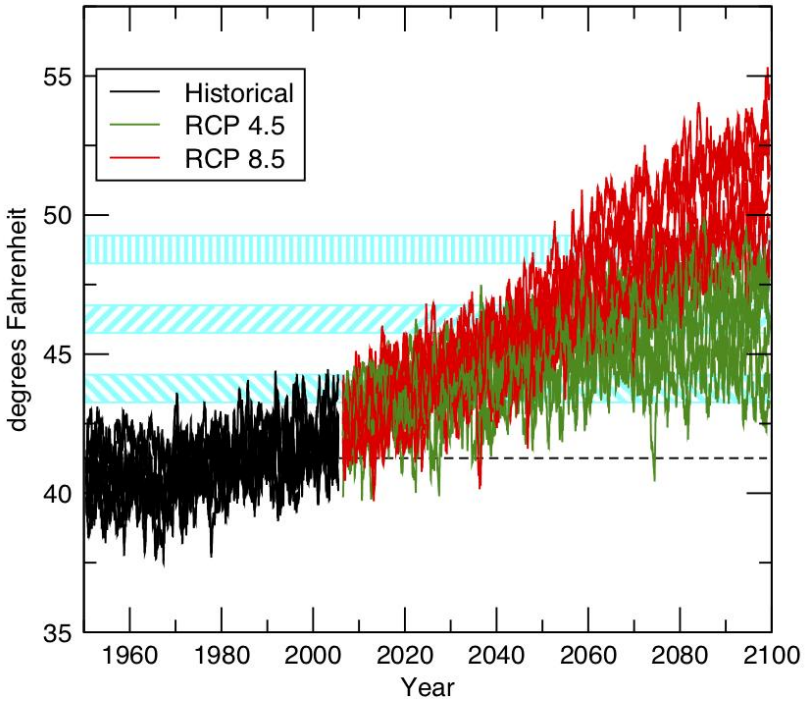

Figure 6.1. Ensemble of time series of annual temperatures in the Upper Truckee River subbasin, reprised from Figure 4.2a, with three temperature bands highlighted—2-3ºF (cyan, back hachured), 4.5-5.5ºF (cyan, front-hachured), and 7-8ºF (cyan, vertical hachures) warmer than the 1971-2000 normal (dashed black line).

Figure 6.2 illustrates schematically when the 30-yr segments that we will use appear in the ensemble and which emissions scenario led to them reaching those temperatures. Notice that, of the 17 segments in the +2–3ºF warmer band, roughly equal numbers of RCP 4.5 and 8.5 projections are included, and all but one (from an RCP 4.5 projection by the GFDL-ESM2M GCM) appear in more or less the present-day parts of the ensemble. The segment that appears later (starting in 2043) reflects the lesser greenhouse forcing in the RCP 4.5 and the fact that the GFDL model "runs somewhat cooler" than most of the other GCMs. The 13 segments that are retrieved from the +4.5–5.5ºF temperature band are also from both among the RCP 4.5 and 8.5 projections (with eight coming from RCP 8.5), and are generally distributed around midcentury. Finally seven segments in the +7–8ºF range were retrieved from the ensemble, all from RCP 8.5 scenarios and from the last half of the century. Notice that these collections of segments are all more numerous or (in the +7–8ºF case) more or less the same number as the subsets displayed in section 5, wherein each of the maps corresponded to 8 30-yr averages from the ensemble.

When the projections summarized in Figure 5.2 are re-summarized instead for these of these "temperature bands", Figure 6.3 results. The April 1 SWE patterns in Figure 6.3 are similar to those in Figure 5.2, with the +2–3ºF-warmer subset in Figure 6.3 being similar to the midcentury-RCP4.5 average in Figure 5.2. The +4.5–5.5ºF-warmer subset in Figure 6.3 is similar to the late-century-RCP4.5 and midcentury-RCP8.5 projections in Figure 5.2, and the patterns of the +7–8ºF-warmer subset in Figure 6.3 is similar to (albeit with somewhat less snow loss than)

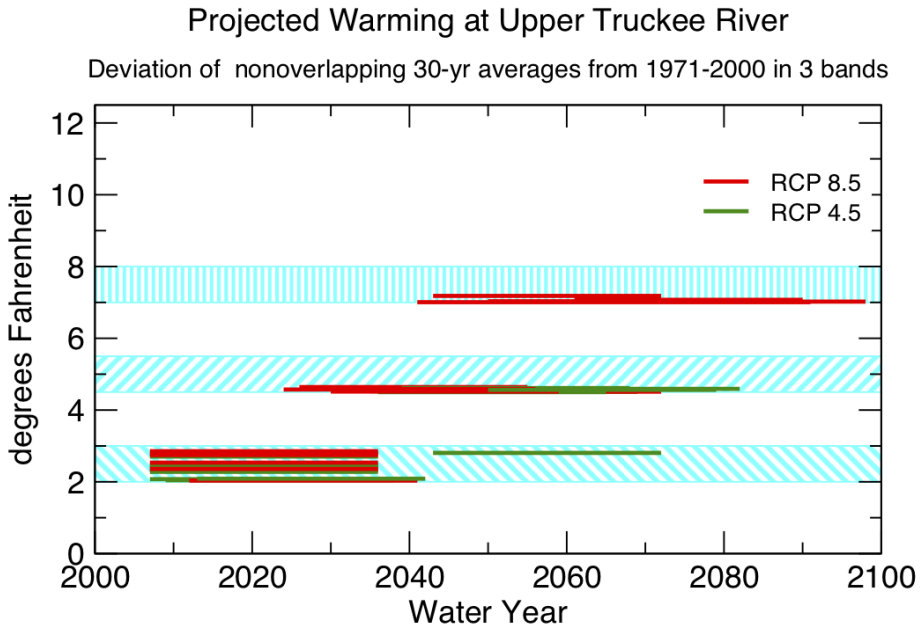

Figure 6.2. Three temperature-change bands from Figure 6.1 plotted versus time in the 21st Century, with green and red bars (RCP4.5 and RCP8.5, respectively) indicating non-overlapping 30-yr periods with projected mean temperatures falling in those bands; the 30-yr periods indicated are derived from the 8-GCM, 2-emissions scenarios ensemble studied throughout this report.

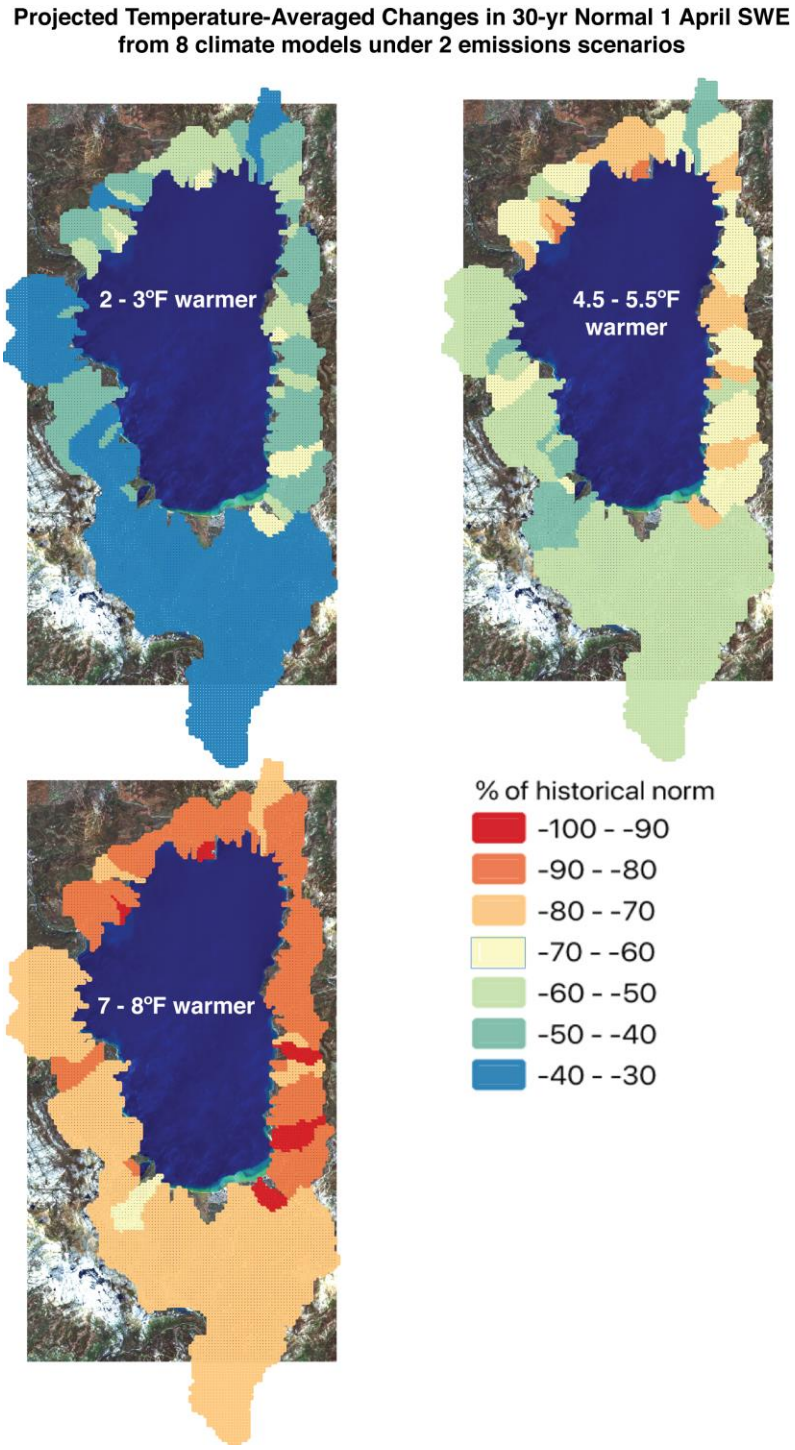

Figure 6.3. Temperature-band-mean changes in 30-yr normals of April 1 snowwater contents, over the Lake Tahoe subbasins, as projected by eight climate models downscaled and run through the basin PRMS model; three sets of 30-yr segments of hydrologic simulations responding to parts of the climate projections that fall within the temperature bands indicated, and as described in the text, are averaged to estimate these subbasin responses. These maps are another way of summarizing the changes suggested by Figure 5.2.

the late-century-RCP8.5 average in Figure 5.2. The point of the temperature-banding exercise here is that Figure 6.3 is now largely just reliant on the hydrologic-model simulations rather than depending also on specific rates of (temperature) change in the individual GCMs. In theory, one could monitor and track long-term (e.g., 30-yr normals here) temperature changes in the Tahoe Basin, and strive to be prepared for the various levels of snowpack change indicated in Figure 6.3 by the time those temperature increases arrive at some as-yet-uncertain time in the future, rather than basing plans on GCM-based assumptions regarding when that amount of warming will arrive. Thus climate-banded planning could reduce reliance on assumptions about which climate models, or mix of climate models, will prove to be most accurate, and instead can rely more on the changes observed as they happen. Perhaps most notably, this approach reduces the need to guess which of the emissions scenarios society will follow as this century plays out, probably the hardest decision and thus prediction facing us currently. On the other hand, efficacy of this observations-driven approach to planning will depend on the lead times required to implement plans; adaptations that can be implemented quickly can track observations more readily than adaptations that require a decade or more of study, lobbying, and preparation.

A similar exercise, based on the same subsets of the climate-projection ensemble, applied to annual streamflow totals is shown in Figure 6.4. Notably, the +2–3ºF-warmer total-streamflow responses are almost minimal, suggesting that we should not expect to have observed actual climate-change responses with respect to this variable yet, in the real world. The average total-streamflow pattern in the +4.5–5.5ºF-warmer subset is fairly similar to the changes indicated for late-century-RCP4.5 and mid-century-RCP8.5 projections in Figure 5.9, although the magnitude of the change falls somewhat between those two time-based averages. The +7–8ºF-warmer averages in Figure 6.4 are quite similar to the late-century-RCP8.5 average in Figure 5.9. Again, as with Figure 6.3, one could choose to make plans based on observations-based indications of whether (and even, by extrapolation, when) this +7–8ºF-warmer outcome is approaching.

Given these temperature-banded projections of snowpack and streamflow responses, a corresponding analysis of streamflow timing is worthwhile. Figure 6.5 shows the temperature-banded changes in center-of-streamflow timing, and clarifies somewhat the temperature-driven effects mapped (by era and emissions) in Figure 5.7. Finally, Figure 6.6 illustrates the temperature-banded changes in 3-day maximum streamflows, as indicated for eras and emissions in Figure 5.13. Notice that these 3-day maximum “flood” flows are projected to nearly doubled in many subbasins (especially on the east side of the Lake) by the time warming reachs about +5ºF, and another 50% more by the time warming reaches about +7–8ºF.

The specifics of the temperature-banded strategy demonstrated here (e.g., using only temperatures, the particular temperature bands, and the use of 30-yr averages rather than some other metric of change) are not intended to be the final version of this strategy. Rather the projection summaries presented above are offered, as an example, in the interests of sparking conversation about other possible ways of ingesting and using available climate projections in real-world planning for the future.

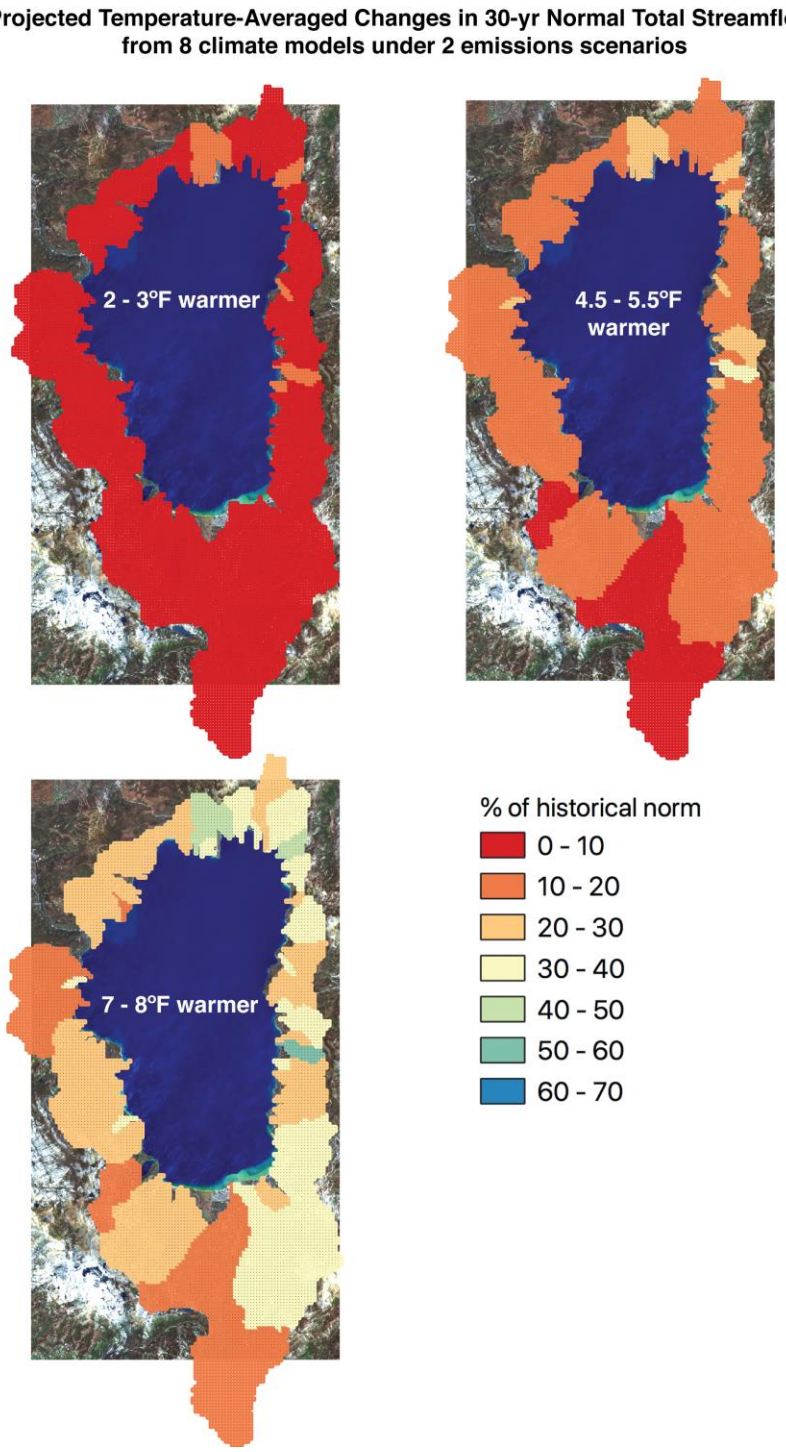

Figure 6.4. Similar to Figure 6.3, except showing averaged changes in 30-yr mean annual streamflow totals. These maps are another way of summarizing the changes suggested by Figure 5.9.

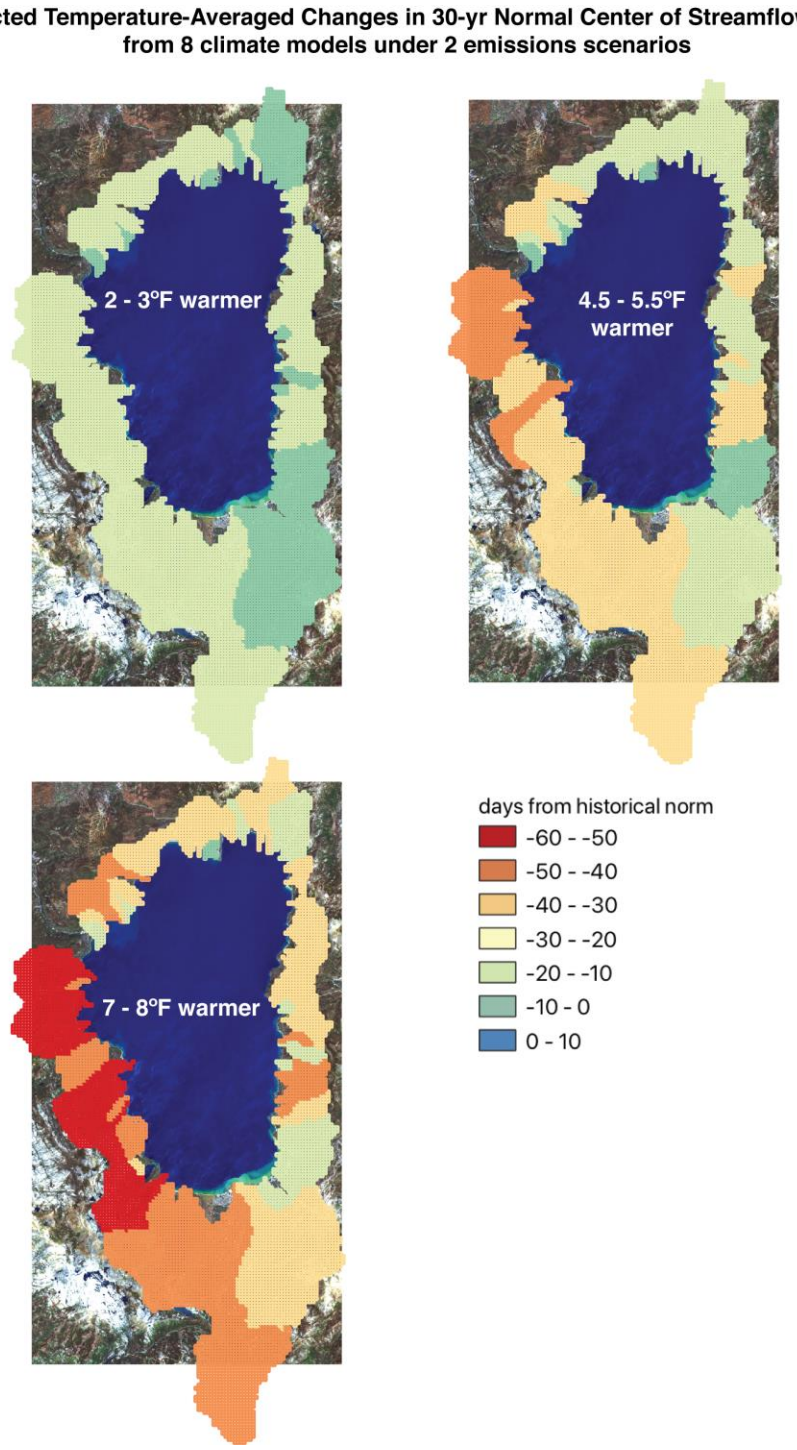

Figure 6.5. Similar to Figure 6.3, except showing averaged changes in 30-yr mean center-of-streamflow timing. These maps are another way of summarizing the changes suggested by Figure 5.7.

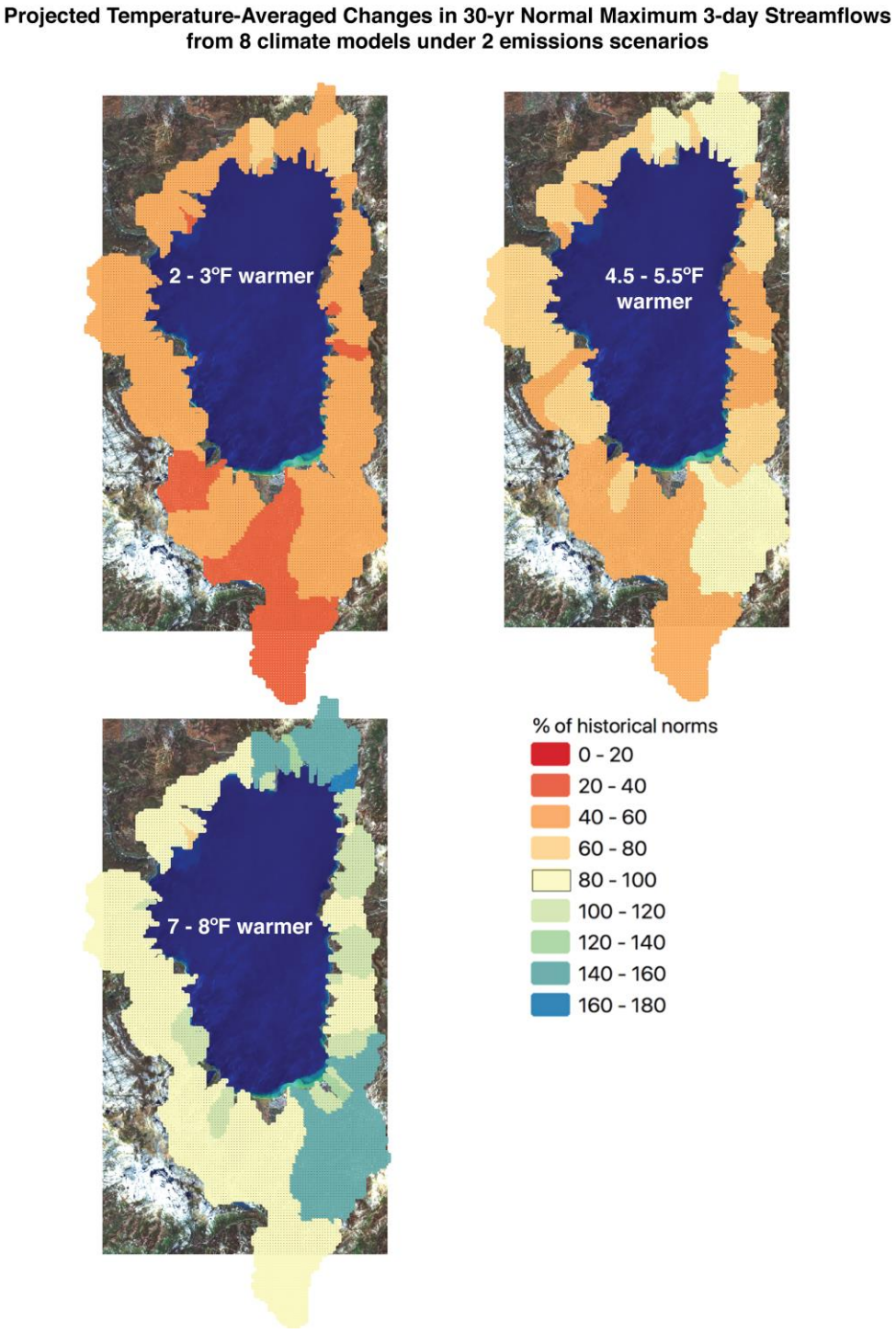

Figure 6.6. Similar to Figure 6.3, except showing averaged changes in 30-yr mean 3-day maximum streamflows. These maps are another way of summarizing the changes suggested by Figure 5.13.

7. SUMMARY OF PROJECTIONS AND WAYS FORWARD

To summarize, when expressed relative to historical normals at subbasin scales, projected warming and changes in precipitation totals are spatially fairly uniform within the Tahoe Basin. Consequently, most of the subbasin-to-subbasin variations in hydrologic responses projected and reported here are reflections of the different hydrologic conditions from subbasin to subbasin. Overall, by end of century, temperatures are projected to increase by about +4F to as much as +9F depending on how greenhouse-gas emissions play out globally over coming decades. Annual precipitation totals are projected to increase (in the ensemble of climate models evaluated here) by between 0% and to about 15%, depending on which emissions scenario and subbasin is considered. However, these ensemble-mean precipitation changes are less than ensemble-standard deviations, suggesting that the changes are not consistent from model to model. The changes in ensemble-mean projections are also small compared to year-to-year precipitation variations, indicating that the long-term mean precipitation changes will be well within the large range of natural variations that we are already used to. Thus the projection of wetter future conditions by this particular ensemble of climate models is probably the most uncertain projection in this study. On the other hand, 3-day precipitation maxima are projected to increase by between about 10% and 25% depending on emissions scenario, and these increases are larger than the ensemble-standard deviations, indicating a significant level of agreement among models, making this a fairly confident outcome.

Given the projected warming of the Basin, projections of significant snowpack declines are no surprise. April 1 snow-water equivalents (SWEs) and annual snowmelt amounts (as a metric of water availability and of how much total snowfall occurs) decline substantially, with maximum declines mostly along the south- and west-facing subbasins. April 1 SWEs all but disappear in the northern and eastern subbasins and decline by about 80% in the rest of the Basin under the more extreme emissions scenario (RCP8.5). This decline reflects less snow overall but also is a consequence of changes in the time when snowpack is present. Snow-season lengths are projected to be a month to more than three months shorter by end of century, depending on location and emissions scenario, and snowmelt timing comes 20 to about 50 days earlier. Mostly as a consequence of these warming-induced snowmelt changes (precipitation timing is not projected to change significantly), overall streamflow timing also is projected to come about 20 to 50 days earlier, depending on locations and emissions.

As a result of a complex interplay of the changes in snowmelt-and-streamflow timing with the seasonality of evaporative demands in the projected future climates, annual streamflow totals on long-term average do not decline, despite overall warming-induced increases in those demands. Indeed flows increase somewhat overall, since much of the runoff occurs before seasonal upturn in potential evapotranspiration, with largest increases in the eastern subbasins. Year-to-year fluctuations in annual streamflow will increase, resulting in hydrologic whiplash conditions and wetter wet-years in the midst of drier dry years.

Finally annual streamflow maxima (floods) are projected to increase on average with flood flows in some subbasins almost tripling under the most severe emissions scenario by end of century. More typically flow maxima increase by between about 30% to almost 150% of the historical maxima. These projected increases in flow maxima result in more flow arriving at the Lake at higher rates in shorter periods of time in the future; to be specific, the amount of high inflows that currently occurs in the 10% of days with highest inflows to the Lake is projected (on average) to occur in 30-60% LESS time by end of century, requiring that the flows and potentials for erosion and transports during that those days are correspondingly much higher. These increasingly "concentrated" inflows to the Lake likely represent increased opportunities for increasing sediment and nutrient loads. Rain-on-snow events happen more frequently in the first part of the century but then decline, as there is less snow cover to rain upon by end of century.

Another way to summarize the projections of climate-change responses in the Lake Tahoe Basin is to compare aggregated responses at all of the various subbasins across multiple response metrics. Each of the subbasins responds to climate changes in its own way, reflecting distinctive elevations, aspects, distances from the main ridgeline of the Sierra Nevada and thus precipitation regimes, forest patterns, and so on. Subbasin responses differ in terms of their changes in snowpacks, streamflow totals, and flood regimes. For planning purposes, it will be useful to be able to distinguish which subbasins are more vulnerable overall to climate change and which are less so. Such distinctions could provide a basis for deciding where to invest to hold the line against future changes ("hot spots"), versus areas where relatively muted future changes might provide some refuge against the worst climate-change impacts.

An example of such a "hot spot versus refuge" mapping is shown in Figure 7.1, where projected percentage or day-of-year changes (e.g., from Figures 4.11 or 5.7) at each of the 60 subbasins were ranked separately for each of 10 measures of climate-change reponse. Then at each subbasin the 10 ranks were averaged to distinguish the overall most-responsive subbasins from less-responsive subbasins.

Overall, at both middle and end of the century, subbasins on the north and east sides of the Basin respond more than the west and south sides. At a finer scale, by end of century under the greater-emissions scenario (RCP8.5), Trout Creek in the southeast corner of the Basin, and Mill Creek in the Incline Village area in the northeast corner of the Basin, are subbasins that are most impacted on average and might be examples of hot spots for climate change. Eagle and Cascade Creeks near Emerald Bay are projected to be least impacted overall. By midcentury under the less-emissions scenario (RCP4.5), representing nearest term responses, the Upper Truckee River and Eagle and Cascade Creeks are projected to be less impacted overall, and subbasins all along the northern end of the Lake are projected to respond first and worst. Results of hot-spot determinations will depend on the particular decades and emissions analyzed, as well as on the particular subset of impacts ranked but, in consultation with agencies of the Basin, hotspot-versus-refuge analyses can add geographic detail to planning and adaptation efforts.

Looking forward, the model errors illustrated in section 3 suggested that the PRMS model used here is probably not capable of providing reliable low-flow projections, and so the present study did not concentrate on changes in warm-season flows. Our best understanding of why low-flow simulation presented problems is that those low flows rely upon deeper subsurface, groundwater flows within the Basin that the PRMS model does not include or represent. A future study using a well-calibrated GS-FLOW model of the Basin might provide reliable low-flow projections, but that improved calibration of a basin-wide GS-FLOW model will probably depend on the availability of more groundwater data collected in more parts of the Basin than is being collected now.

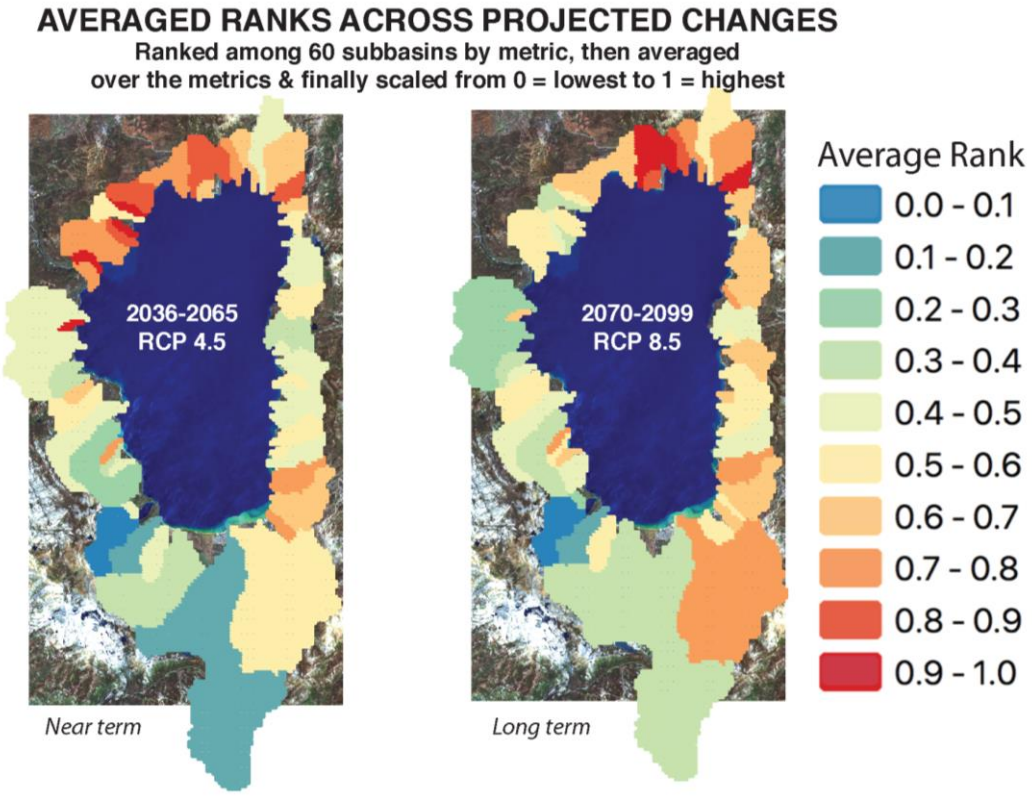

Figure 7.1. Overall average of subbasin ranks of projected climate-change impacts in the Tahoe basin by (left) middle of 21st Century under RCP4.5 emissions, and by (right) end of 21st Century under RCP8.5 emissions. Measures included in this calculation are the projected changes of (1) annual precipitation, (2) maximum 3-day precipitation totals, (3) April 1 SWE, (4) snow-season length, (5) snowmelt timing, (6) annual snowmelt, (7) annual streamflow, (8) streamflow timing, (9) maximum 3-day streamflow totals, and (10) amount of rainfall on snow. Measure-by-measure, the subbasin responses are ranked from smallest to largest, and then all the ranks for each subbasin are averaged to arrive at a single average ranking for that subbasin. Then those average ranks are rescaled from 0 (subbasin with lowest average rank) to 1 (subbasin with highest average rank) for the maps below.

The PRMS models as used here does not simulate changes in forest cover and other land uses. Some changes, like thinning or extirpation of forest densities in some parts of the Basin, are likely to occur in partial response to the same climate changes explored here, e.g., due to major increases in wildfire risks and scales that are being projected by other studies. An improved modeling system for the kinds of hydrologic projections developed here could also include hydrologic models informed by even more detailed forest-stand information (e.g., from airborne lidar surveys) and might be coupled to projections of the canopy changes associated with future fires and other causes of land-cover and snowpack-and-transpiration changes to come.

For most of the past 20 years, statistically downscaled climate projections like those used here have had the advantage of being more readily available and generally more accurate (in terms of having smaller systematic biases) than projections taken directly from global climate models or higher-resolution regional climate models (CCTAG, 2015). Currently, though, the state-of-science is on the verge of a transition to having more available, more accurate, and physically more comprehensive projections from an emerging generation of high-resolution regional climate models. Examples of these kinds of high-resolution "dynamically downscaled" projections (or hybrids of dynamic and statistically downscaled projections) are expected to be included for the first time in the next California Climate Change Assessment process within the next two years. Such projections will more than likely include even warmer futures in the Tahoe Basin (as snow-cover declines are incorporated in ways that allow "new" albedo-warming feedbacks to add additional warming) and potentially different patterns of storm extremes and precipitation-form changes (Schwartz *et al.,* 2017). Statistically downscaled projections to date simply have not been able to capture and portray these local-scale climate feedbacks and impacts as well as the current regional models are beginning to.

The upshot of these (and other) limitations of the PRMS model and climate projections used here, together with the prospects for future modeling improvements, is that the projections provided here, while providing some information that could not be obtained from previous larger scale studies, are not the final word as to changes to come. New climate projections emerge regularly on about a 5-10 year cycle, and should be tracked to identify any major changes in projected futures for the Basin. In the meantime, a more comprehensive GS-FLOW-style surface- and groundwater model could be improved (with the addition of some necessary groundwater monitoring) to provide more comprehensive hydrologic projections with the next round of higher-resolution regional climate projections. Even more ambitiously, a model system that integrates (projected) land-cover changes with hydrologic-process modeling would provide an even more comprehensive basis for future projections and planning.

8. REFERENCES CITED

Abatzoglou, J.T., and Brown, T.J., 2012, A comparison of statistical downscaling methods suited for wildfire applications: International Journal of Climatology, 32, 772-780.

Albano, C.M., Abatzoglou, J.T., McEvoy, D., Huntington, J., Morton, C., Dettinger, M., Ott, T., 2022, A multi-datset assessment of climatic drivers and uncertainties of recent trends in evaporative demand across the continental US: J. Hydrometeorology, 23, 15 p., doi: 10.1175/JHM-D-21-0163.1

Ban, Z., and Lettenmaier, D.P., 2022, Asymmetry of western US river basin sensitivity to varying climate warming: Water Resources Research, 58, e2021WR030367.

California DWR Climate Change Technical Advisory Group (CCTAG), 2015, Perspectives and guidance for climate change analysis: California Department of Water Resources Technical Information Record, 142 p.

Christensen, N.S., and Lettenmaier, D.P., 2007, A multimodel ensemble approach to assessment of climate change impacts on the hydrology and water resources of the Colorado River basin: Hydrology and Earth System Sciences, 11, 1417-1434.

Coats, R., Sahoo, G., Riverson, J., Costa-Cabral, M., Dettinger, M., Wolfe, B., Reuter, J., Schladow, G., and Goldman, C., 2013, Historic and likely future impacts of climate change on Lake Tahoe [chapter 14], in C.R. Goldman, M. Kumagai, and R.D. Robarts [eds.], Climate change and inland waters—Impacts and mitigation approaches for ecosystems and society: Wiley-Blackwell, 231-254, DOI: 10.1002/9781118470596.ch14.

Daly, C., Halbleib, M., Smith, J.L., Gibson, W.P., Doggett, M.K., Taylor, G.H., Curtis, J., and Pasteris, P.P., 2008, Physiographically sensitive mapping of climatological temperature and precipitation across the conterminous United States: International Journal of Climatology, 28, 2031-2064.

Das, T., Pierce, D.W., Cayan, D.R., Vano, J., and Lettenmaier, D., 2011, The importance of warm season warming to western US streamflow changes: Geophysical Research Letter, 38, https://doi.org/10.1029/2011GL049660.

Dettinger, M.D., 2013, Projections and downscaling of 21st Century temperatures, precipitation, radiative fluxes and winds over the southwestern US, with a focus on Lake Tahoe: Climatic Change, 116, 17-33, doi:10.1007/s10584-012-0501-x.

Dettinger, M., Alpert, H., Battles, J., Kusel, J., Safford, H., Fourgeres, D., Knight, C., Miller, L., and Sawyer, S., 2018, Fourth California Climate Assessment--Sierra Nevada Region Report: California's Fourth Climate Change Assessment report SUM-CCCA4-2018-004, 94 p.

Dettinger, M.D., Cayan, D.R., Meyer, M.K., and Jeton, A.E., 2004, Simulated hydrologic responses to climate variations and change in the Merced, Carson, and American River basins, Sierra Nevada, California, 1900-2099: Climatic Change, 62, 283-317.

Erkman, C., Coors, S., Powell, A., and Noe, P., 2020, TMWA Climate change analysis (contract # PO-004638): Precision Water Resources Engineering report to Truckee Meadows Water Authority, 50 p.

Franco, G., Cayan, D., Pierce, D., Westerling, A., & Thorne, J., in review, Cumulative global CO2 emissions and their climate impacts from local through regional scales: California Fourth Assessment Report, 28 p.

Ghil, M. and Childress, S., 1987, Topics in GeophysicaI Fluid Dynamics: Atmospheric Dynamics, Dynamo Theory, and Climate Dynamics: Springer-Verlag, New York, 485 pp.

Hayhoe, K., Wuebbles, D.J., Easterling, D.R., Fahey, D.W., Doherty, S., Kossin, J., Sweet, W., Vose, R., and Wehner, M., 2018, Our Changing Climate: In Impacts, Risks, and Adaptation in the United States: Fourth National Climate Assessment, Volume II [Reidmiller, D.R., C.W. Avery, D.R. Easterling, K.E. Kunkel, K.L.M. Lewis, T.K. Maycock, and B.C. Stewart (eds.)]. U.S. Global Change Research Program, Washington, DC, 72–144.

Hidalgo, H., Dettinger, M., and Cayan, D., 2008, Downscaling with constructed analogues—Daily precipitation and temperature fields over the United States: California Energy Commission PIER Final Project Report CEC-500-2007-123, 48 p.

Huntington, J.L., and Niswonger, R.G., 2012, Role of surface-water and groundwater interactions on projected summertime streamflow in snow dominated regions--An integrated modeling approach: Water Resources Research, vol. 48, W11524, doi: 10.1029/2012WR012319.

Jeton, A.E., 1999, Precipitation-runoff simulations for the Lake Tahoe Basin, California and Nevada: USGS Water Resources Investigations Report 99-4410, 61 p.

Jeton, A.E., Dettinger, M.D., and Smith, J.L., 1996, Potential effects of climate change on streamflow, eastern and western slopes of the Sierra Nevada, California and Nevada: U.S. Geological Survey Water Resources Investigations Report 95-4260, 44 p.

Karl, T.R., Melillo, J.M., and Peterson, T.C. (eds.), 2009, Global Climate Change Impacts in the United States: Cambridge University Press, 196 p.

Leavesley, G.H., Litchy, R.W, Troutman, M.M., and Saindon, L.G., 1983, Precipitation-runoff modeling system User's manual: U.S. Geological Survey Water-Resources Investigations Report 83-4238, 207 p.

Liang, X., Lettenmaier, D. P., Wood, E., & Burges, S. J., 1994, A simple hydrologically based model of land surface water and energy fluxes for general circulation models, J. Geophys Res., 99, 14415–14428.

Lorenz, E., 1963, Deterministic nonperiodic flow. *J. Atmos. Sci.*, **20,** 130-141.

Markstrom, S.L., Niswonger, R.G., Regan, R.S., Prudic, D.E., and Barlow, P.M., 2008, GSFLOW - Coupled groundwater and surface-water flow model based on the integration of the Precipitation-Runoff Modeling System (PRMS) and the Modular Groundwater Flow Model (MODFLOW-2005): USGS Techniques and Methods 6-D1, 240 p., doi: 10.3133/tm6D1.

McCabe, G.J., Clark, M.P., & Hay, L.E., 2007, Rain-on-snow events in the western United States: Bull. Amer. Meteorol. Soc. 88, 319-328.

McEvoy, D.J., Pierce, D.W., Kalansky, J.F., Cayan, D.R., and Abatzoglou, J.T., 2020, Projected changes in reference evapotranspiration in California and Nevada—Implications for drought and wildland fire danger: Earth's Future, 8, https://doi.org/10.1029/2020EF001736.

Pierce, D.W., D.R. Cayan, & B.L. Thrasher, 2014: Statistical Downscaling Using Localized Constructed Analogs (LOCA). J. Hydrometeor., 15, 2558–2585.

Schwartz, M., Hall, A., Sun, F., Walton, D., and Berg, N., 2017, Significant and inevitable end-of-twenty-first-century advances in surface runoff timing in California's Sierra Nevada. J. Hydrometeor. 18:3181–3197.

Stewart, I., Cayan, D.R., and Dettinger, M.D., 2004, Changes in snowmelt runoff timing in western North America under a 'Business as Usual' climate change scenario: Climatic Change, 62, 217-232.

Swain, D.L., Langenbrunner, B., Neelin, J.D., and Hall, A., 2018, Increasing precipitation volatility in 21st century California: Nature Climate Change, 8, 427-438.

Tarboton, D.G., 2003, Rainfall-Runoff Processes: Utah State University Web module, available at: https://www.researchgate.net/publication/265265983_RAINFALL-RUNOFF_PROCESSES .

Thrasher, B., Maurer, E.P., McKellar, C., and Duffy, P.B., 2012, Correcting climate model simulated daily temperature extremes with quantile mapping: Hydrology and Earth System Sciences, 16, 3309-3314.

Touze-Peiffer, L., Barberousse, A., and Le Truet, H., 2020, The Coupled Model Intercomparison Project—History, uses, and structural effects on climate research: WIREs Climate Change, 11, e648, https://doi.org/10.1002/wcc.648.

Walsh, J., Wuebbles, D., Hayhoe, K., Kossin, J., Kunkel, K., Stephens, G., Thorne, P., Vose, R., Wehner, M., Willis, J., Anderson, D., Doney, S., Feely, R., Hennon, P., Kharin, V., Knutson, T., Landerer, F., Lenton, T., Kennedy, J., and Somerville, R., 2014, Ch. 2: Our Changing Climate: in *Climate Change Impacts in the United States: The Third National Climate Assessment*, J. M. Melillo, Terese (T.C.) Richmond, and G. W. Yohe, Eds., U.S. Global Change Research Program, 19-67.

STANDING DISTRIBUTION LIST

*Whitney Brennan, Landscape Resilience Program Supervisor
*Also: Jason Vasques, Executive Director
*Also: Jane Freeman, Deputy Director
Also: Scott Carroll
California Tahoe Conservancy
1061 Third Street
South Lake Tahoe, CA 96150
Whitney.Brennan@Tahoe.ca.gov
Jason.Vasques@Tahoe.ca.gov
Jane.Freeman@Tahoe.ca.gov
Scott.Carroll@Tahoe.ca.gov

*Robert Larsen
Sudeep Chandra, Co-Chair
Tahoe Science Advisory Council
291 Country Club Drive
Incline Village, NV 89451
Robert.Larsen@resources.ca.gov

Patrick Wright, Director
Governor's Wildfire and Forest Resilience Task Force CA Natural Resources Agency,
715 P Street
Sacramento, CA 95814
Patrick.wright@gov.ca.gov

Dorian Fougères
Commission on Ecosystem Management
International Union for the Conservation of Nature Gland, Switzerland
fougeres@gmail.com

*Michael Anderson
*Also: John Andrew
Also: Romain Maendly
California Department of Water Resources
P.O. Box 942836
Sacramento, CA 94236
Michael.L.Anderson@water.ca.gov
Romain.Maendly@water.ca.gov
jandrew@water.ca.gov

*Geoff Schladow, Director
UC Davis Tahoe Environmental Research Center
291 Country Club Drive
Incline Village, NV 89451
gschladow@ucdavis.edu

*Alex Hall, Professor
Dept of Atmospheric and Oceanic Sciences
7955 MSB
Los Angeles, CA 90095
alexhall@g.ucla.edu

Justin Huntington
Also: Christine Albano
Also: Tamara Wall
Also: Maureen McCarthy
Also: Alan Heyvaert
Also: Mark Hausner
Desert Research Institute
2215 Raggio Parkway
Reno, NV 89512

Nevada State Library and Archives
State Publications
100 North Stewart Street
Carson City, NV 89701-4285
NSLstatepubs@admin.nv.gov

Archives Getchell Library
University of Nevada, Reno
1664 N. Virginia St.
Reno, NV 89557
tradniecki@unr.edu

Document Section, Library
University of Nevada, Las Vegas
4505 Maryland Parkway
Las Vegas, NV 89154
sue.wainscott@unlv.edu

†Library
Southern Nevada Science Center
Desert Research Institute
755 E. Flamingo Road
Las Vegas, NV 89119-7363

All on distribution list receive one PDF copy, unless otherwise noted.

---

† 2 copies; CD with pdf (from which to print)

*** Receive one hard copy**

Ramon Naranjo
U.S. Geological Survey, Nevada Water Science Center
2730 N. Deer Run Road
Carson City, NV 89701
rnaranjo@usgs.gov

Richard Niswonger
US Geological Survey
345 Middlefield Road
Menlo Park, CA 94025
rniswon@usgs.gov

Jill D. Frankforter, Center Director
US Geological Survey
Nevada Water Science Center
2730 N. Deer Run Road
Carson City, NV 89701
jdfrankf@usgs.gov

Anke Mueller-Solger, Center Director
Also: Joe Domagalski
US Geological Survey
California Water Science Center
6000 J Street, Placer Hall
Sacramento, CA 95819
amueller-solger@usgs.gov

Julie Kalansky
Also: Dan Cayan
Scripps Institution of Oceanography
California-Nevada Climate Applications Program
9500 Gilman Drive
La Jolla, CA 92093
jkalansky@ucsd.edu
dcayan@ucsd.edu

Kristen Averyt
Office of VP for Research
University of Nevada, Las Vegas
4505 S. Maryland Parkway
Las Vegas, NV 89154
kristen.averyt@unlv.edu

Allison Wolff
Vibrant Planet
1314 Tirol Drive
Incline Village, NV 89451
allison@vibrantplanet.net

Adrian Harpold
Department of Natural Resources & Environmental Science
University of Nevada, Reno
1664 N. Virginia Street
Reno, NV 89557
aharpold@unr.edu

Ivo Bergsohn
South Tahoe Public Utility District
1275 Meadow Crest Drive
South Lake Tahoe, CA 96150
ibergsohn@stpud.dst.ca.us

Jason Kuchnicki
Nevada Division of Environmental Protection
901 S. Stewart St, Suite 4001
Carson City, NV 89701
jkuchnic@ndep.nv.gov

Meredith Gosejohan
Tahoe Program Manager
Nevada Division of State Lands
901 S Stewart St, Suite 5003
Carson City, NV 89701
mgosejohan@lands.nv.gov

Dan Segan
Tahoe Regional Planning Agency
PO Box 5310
Stateline, NV 89449
dsegan@trpa.org

Laurie Scribe
Lahontan Regional Water Quality Control Board
2501 Lake Tahoe Blvd
South Lake Tahoe, CA 96150
laurie.scribe@waterboards.ca.gov

Brian Garrett
Also: Theresa Cody
US Forest Service, Lake Tahoe Basin Management Unit
35 College Drive
South Lake Tahoe, CA 96150
brian.garrett@usda.gov
Theresa.cody@usda.gov